Western University
Scholarship@Western

Digitized Theses | Digitized Special Collections

2009

Behaviour of Reinforced Concrete Beams Retrofitted/Repaired in Shear with Fibre Reinforced Polymers

Hasan Nikopour Deilami

Follow this and additional works at: https://ir.lib.uwo.ca/digitizedtheses

Recommended Citation
Deilami, Hasan Nikopour, "Behaviour of Reinforced Concrete Beams Retrofitted/Repaired in Shear with Fibre Reinforced Polymers" (2009). *Digitized Theses*. 3763.
https://ir.lib.uwo.ca/digitizedtheses/3763

This Thesis is brought to you for free and open access by the Digitized Special Collections at Scholarship@Western. It has been accepted for inclusion in Digitized Theses by an authorized administrator of Scholarship@Western. For more information, please contact wlswadmin@uwo.ca.

Behaviour of Reinforced Concrete Beams Retrofitted/Repaired in Shear with Fibre Reinforced Polymers

(SPINE TITLE: Behaviour of RC Beams Retrofitted/Repaired in Shear with FRP)
(Thesis Format: Integrated Article)

By

Hasan Nikopour Deilami

Graduate Program in Engineering Science
Department of Civil and Environmental Engineering

Submitted in partial fulfillment of the requirements for the degree of Master of Engineering Science

School of Graduate and Postgraduate Studies
The University of Western Ontario, London, Ontario
August 2009

© Hasan Nikopour Deilami, 2009

ABSTRACT

This study aims to explore the shear behaviour of externally Fibre-Reinforced Polymer (FRP) bonded reinforced concrete beams under quasi-static or monotonic loading. The effects of key parameters such as the shear span to effective depth ratio, FRP type and scheme, and stiffness of FRP sheets on shear behaviour aspects such as the ultimate load capacity, deflection, crack pattern, mode of failure, and final strain in the FRP sheets were investigated. This study consists of two main phases incorporating experimental and numerical parts. In the experimental part, six beams were tested using different types of FRP sheets under quasi-static cyclic load and then three of these beams were repaired using epoxy injection along with new CFRP sheets and retested. A finite Element Model (FEM) was developed to predict the results of the first phase of the experimental study. The Genetic Algorithms (GAs) approach was used to develop simple, yet more accurate, formulas for predicting the ultimate load of RC beams under monotonic loading based on experimental data found in the open literature. The accuracy of the proposed model was found to be superior to that of common design guidelines namely, the ACI 440, Eurocode (EC2), Matthys model, Colotti model, and the ISIS Canada guidelines. Considerable improvement of the ultimate shear capacity of beams retrofitted using externally bonded hybrid FRP sheets was observed. The simultaneous application of epoxy injection and externally bonded FRP sheets can significantly improve the ductility and load capacity of damaged beams.

Keywords: Shear, reinforced concrete, fibre-reinforced polymers, finite element modeling, artificial intelligence.

CO-AUTHORSHIP

This thesis has been prepared in accordance with the regulation of integrated article format stipulated by the Faculty of Graduate Studies at the University of Western Ontario. Substantial parts of this thesis were submitted for publication to peer-reviewed technical journals or conferences. All experimental work, data analysis, modeling developments, and writing of the first version of publications listed below were conducted by the candidate himself. The contribution of his co-authors consisted of either providing advice, and/or helping in improving of the final version of publications:

[1] **Nikopour, H.**, Nehdi, M., Broumand, P., 2009, Experimental and Numerical Investigation of FRP Bonded-Reinforced Concrete Beams under Quasi-Static Cyclic Loading, submitted to **Canadian Journal of Civil Engineering**.

[2] **Nikopour, H.**, Nehdi, M., 2009, Shear Repair of Concrete Beams Using External FRP Sheets and Epoxy Injection Methods, submitted to **ACI Materials Journal**.

[3] **Nikopour, H.**, Nehdi, M., 2009, Modeling Shear Capacity of FRP Bonded-Reinforced Concrete Beams Using Genetic Algorithms Approach, submitted to **Journal of Materials and Structures.**

ACKNOWLEDGMENTS

I would like to express my sincere appreciation and gratitude to my thesis supervisor Prof. Moncef Nehdi for his advice and encouragement throughout all stages of my study. I also wish to thank Prof. Nehdi's research group for all the support and help during my research work.

I would like to thank Wilbert Logan for his technical advice regarding my experimental work in the Structures Lab. I would also like to thank all the administrative and technical staff in the Civil and Environmental Engineering Department for their support and cooperation.

The support of my family during my stay in Canada for this study has been most valuable.

Finally, I appreciate the support of companies which cooperated with me by providing materials or technical support including BASF, A-1 Restoration, Fibrewrap, and the Hoskin Company.

TABLE OF CONTENTS

LIST OF TABLES

LIST OF FIGURES

NOTATIONS

A_f = area of FRP external reinforcement, mm^2

A_{sl} = total area of transverse steel reinforcement, mm^2

A_{st} = total area of transverse steel reinforcement, mm^2

a = shear span of beam, mm

b = width of beam, mm

d = effective depth of beam section, mm

d_f = depth of FRP shear reinforcement, mm

d_v = $0.9d$ = effective shear depth, mm

E_c = concrete Young's modulus, MPa

E_f = tensile modulus of elasticity of FRP, MPa

E_{fl} = tensile modulus of elasticity of FRP in primary direction, MPa

E_{f2} = tensile modulus of elasticity of FRP in transverse direction, MPa

E_s = steel Young's modulus, MPa

f_{bo} = concrete biaxial compressive strength, MPa

f_{co} = concrete uniaxial compressive strength, MPa

f'_c = compressive stress in concrete, MPa

f_{fe} = effective stress in FRP, MPa

f_{fu} = design ultimate tensile strength of FRP, MPa

f_{ful} = design ultimate tensile strength of FRP in primary direction, MPa

f_{fu2} = design ultimate tensile strength of FRP in transverse direction, MPa

f_{ly} = specified yield strength of longitudinal reinforcement, MPa

f_y = specified yield strength of transverse steel, MPa

K = ratio of second stress invariant on tensile meridian to that on compressive meridian

K_1 = first modification factor for k_v

K_2 = second modification factor for k_v

L_e = active bond length of FRP, mm

n = number of plies of FRP reinforcement

R_σ = concrete stress-strain model (eq. 9) parameter usually taken as 4,

$R\varepsilon$ = concrete stress-strain model (eq. 9) parameter usually taken as 4

s = spacing of internal steel stirrups, mm

s_f = spacing of FRP shear reinforcement, mm

T_g = glass transition temperature of epoxy, °C

t_f = nominal thickness of FRP sheet, mm

V_c = nominal shear strength provided by concrete, kN

V_n = nominal shear strength, kN

V_s = nominal shear strength provided by steel, kN

V_f = nominal shear strength provided by FRP, kN

w_f = strip width of the FRP reinforcing plies, mm

α = ratio of shear span to effective shear depth

τ = nominal shear stress, MPa

τ_u = concrete-FRP bond strength, MPa

k_v = bond-dependent coefficient for shear

υ_c = Poisson's ratio of concrete

v_{co} = effectiveness factor of concrete

υ_s = Poisson's ratio of steel

ε_0 = strain corresponding to peak compressive stress of concrete, MPa

ε_c = strain in concrete

ε_{fe} = effective FRP strain

ε_{fu} = design rupture strain of FRP

ρ = tension reinforcement ratio

ρ' = compression reinforcement ratio

ρ_f = FRP strengthening ratio

ρ_w = transversal steel reinforcement ratio

ψ = degree of shear reinforcement

ψ_e = degree of external shear reinforcement

ψ_i = degree of internal shear reinforcement

ψ_f = additional FRP strength-reduction factor

CHAPTER 1

Introduction

1.1 Background

Repairing deteriorated concrete structures for shear is essential not only to utilize them for their intended service-life, but also to assure their safety and serviceability. Several techniques have been utilized for the shear repair of RC beams such as drilling and plugging, stitching, routing and sealing, etc. More recently, the application of externally bonded FRP sheets has gained popularity compared to conventional methods. Structural strengthening with externally bonded fibre-reinforced polymers (FRP) has been recognized as a cost-effective, structurally sound and practical method for rehabilitating reinforced concrete (RC) structures (Mosallam *et al.* 2007).

The behaviour of reinforced concrete (RC) beams under shear loading is complex and difficult to predict analytically. For this reason, the shear capacity of RC beams in design codes is generally calculated using empirical or semi-empirical methods. In particular, the shear behaviour of FRP-bonded RC beams depends on the beam size, reinforcement type and amount, FRP laminate characteristics and detailing, as well as the type and position of the applied loading. In addition to the resistance of concrete, additional shear resistance contributions come from the external and/or internal reinforcements of the RC

beam. The reinforcements provided can transform the failure from brittle to ductile (Nehdi *et al.* 2007).

Several experimental and analytical studies have been carried out on RC beams retrofitted with FRP sheets having long unidirectional fibres. Currently, in the calculation of the shear capacity of FRP-bonded RC beams, design codes do not generally provide sufficient information either on various loading patterns, such as cyclic loading, or on the application of hybrid FRP sheets. Therefore, much research is needed to explore the behaviour of RC beams retrofitted with hybrid FRP sheets. In particular, their ultimate strength, pattern of failure and performance under cyclic loading need to be understood to pave the way for their full-scale use in construction.

1.2 Objectives of study

The main objectives of this study are to:

1) Develop experimental data on the ultimate shear load capacity, deflection, crack pattern, mode of failure, and strain in FRP sheets for reinforced concrete beams retrofitted using hybrid FRP sheets as external reinforcement under quasi-static cyclic loading.
2) Experimentally investigate the effect of repairing cracks using epoxy injection for damaged reinforced concrete beams retrofitted using FRP sheets, under shear loading.

3) Investigate the effects of main parameters that affect the shear behaviour of reinforced concrete beams retrofitted by FRP sheets, such as the shear span to depth ratio *a/d*, longitudinal reinforcement ρ, and the mechanical and geometrical characteristics of the attached FRP sheets.
4) Using the Genetic Algorithm's approach for the prediction of the shear capacity of reinforced concrete beams retrofitted by FRP sheets.

1.3 Scope of Research

This thesis consists of five chapters. Chapter 1 provides an introduction on using FRP sheets as external reinforcement in concrete structures, presents the objectives of the study, and summarizes the layout of the thesis. Chapter 2 analyses previous work in the open literature, with particular focus on existing research developing numerical equations or experimental databases on retrofitting or repairing concrete beams using externally bonded FRP sheets or epoxy injection. Chapter 3 describes in detail the experimental program on reinforced concrete beams retrofitted by FRP sheets along with finite element method to model the results of experimental work. Chapter 4 describes experimental work on repairing damaged RC beams using epoxy injection and FRP sheets and testing them under monotonic loading. Chapter 5 presents a numerical study on the effects of different parameters such as the shear span to depth ratio *a/d*, longitudinal reinforcement ρ, mechanical and geometrical characteristics of attached FRP sheets using artificial intelligence namely Genetic Algorithms approaches. Chapter 6 presents the conclusions reached in this study along with some recommendations for future research.

CHAPTER 2

Overview of Previous Work on Application of Externally Bonded FRP Sheets and Epoxy Injection for Rehabilitation

Historically, concrete members have been repaired by post-tensioning or jacketing with new concrete in conjunction with surface adhesives (Klaiber *et al.* 1987). Since the mid 1960's, epoxy bonded steel plates have been used in Europe and South Africa to retrofit flexural members (Dussek 1987). Steel plates have a durability problem unique to this application, because corrosion may occur along the adhesive interface. This type of corrosion adversely affects the bond at the steel plates/concrete interface and is difficult to monitor during routine inspections. Additionally, special equipment is necessary to install the heavy plates. As a result of these problems, alternative materials have been sought by engineers.

2.1 External FRP for Rehabilitation of Concrete Beams

There is a large need for strengthening and retrofitting concrete structures all over the world. The reasons for such a need include, increased load demand, design and construction faults, problems initiated by temporary overload, and so on. Some structures are in such a bad condition that they need to be replaced. Since environmental and economic factors preclude replacing all such structures, they should instead be strengthened or retrofitted as much as possible. A repair and strengthening method that

has gained acceptance all over the world is plate bonding with fibre-reinforced polymers (FRPs), (Burgoyne 1999; Labossière 2000; Bencardino *et al.* 2002; Shin and Lee 2003). This method, which has now been used for over a decade, consists of a thin layer of fibre composite epoxy bonded externally to a structure's surface so that the composite acts as an outer reinforcement.

2.1.1 *Fibre reinforced polymers (FRP)*

FRPs are used in the aerospace and automotive fields because of their high strength to weight ratio, durability, and ability to form complex shapes. They are generally constructed of high performance fibres such as carbon, Aramid, or glass which are placed in a resin matrix. By selecting among the many available fibres, geometries and polymers, the mechanical and durability properties can be tailored for a particular application. This quality makes FRP a good choice for civil engineering applications.

Carbon fibres have a high elastic modulus and high strength in both tension and compression. Composed almost entirely of carbon atoms, the fibres are generally available as bundles of 500-150,000 filaments of approximately five microns in diameter called "yarn". These are then assembled directly into FRP products or into intermediate forms such as continuous fibre sheets or fabrics. Continuous fibre sheets are made of parallel yarns attached to flexible backing tape for handling. Fabrics are made of yarns stitched into a geometric form. The yarns may run unidirectionally like continuous fibre sheets, or be woven at different angles into a fabric. Carbon fibre-reinforced polymers

(CFRPs) have a high strength and stiffness-to-weight ratio, show excellent fatigue Behaviour and corrosion resistance, and are not magnetic. The structure of carbon fibres is represented schematically in Fig. 2.1. Table 3.1 shows mechanical properties of typical fibres. As illustrated in Table 3.1 carbon fibres are highly anisotropic and have different strength and stiffness in the axial and radial directions.

Most glass fibres are based on silica (SiO_2), with additions of oxides of calcium, born, sodium, iron and aluminum. These glasses are usually amorphous, although some crystallization may occur after prolonged heating at high temperature, leading to a reduction in strength. There are three types of glass fibres. The most commonly used glass fibre, E-glass (E for electrical), draws well and has good strength, stiffness, electrical and weathering properties, In some cases, C-Glass (C for corrosion) is preferred, having a better resistance to corrosion than E-glass, but a lower strength. Finally S-glass (S for strength) is more costly than E-glass, but has a higher strength, Young's modulus and temperature resistance. The diameter of E-glass fibre is usually between 8 and 15 μm. An example is given in Fig. 2.2 of a section cut normal to the fibre direction in a lamina with high glass fibre content.

Aramid is one of the most common organic fibres. It was first developed by Du Pont with the trade name Kevlar. The principles involved are best understood by considering fibres based on a simple polymer, polyethylene. Chain-extended polyethylene single crystals consist of straight zig-zag carbon backbone chains, fully aligned and closely packed. These have a Young's modulus of about 220 GPa parallel to the chain axis. Fairly good

chain alignment can be achieved in a fibre by drawing and stretching resulting in a modulus of 70 GPa. As for carbon fibres, the modulus normal to the fibre axis is much less than that along the fibre axis.

Since there is usually no adhesion between individual fibres, a polymer resin matrix is used to transmit forces between the fibres. Polymers, such as epoxy have the advantages of lower cost, ease of workability, and some have good resistance to environmental effects. The hand or contact layup is the oldest method of assembling an FRP. The epoxy is applied to one or both sides of the fabric and worked between the fibres using an ordinary paint roller and hand pressure. The surface may then be finished with a flexible blade to remove excess epoxy before curing occurs. Fibres may be mixed in random directions with suitable epoxy or they may be arranged in specific directions (Fig. 2.3). Another method for the arrangement of fibres is the woven structure, which is shown in Fig. 2.4.

The most commonly used test method for determining the properties of a composite material is the uniaxial tension test (ASTM D3552 -96, 2007). In this test, a specimen of FRP is instrumented either using an extensiometer or strain gages and is loaded in tension. The elastic modulus varies for different fibre orientations. When the load is applied at 0^{o} or 90^{o} to the fibres, the behaviour is almost linear elastic. However, when the load is applied at an angle to the fibres, the behaviour is nonlinear.

2.1.2 *Shear retrofit of RC beam using FRP*

Several experimental researches have been carried out on the investigation of the shear retrofit of damaged or low strength reinforced concrete RC beams using externally bonded FRP sheets under monotonic loading. They have used different schemes and materials. The most typical schemes are two side, three sides bonded or completely wrapped patterns. Some of the experimental work includes researches by Mosallam *et al.* 2007, Khalifa *et al.*1999, Cao *et al.* 2005, Abdel-Jaber *et al.* 2003, Kachlakev *et al.* 1999, Kage *et al.* 1997, Mitsui *et al.* 1998, Sato *et al.* 1996, Triantafillou 1998, Uji 1992, Huthchinson *et al.* 1999, Taerwe *et al.* 1997, Taljsten *et al.* 1999, Michael *et al.* 1995, Carolin *et al.* 2005, Pellegrino *et al.* 2006, Hadi 2003, Monti *et al.* 2006, Matthys 2000, Spadea *et al.* 1998, Swamy *et al.* 1996, Norris *et al.* 1997, Umezu *et al.* 1997, Araki *et al.* 1997, Swamy *et al.* 1999, Chajes *et al.* 1995, Al-Sulaimani *et al.* 1994. Their results show completely wrapped schemes provide better results for shear retrofitting of RC beams compared to other schemes. Moreover it was concluded even though external FRP increase ultimate shear capacity, it may decrease ductility in some circumstances. Failure of the beam can be cause by debonding or rupture of FRP sheets or failure mode may turn to a flexural one.

2.1.3 *Current shear design guidelines for FRP-RC beams*

Some analytical and empirical models have been developed to theoretically predict the shear capacity of externally bonded FRP reinforced concrete beam specimens, and are described below.

ACI 440, CSA 860, ISIS Canada models

The model proposed by ACI 440 (2003) is applicable to reinforced concrete beams with externally applied FRP reinforcement. According to this model, the nominal shear strength V_u of such beams is given by

$$V_n = V_c + V_s + \psi_f V_f \tag{2.1}$$

Where V_c is the nominal shear capacity provided by concrete, V_s is the nominal shear capacity provided by steel, V_f is nominal shear capacity provided by the fibre-reinforced polymer sheet, and ψ_f is the additional reduction factor given in Table 10.1 of the ACI 440 document.

The shear strength contribution from the FRP is:

$$V_f = \frac{A_f E_f \varepsilon_{fe} d_f}{s_f} \tag{2.2}$$

and

$$V_c = \left(0.16\sqrt{f_c'} + 17\frac{\rho_l V_u d}{M_u}\right)bd \tag{2.3}$$

$$V_s = \frac{A_{st} f_{ty} d}{s} \tag{2.4}$$

In the above formulas, d is the effective depth of the beam section, $M_u/V_u d$ represents the shear span to depth ratio a/d, and $d_f = h_f - d'$ is the effective depth of the external reinforcement, d' being the concrete cover. Furthermore, ε_{fe} is the effective tensile strain in the FRP and E_f is the elastic modulus of the FRP in the principal fibre orientation.

The effective strain, ε_{fe} in the FRP is assumed to be smaller than the ultimate strain, ε_{fu}. This can be computed as

$$\varepsilon_{fe} = \begin{cases} 0.004 \le 0{,}75\varepsilon_{fu} & \text{completely wrapped beams} \\ k_v\varepsilon_{fu} \le 0.004 & \text{two or three sides laminated} \end{cases} \tag{2.5}$$

$$k_v = \frac{k_1 k_2 L_e}{11{,}900\varepsilon_{fu}} \le 0.75 \tag{2.6}$$

$$L_e = \frac{23{,}300}{(nt_f E_f)^{0.58}} \tag{2.7}$$

$$k_1 = \left(\frac{f_c'}{27}\right)^{2/3} \tag{2.8}$$

$$= \begin{cases} \dfrac{d_f - L_e}{d_f} & \text{U - wraps} \\ \dfrac{d_f - 2L_e}{d_f} & \text{two sides laminated} \end{cases} \tag{2.9}$$

Where, f_c' and E_f are in MPa, and t_f in mm, respectively. The Canadian Standards Association CSA S806 (2002) and ISIS Canada (2001) design manuals use similar methodology to the ACI code. Figure 2.5 illustrates parameters used in the ISIS approach.

Triantafillou and Antonopoulos model

This model proposed by Triantafillou and Antonopoulos (2000) has been adopted by the Eurocode (EC2). According to this model

$$V_n = V_c + V_s + V_f \le V_{R2} = 0.4 v_{co} f_c' \, bd \tag{2.10}$$

Where

$$V_c = \tau_R k(1.2 + 40\rho_l)bd \tag{2.11}$$

$$V_s = \frac{0.9A_{st}f_{ty}d}{s} \tag{2.12}$$

$$V_f = \frac{0.9A_f E_f \varepsilon_{fe} d_f}{s_f} \tag{2.13}$$

The tensile strength of concrete, $f_{ct} = 0.3(f_c')^{2/3}$, the concrete shear resistance, $\tau_R = 0.025 f_{ct}$, k=*1.6-d* >*1* (*d* is in m), $\rho_l = \frac{A_{sl}}{bd}$, $\rho_f = \frac{A_f}{bs_f}$, and $v_{co} = 0.7 - f_c'/200 \geq 0.5$ (f_c' is in MPa).

The effective strain in this model is:

$$\varepsilon_{fe} = \begin{cases} 0.17\left(\frac{f_c^{2/3}}{E_f\rho_f}\right)^{0.30}\varepsilon_{fu}\text{, for beams fully wrapped with CFRP} \\ min\left[0.00065\left(\frac{f_c^{\frac{2}{3}}}{E_f\rho_f}\right)^{0.56};0.17\left(\frac{f_c^{\frac{2}{3}}}{E_f\rho_f}\right)^{0.3}\varepsilon_{fu}\text{, for two or three sides laminated with CFRP}\right] \end{cases} \tag{2.14}$$

Matthys and Triantafillou model

Matthys and Triantafillou (2001) made a modification to the Trinatafillou and Antonopoulos model and incorporated the effect of the shear span to beam depth ratio in the calculation of the effective strain. In practice, it was proposed to calibrate the

effective FRP strain, ε_{fe} not only in terms of the FRP axial rigidity, $E_f \times \rho_F$ and the concrete tensile strength, f_{ct}, but also taking into account the influence of the shear span ratio *a/d*. According to their modification, the effective strain can be expressed as:

$$\varepsilon_{fe} = \begin{cases} 0.72\varepsilon_{fu} e^{-0.0431\Gamma_f} & \text{fully wrapped wit CFRP} \\ 0.56\varepsilon_{fu} e^{-0.0455\Gamma_f} & \text{two or three sides laminated CFRP} \end{cases} \quad (2.15)$$

Where

$$\Gamma_f = \frac{E_f \rho_f}{f_c^{\frac{2}{3}} \left(\frac{a}{d}\right)} \quad (2.16)$$

The remaining expressions for the evaluation of the ultimate shear capacity V_u in this model are the same used in the Triantafillou and Antonopoulos model, expressed in equations 2.12, 2.13 and 2.14.

Colotti *et al.* model

Colotti *et al.* (2004) proposed that the total contribution to shear reinforcement can be expressed as:

$$\psi = \psi_i + \psi_e \quad (2.17)$$

The internal shear strength contributed by the internal steel reinforcement is:

$$\psi_i = \frac{A_{st} f_y}{bsf_c'} \tag{2.18}$$

whereas, the external contribution from FRP is:

$$\psi_e = \begin{cases} \dfrac{2w_f t_f}{bs_f f_c'} f_{fe} & \text{for completely wrapped beams} \\ min\left(\dfrac{w_f d_f}{bs_f f_c'} \tau_u ; \dfrac{2w_f t_f}{bs_f f_c'} \right) & \text{two or three sides laminated} \end{cases} \tag{2.19}$$

where the effective stress, $f_{fe} = v_f \times f_{fu}$.

The shear strength of a beam specimen is given by:

$$V = (\frac{\tau}{f_c'}) bd_v f_c' \tag{2.20}$$

where τ / f_c' is the minimum value from the following failure cases:

Failure case (1)

$$\frac{\tau}{f_c'} = \begin{cases} \dfrac{1}{2}\left[\sqrt{1+\alpha^2} - \alpha\right] + \psi\alpha & 0 \le \psi \le \psi_0 = \dfrac{\sqrt{1+\alpha^2} - \alpha}{2\sqrt{1+\alpha^2}} \\ \sqrt{\psi(1+\psi)} & \psi_0 \le \psi \le 0.5 \\ \dfrac{1}{2} & \psi > 0.5 \end{cases} \tag{2.21}$$

Failure case (2)

For $\psi \le \psi_0$

$$\frac{\tau}{f_c'} = \begin{cases} \frac{1}{2}\left[\sqrt{4\eta(1-\eta)+\alpha^2} - \alpha\right] & \eta \le 0.5 \\ \frac{1}{2}\left[\sqrt{1+\alpha^2} - \alpha\right] & \eta > 0.5 \end{cases} \tag{2.22}$$

For $\psi > \psi_0$

$$\frac{\tau}{f_c'} = \psi\left[\sqrt{\frac{2\eta}{\psi}+\alpha^2} - \alpha\right] \tag{2.23}$$

where $\eta = \frac{A_{sl} f_{ly}}{b d_v f_c'}$ and $\alpha = \frac{a}{d_v}$.

The effectiveness of this design procedure can be assured by predicting the internal strengths corresponding to the different failure modes of the member. Thus, it is possible to select the geometry and mechanical properties of the composite material to ensure fewer unfavourable failure modes.

All design guidelines presented in this chapter do not consider the interaction between the internal shear reinforcement and the shear capacity owing to the FRP. Also, design provisions are not applicable for hybrid or bidirectional FRP sheets. Except the Matthys and Triantafillou model, other formulas do not consider the effect of the shear span-to-depth ratio on the shear capacity contributed by the FRP. Mosallam *et al.* (2007) argued that shear span-to-depth ratio *a/d*, is an important factor that actively controls the shear failure mode of beam and consequently influences the shear strength enhancement. Pellegrino (2006) showed that there is a considerable interaction between steel stirrups and external FRP laminates and that it is possible at failure, weather in-debonding or

rupture, stress level in steel stirrups are much lower than the yield stress. Sakar *et al.* (2009) presented an experimental research on RC beams with bidirectional FRP sheets as external reinforcement. He concluded that current design codes have a substantial error due of ignoring the FRP effect in the transverse direction.

2.2 Repairing of Cracks in Damaged RC Beams

Concrete is one of the most versatile construction materials and the most consumed material worldwide after water. It is relatively inexpensive, durable, strong, and it can be molded into any shape. The development of concrete as a construction material dates back to several thousand years, while steel was introduced to reinforce concrete about two centuries ago. There have been tremendous advancements in the use of reinforced concrete for construction over the last decades (Shah, 2005).

Although the majority of concrete structures have generally performed satisfactory, many problems have been reported due to one or more of the following causes: (i) improper quality of materials, (ii) incorrect specifications, (iii) faulty design, (iv) errors in the construction process, and (v) exposure of structures to extreme environmental conditions. All of these problems may lead to insufficient structural capacity and/or the development of cracks which can decrease the service life of structures. A successful repair technique improves the performance of a structure, restores and/or increases its strength and stiffness, enhances the appearance of the concrete surface, prevents the ingress of

moisture, chloride ions and carbon dioxide to the reinforcing steel, and improves the overall durability.

Cracks can be categorized into three groups: (i) cracks due to inadequate structural performance, (ii) cracks due to inadequate material performance, and (iii) acceptable cracks. Structural cracks are caused primarily by overloading; material related cracks are due to shrinkage and chemical reactions; and acceptable cracks are those that develop due to service loading for tensile stresses to be distributed properly along the length of the material (Tsisatas *et al.* 1994). Cracks in structural elements can also be classified as dormant or active. Active cracks, such as cracks caused by foundation settlement, cannot generally be fully repaired, whereas dormant cracks can be successfully repaired (Ekenel *et al.* 2007).

Various systems for crack repair have been developed and used for many years. The most common crack repair materials are cementitious and polymer products and include epoxy injection and grouting. The ACI Publication 546R-96 (1996) "Concrete Repair Guide" documents standard techniques for concrete repair with cementitious and polymer materials. Two other ACI publications, which are directly related to crack repair, include 224R-80 "Control of Cracking in Concrete Structures" (1980), and ACI 224.1R-93 "Cause, Evaluation, and Repair of Cracks in Concrete Structures" (1993). According to ACI 224.1R-93, any crack repair material and method must not only address the cause of the cracking, but also repair the crack itself. Epoxy resins are commonly used repair materials that generally have very good bonding and durability characteristics. In the

following sections the most common methods for repairing cracks have been briefly discussed.

2.2.1 *Conventional methods for repairing cracks*

Three common methods for repairing cracks in concrete structures are as follows:

- Routing and sealing
- Stitching
- Drilling and plugging

Routing and sealing

Figure 2.6 illustrates different steps of this method. It involves enlarging the crack along its exposed face and filling and sealing it with a suitable joint sealant. It is a useful technique for horizontal surfaces such as floors and pavements owing to as ease of application. Materials which are usually used for this approach are epoxies, urethanes, silicones, polysulfides, asphaltic materials, and polymer mortars (Johnson, 1965). The procedure consists of:

1-Preparing a groove at the surface

2-Cleaning by air blasting or water blasting followed by drying

3-Sealant is placed into the dry groove and allowed to cure

Stitching

The most common stitching methods use stitching dogs (U-shaped metal units), thin metal interlocking plates, or dowel bars for reinforcement. In each method, the reinforcement is installed across the crack and is bonded to each side of the crack with epoxy or cementitious materials. The amount of reinforcement can be varied to achieve the desired strength restoration. Unlike interlocking plates and dowel bars, which are embedded in the concrete, stitching dogs are surface mounted. Since concrete is usually weak in axial tension, stitching dogs are placed on both faces. Stitching dogs are most effective when restoring tension in bending members since they are placed at the critical location-the tension face.

To install stitching dogs, holes are drilled on both sides of the crack, the holes are cleaned, and the legs of the dog are anchored in the holes with non-shrink grout or epoxy. The length, orientation, and location of the stitching dogs are varied so that the tension is transmitted across the area, not across a single plane within the section.

Because dogs are thin and long and are not supported laterally, they cannot take much compressive force. If the crack closes as well as opens, the dogs must be stiffened and strengthened to prevent buckling. One method to prevent buckling is to embed the dogs in an overlay.

Dowel bars are also used to repair concrete cracks. To install dowel bars, two holes are drilled diagonally through the crack, one from each side. The holes are filled with non-shrink cementitious or epoxy materials, then a dowel bar is driven into each hole. The bonded dowel bars transmit force across the crack face. The angled dowel bars restore shear transfer and transmit axial tension, but are not very effective for restoring tension in flexural members. (Contrasto, 1995). Figure 2.7 presents an example of using this method.

Drilling and plugging

This method consists of drilling down the length of the crack and grouting it to form a key. It is most often used to repair vertical cracks in retaining walls.

2.2.2 *Epxoy injection*

One way to repair extensive cracks is the use of epoxy injection. This technology was developed in Germany and Switzerland in the 1930's. It can be used to restore tensile strength to a cracked concrete member such as slabs and pavements, beams, walls and columns. Usually a two component epoxy is used in this method, one of which is a resin and the other is a hardener material. Figure 2.8 shows crack repair using epoxy injection. The typical installation procedure is as follows:

- Prepare the surface
- Seal cracks and install injection ports

- Inject the resin
- Cure
- Grind off seal and ports

The common installation problems associated with the epoxy injection can be summarized as follows:

- Improper resin
- Improper mixing
- Inadequate surface sealing
- Improper pressure
- Improper port spacing
- Improper sequence of pumping
- Excessive crack width

Calder and Thompson (1998) reported that the overall structural performance of RC slabs repaired using epoxy resin injection performed best compared to other repair materials such as polyester and methyl methacrylate resins. The stiffness of the cracked slabs in their study was about one quarter of that of the un-cracked slabs and the repairs reinstated only about half of the stiffness loss. According to Minoru *et al.* (2001), the bond between concrete and the injection material is very critical; a good bond may restore the original stiffness of the repaired material and prevent further penetration of chloride ions and water. The crack should also be clean and dry prior to injection. Epoxy injection is not

applicable if the cracks are actively leaking or cannot be dried out, unless moisture tolerant epoxies are used which can flush the moisture from the inner crack surfaces.

2.3 Conclusions and Motivation of the Research

A literature review was carried out to critically examine the research available on using externally FRP bonded and epoxy injection as renovation and upgrading methods for RC beams. It was argued that FRP sheets have a great potential for retrofitting concrete structures. The main advantage of FRP sheets is their ability to mitigate corrosion problems while having a high strength-to-weight ratio. Research on the application of externally bonded unidirectional FRP sheets for reinforced concrete (RC) beams under monotonic loading is well established. However, very limited research on the shear behaviour of externally FRP-bonded reinforced concrete beams is available using hybrid FRP sheets or under other types of loading such as cyclic loading. Some design provisions were discussed in this chapter, but they do not consider the interaction between the internal shear reinforcement and the shear capacity imparted by the FRP. Moreover, design codes are not applicable for hybrid or bidirectional applications of FRP sheets. The effect of the shear span-to-depth ratio a/d is also ignored in all models, expect the Matthys and Triantafillou model. Thus, more research is still needed to improve the accuracy of design provisions and to develop a data-base on other patterns of loading and FRP materials.

Three conventional methods for repairing cracks were discussed. Epoxy injection was found to be a powerful and simple method for repairing damaged concrete structural members. However, data on the simultaneous application of epoxy injection and externally bonded FRP sheets is scarce.

Table 2.1: Typical fibre properties

Fibre	Density, P ($Mg\ m^{-3}$)	Young's modulus E (GPa)	Poisson's Ratio ν	Tensile strength σ (GPa)	Failure strain ε (%)	Thermal expansivity α ($10^{-6}K^{-1}$)	Thermal conductivity α ($W\ m^{-1}\ K^{-1}$)
HM[a] Carbon	1.95	axial 380 radial 12	0.2	2.4	0.6	axial -0.7 radial 10	axial 105
HS[b] Carbon	1.75	axial 230 radial 20	0.2	3.4	1.1	axial -0.4 radial 10	axial 24
E-glass	2.56	76	0.22	2.0	2.6	4.9	13
Kevlar	1.45	axial 130 radial 10	0.35	3.0	2.3	axial -6 radial 54	axial 0.04

[a] High modulus
[b] High strength

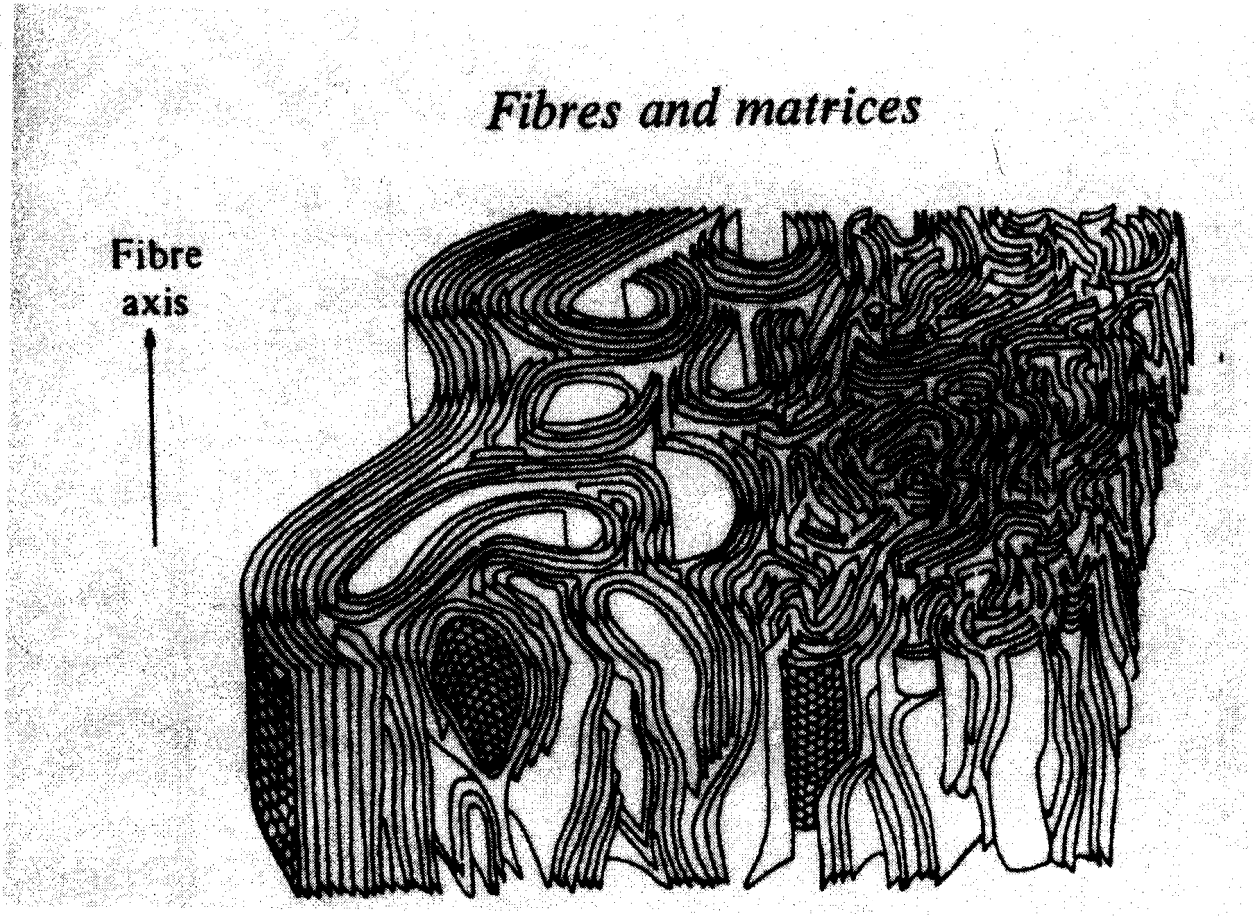

Fig. 2.1: Schematic representation of the structure of carbon fibres (From Bennett and Johnson, 1978).

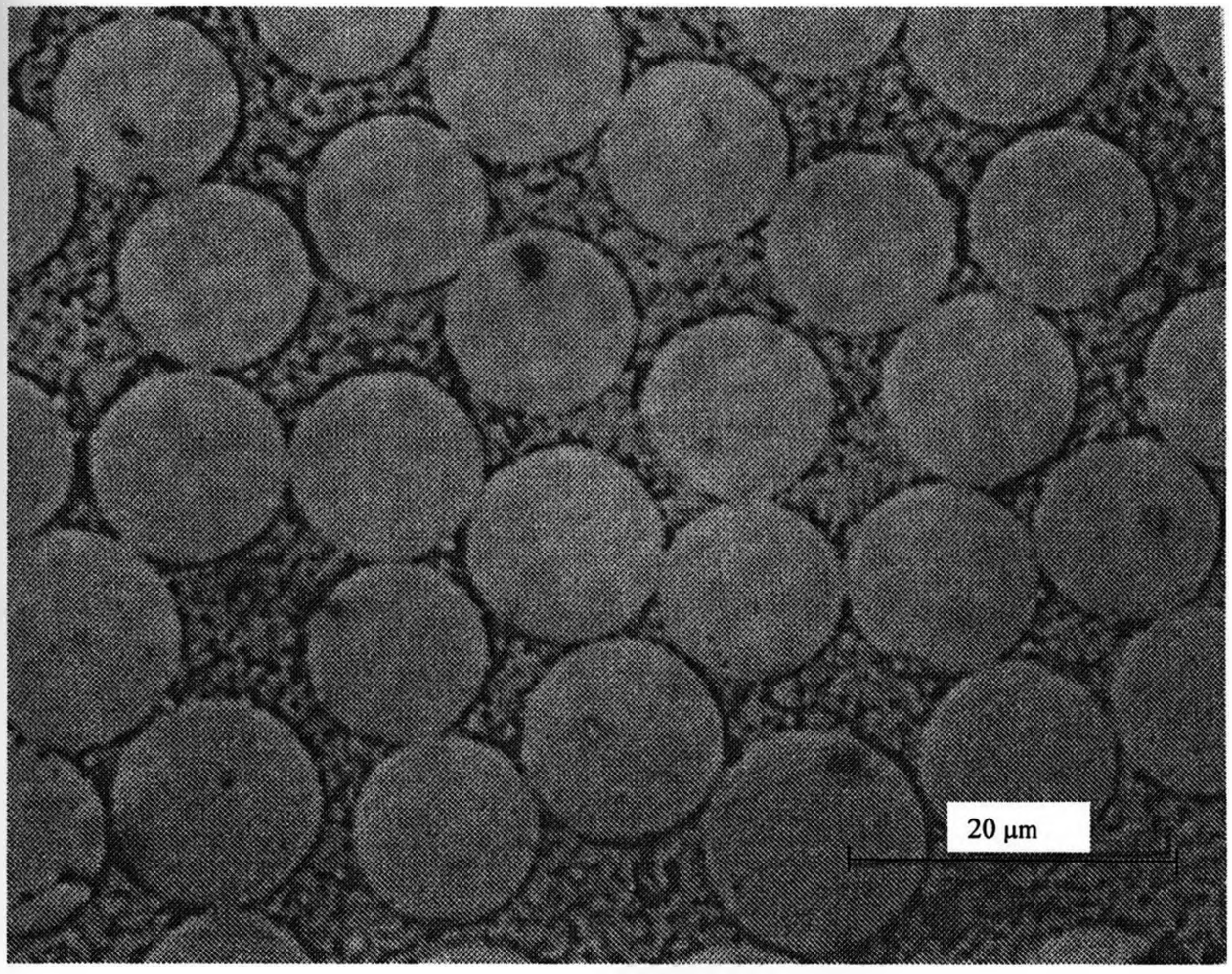

Fig. 2.2: Optical micrograph of a section cut at right angles to fibres in a unidirectional laminate of glass fibre/polyester resin (From Hull and Clyne, 1996).

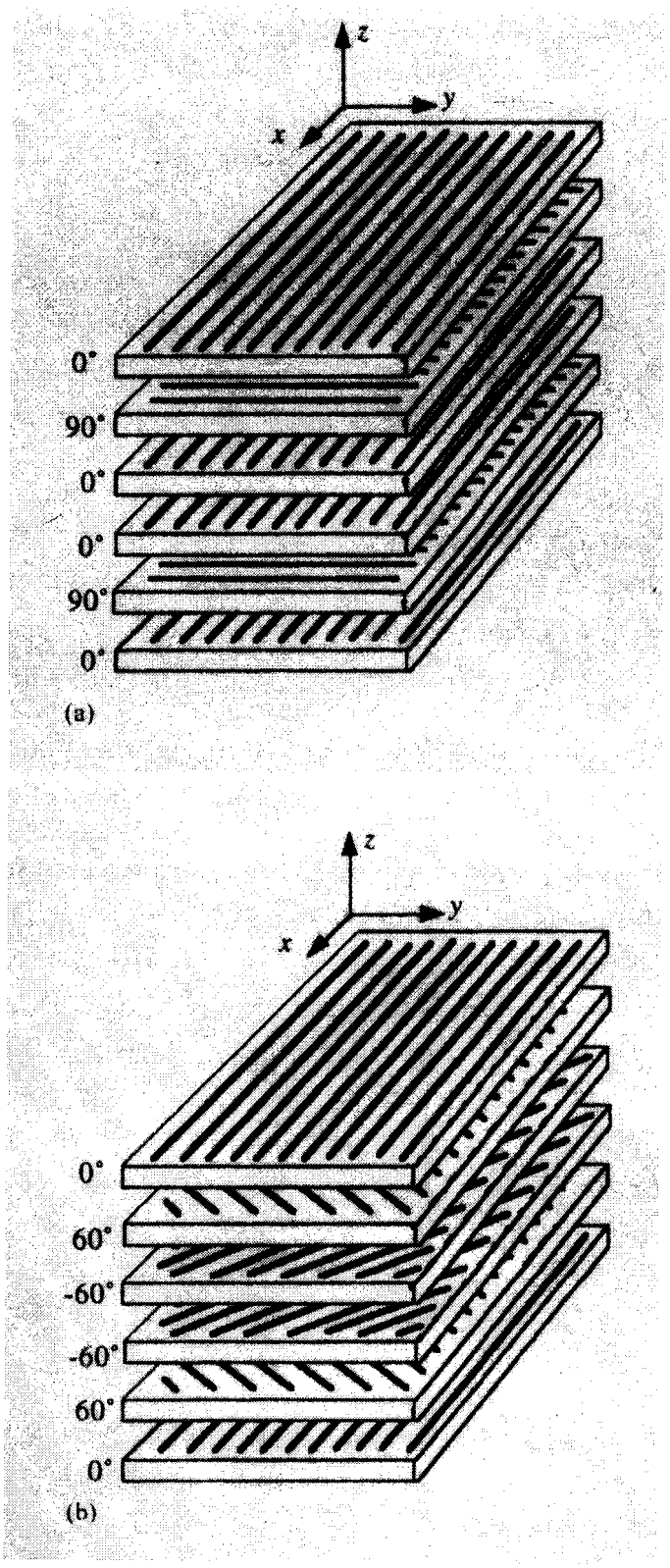

Fig. 2.3: Arrangement of plies in (a) a crossply laminate, and (b) an angle-ply laminate sandwiched between 0^{o} plies (From Hull and Clyne, 1996).

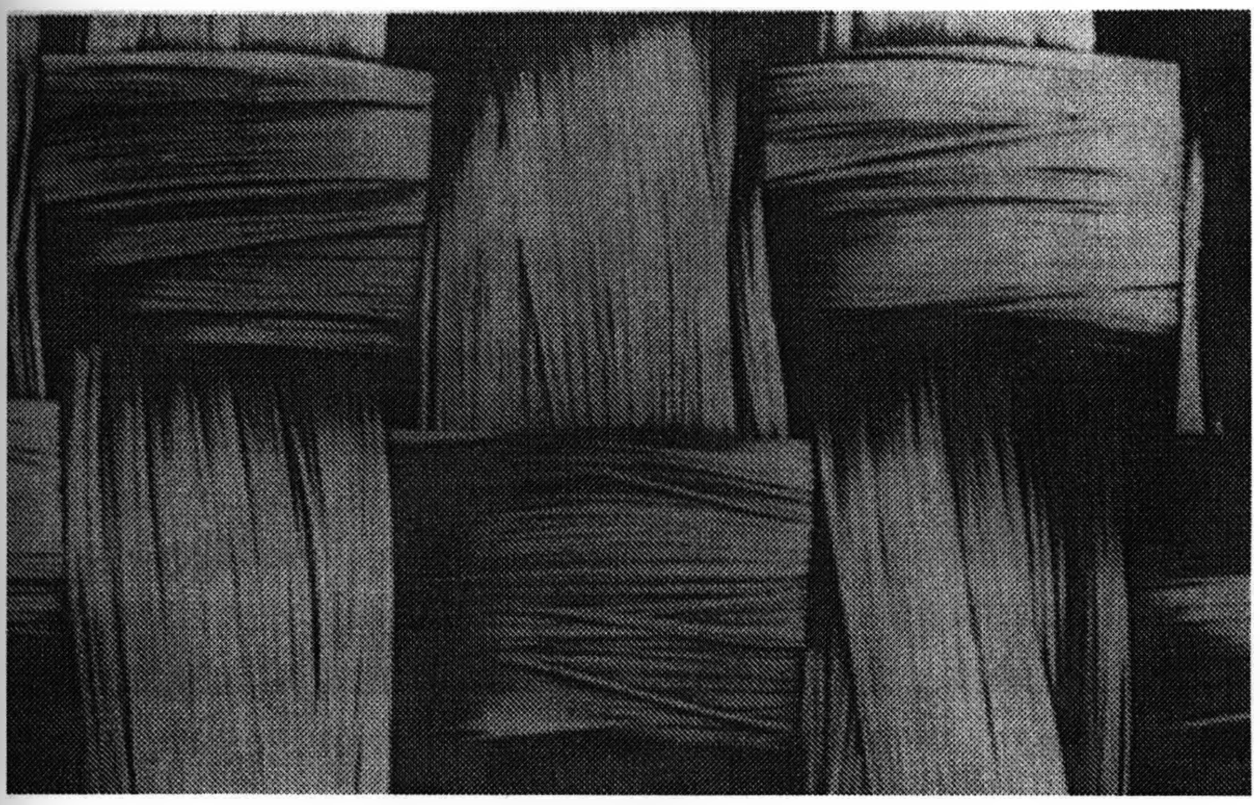

Fig. 2.4: Micrograph of a woven roving before infiltration with resin (From Hull and Clyne, 1996).

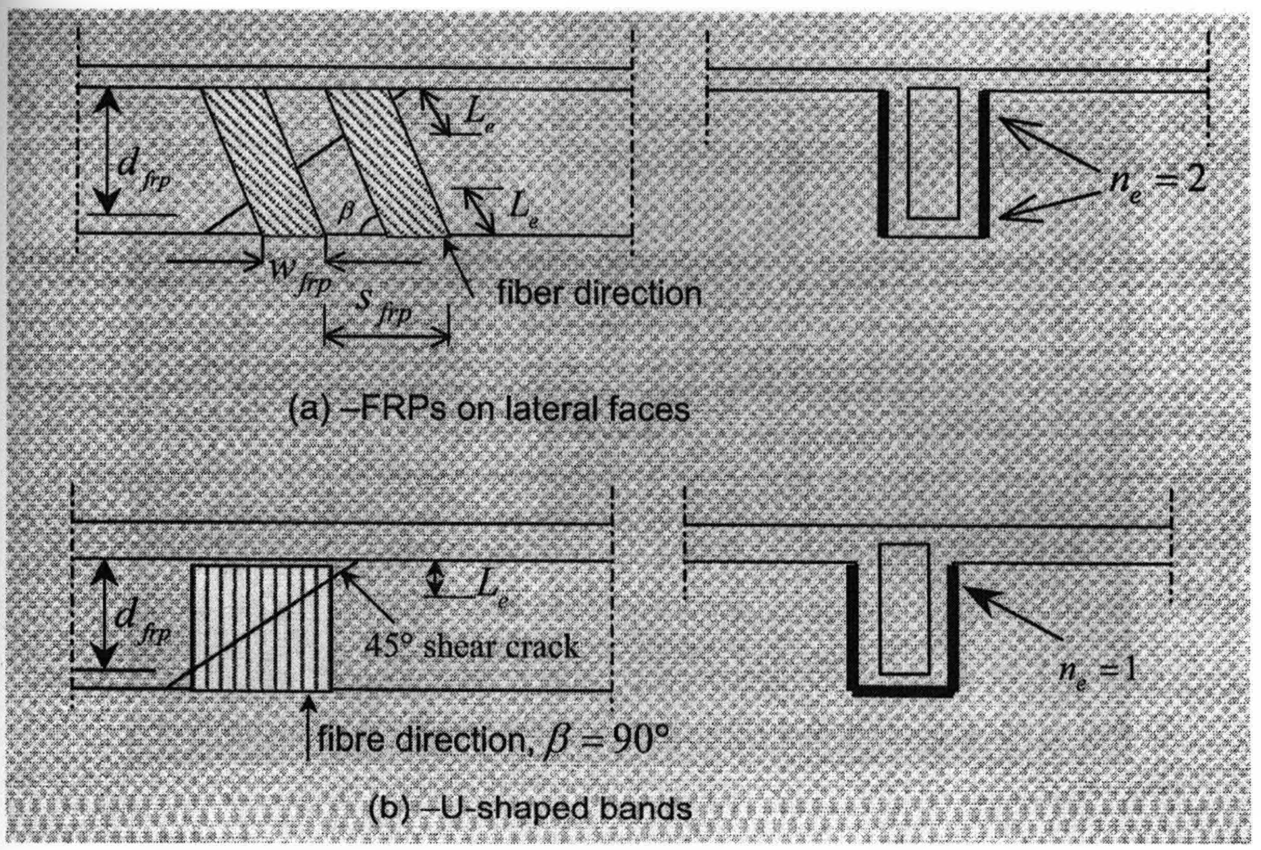

Fig. 2.5: Typical shear strengthening and design parameters (From ISIS Canada Design Manual No.2, 2001).

Fig. 2.6: Repair of crack in pavement by routing and sealing (From *http://www.highwayimprovementinc.com/crack_sealing.htm*).

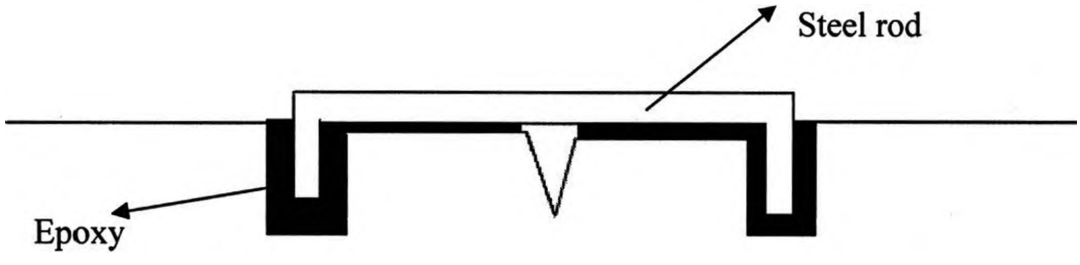

Fig. 2.7: Stitching method for repairing cracks.

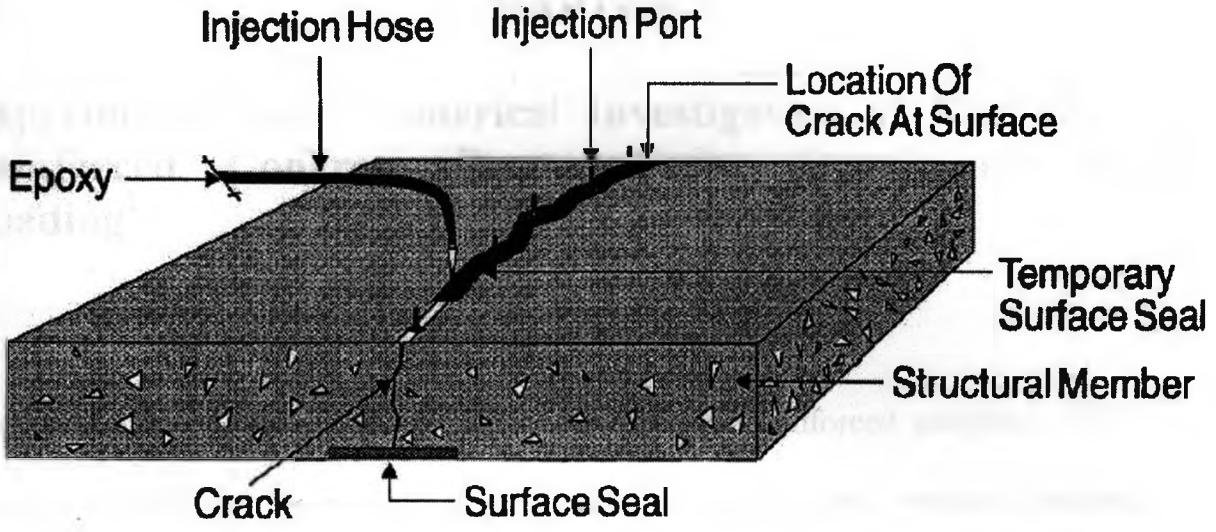

Fig. 2.8: Crack repair using epoxy injection (From Sika Tech Guide, 1990).

CHAPTER 3

Experimental and Numerical Investigation of FRP Bonded-Reinforced Concrete Beams under Quasi-Static Cyclic Loading[1]

Structural strengthening with externally bonded fibre-reinforced polymers (FRP) has been recognized as a cost-effective, structurally sound and practical method for rehabilitating reinforced concrete (RC) structures. Although several experimental and numerical studies have been carried out on the shear capacity of RC beams retrofitted by carbon or glass fibre-reinforced polymers, there has been little work on hybrid FRP sheet applications, particularly under cyclic loading. In the present research, six RC beams were constructed, and four of which were retrofitted using various schemes of FRP sheets. All beams were subjected to quasi-static cyclic loading in an attempt to represent the effect of fatigue and repetitive loading. The experimental crack load, ultimate load, and deflection pattern at mid-span of the beams were measured and compared with predictions of a numerical model based on finite element analysis. Experimental results demonstrated that hybrid applications of FRP sheets can improve the shear performance of retrofitted RC beams and increase the ultimate strain of the FRP sheets at failure. The results of the numerical model were in reasonable agreement with the corresponding experimental results.

[1] A version of this chapter has been submitted for review to a Canadian Journal of Civil Engineering.

3.1 Introduction

Innovative composite materials known as fibre-reinforced polymers (FRP) have shown great promise in the rehabilitation of ageing reinforced concrete (RC) structures. The rehabilitation of these structures is usually in the form of strengthening of structural members, repair of damaged structures, or retrofitting for seismic deficiencies. Composite materials have proven to be an excellent option for external reinforcement because of their high tensile strength, lightweight, resistance to corrosion, high durability, and ease of installation (Khalifa et al. 2000). Externally bonded FRP reinforcement has shown to be applicable to the strengthening of many types of RC structures and structural members such as columns, beams, slabs, walls, tunnels, chimneys, and silos. It can be used to improve the flexural and shear capacities, and also to provide confinement and ductility of structural members, particularly under compressive load (Khalifa et al. 2000).

The shear behaviour of FRP-bonded RC beams depends on a number of parameters including the beam size, reinforcement type and amount, FRP laminate properties and detailing, and the type of the applied loading (Pellegrino et al. 2006). Several studies have been done on the application of unidirectional fibres for retrofitting reinforced concrete beams; however, very little information is available of behaviour of beams retrofitted by hybrid FRP sheets.

Over the past few years, a number of experimental and theoretical studies have been carried out on the behaviour of hybrid FRP sheets used as external reinforcement for RC

structures. For instance, Wu et al. (2008) carried out an experimental research on the application of hybrid FRP sheets as external confinement for concrete cylinders. They concluded that this reinforcement scheme can significantly enhance the strength and ductility, resulting in a large energy absorption capacity of specimens. Li et al. (2002) conducted an experimental study on the reinforcement of concrete beam–column connections with hybrid FRP sheets. Their results show that retrofitting critical sections of concrete frames with FRP reinforcement can provide significant gains in strengthening and stiffening of such frames and improving their behaviour under different types of loading. The selection of the type of FRP and its architecture in order to improve the bond and strength of the retrofitting scheme were also discussed in this study. Li et al. (2005) later reported the results of an experimental study conducted on RC beams retrofitted in flexure using hybrid FRP sheets. It was indicated that hybrid sheets allow the transfer of stress in the hybrid composite between carbon fibres and glass fibres, and further improve ductility. Based on this experimental study, an elastoplastic section analysis method was conducted to predict the bearing capacity of RC beams strengthened with hybrid FRP sheets. Sakar et al. (2009) reported results of an experimental research on the application of bidirectional CFRP sheets for retrofitting RC beams under cyclic loading. It was concluded that adding a horizontal ply in the 0^{o} direction has a considerable effect of increasing the shear capacity.

No research was accessible in the open literature on the application of hybrid sheets of different FRP materials as external reinforcement for the shear rehabilitation of RC beams. To develop experimental data on the ultimate shear load capacity, deflection,

crack pattern, mode of failure, and strain for RC beams retrofitted using hybrid FRP sheets as external reinforcement under quasi-static cyclic loading, six full-scale beams were constructed and tested in this study. One beam specimen was retrofitted using hybrid sheets of carbon fibres in the main direction and Aramid fibres in the transverse direction. The same scheme was implemented using carbon and glass fibres on another RC beam specimen. To compare the results with that for RC beams with normal unidirectional FRP fibres, one beam specimen was retrofitted using unidirectional carbon fibre sheets as external reinforcement. Another beam specimen had woven glass fibres in the both $+45^{\circ}/-45^{\circ}$ diagonal directions. The last two RC beams tested had no external reinforcement.

All beams were loaded using an eight point loading scheme. Strain gauges were installed at three directions on the surface of the four RC beam specimens with varying external FRP types and schemes. All beam specimens were loaded to failure under quasi-static cyclic loading. To relate experimental results to theory, the finite-element technique was utilized.

3.2 Experimental Program

The experimental program was conducted in the Structures Laboratory of the Department of Civil and Environmental Engineering at The University of Western Ontario. It involved six tests on full-scale rectangular RC beams that were designed so that their ultimate shear capacity was reached before their flexural failure.

3.2.1 Materials properties

A relatively low strength concrete (25 MPa) was selected for casting the beam specimens in order to emphasize the need for retrofit. The mix design of the concrete used was as follows: cement = 375 kg/m^3, coarse aggregate (well graded, 28-mm nominal maximum-size rounded gravel) = 1200 kg/m^3, fine aggregate (natural sand with an oven dry relative density of 2.64 and absorption of 0.7%) = 600 kg/m^3. The fineness modulus of the sand was 2.8 and the water to cement ratio (w/c) was 0.5. Cylindrical (150×300 mm) specimens were made to determine the compressive strength (ASTM C39) of concrete, f_c'. Splitting tests (ASTM C496) on cylindrical specimens were also used to measure the splitting tensile strength of the concrete, f_{ct}. The following average values were obtained at 28 days: cylindrical compressive strength of the concrete, f_c' = 25.1 MPa, splitting tensile strength, f_{ct} = 2.5 MPa. The Young's modulus (ASTM C469) was measured as E_c = 223 GPa and the Poisson's ratio (ASTM C469) under uniaxial compression loading was ν_c = 0.2.

The tensile strength of the reinforcing steel, f_y was 465 MPa. Its Young's modulus, E_s and passion ratio υ_s, were 200 GPa and 0.3, respectively. The properties of the FRP sheets used in this study are shown in Table 3.1. Mechanical properties of FRP laminates can be measured following the ASTM D-3039 standard guidelines.

The Tyfo epoxy, which is a two-component material product of Fyfe Company, was used for bonding the FRP sheets to concrete. Its viscosity at room temperature was between

600 cps to 700 cps. The Glass transition temperature, T_g of the epoxy was 82 °C measured following the ASTM D-4065 guidelines. The minimum tensile strength of the epoxy was 50.0 MPa (7.2 ksi), its ultimate elongation capacity was 5%, and it had a tensile modulus of elasticity of 3.18 GPa (461 ksi) measured according to the ASTM D-638 standard provisions.

3.2.2 Specimen preparation

Six identical size wooden frames were constructed and used to cast the concrete beams using the same ready mix concrete batch. Geometrical details of beams were selected by reviewing previous research and also considering the lab limitations. In Table 3.2, geometric details of the specimens are shown. Beams were overdesigned for flexural capacity and transverse steel was used at only one side of the beams to ensure that a shear failure will occur at the other side. In Fig. 3.1, the load scheme and configuration of the transverse and longitudinal steel are shown. The rectangular cross-section of beams has overall dimensions of 150 × 250 mm (5.9 × 9.8 in.).

The beams were smoothed at their edges to eliminate stress concentration effects and to improve the FRP/concrete bondline properties. Two control (not strengthened) RC beam specimens were labeled As-built-1 and As-built-2. All other beam specimens were retrofitted using parallel FRP schemes on two sides for each beam. Two beams were retrofitted using a hybrid composite scheme of Carbon-Glass and Carbon-Aramid (B-Π-CG, B-Π-CA). One beam was retrofitted using a unidirectional carbon fibre fabric (B-I-

C) with an inclination $\alpha = 90$ degrees to ensure interception of diagonal cracks. The last beam was retrofitted using $+45^{\circ}/-45^{\circ}$ glass fibres (B-III-GG). Dimensions and typical laminates details for the shear strengthening of all retrofitted RC beam specimens are shown in Fig. 3.2.

The concrete surface was prepared and made smooth and even before attaching the fibre-reinforced polymer sheets. Small voids on the surface of the RC beams were filled using ordinary cement grout. Using a two-component resin epoxy, the concrete/FRP bondline achieved adequate mechanical properties. Hence, in the numerical modeling, a perfect bond between the concrete and FRP sheets was assumed. Epoxy was combined with the FRP fabrics using the wet-layup method. Approximately 0.8 pounds of epoxy per 1.0 pound of fabric was used.

3.2.3 Loading apparatus and testing

The mechanical load was applied using a 250 kN capacity hydraulic jack. The various signals from the instruments were captured and monitored using an automated data acquisition system. Vertical displacements under the applied load were measured using linear variable differential transducers (LVDTs). Strains in the FRP sheets were also measured in three different directions to be able to calculate deformations in the crack zones and to compare the ultimate strain at failure and the effect of transverse fibres on the ultimate strain of the main vertical fibres. In Fig. 3.3, the instrumentation of the RC beam specimens is illustrated.

To apply quasi-static cyclic loading and to divide the load between two points, a rigid steel beam was utilized on top of the concrete beam. The steel beam was attached to the concrete beam using two steel plates with dimensions of 203×76×38 mm (8.0×3.0×0.5 in.) at the top and bottom of the beams. The steel plates were connected to each other using eight steel rods with a diameter of 12.7 mm (0.5 in.). In Fig. 3.4, the experimental set up and loading cross-section are shown. To prevent the vertical displacement of beams in two directions at the supports, two steel beams were attached vertically on top of the RC beam and connected to the strong floor. The loading was applied in a deflection control manner. The first cycle of loading had a deflection of ±3 mm in the actuator, so that the beam experiences both compression and tension. The actuator displacement frequency was set at 0.005 Hz throughout the test. For every other cycle, the amplitude of the actuator displacement had an increment of 3 mm both in the tension and compression zone. Each loading cycle was repeated three times to ensure a stable behaviour.

3.3 Numerical Analysis

The finite element program ABAQUS (version 6.6, 2006) was used to model the behaviour of the RC beams under monotonic loading up to failure and to predict their ultimate load capacity. Since the experimental loading was quasi-static, monotonic loading can reasonably simulate the overall behaviour of the beam. For instance, the force-displacement diagram of the beam in the monotonic state is the envelope of the quasi-static diagram in the compressive section. Five beams, one control RC beam and

four beams with different externally bonded FRP layers were considered in the numerical analysis.

3.3.1 Materials Properties and Constitutive Models

The materials used in the numerical analysis are concrete, steel and FRP. The constitutive models for the behaviour of these materials are presented below:

3.3.1.1 Steel

The steel rebar is assumed to have an elastic perfectly plastic behaviour as shown in Fig. 3.5. In ABAQUS, the steel reinforcement is treated as an equivalent uniaxial material smeared throughout the element section and can be defined alone or embedded in oriented surfaces. In order to properly model the constitutive behaviour of the steel reinforcement, the cross-sectional area, spacing, position and orientation of each layer of steel bar within each element needs to be specified. In the present model, two surface sections were defined for the top and bottom rebars with one layer of rebar in each surface. Steel ties were defined in surface sections using the same approach. These surfaces were embedded in the concrete section. Material parameters for steel rebars were obtained from experimental data as discussed earlier in section 3.2.1.

3.3.1.2 Concrete

Damage plasticity was used to model the concrete. It is a continuum, plasticity-based damage model for concrete, which uses concepts of isotropic damage elasticity in

combination with isotropic tensile and compressive plasticity to represent the inelastic behaviour of concrete. The model assumes that the main two failure mechanisms are tensile cracking and compressive crushing of the concrete material. Beyond the failure stress, the formation of micro-cracks is represented macroscopically with a softening stress-strain response, which induces strain localization in the concrete structure.

The inputs for the model are the compressive and tensile stresses of the concrete along with damage parameters in terms of plastic strains. The concrete strain, ε_o corresponding to the peak stress, f_c' is usually in the range of 0.002–0.003. A representative value suggested by the ACI Committee 318 and used in the analysis is ε_o = 0.003. For the compressive behaviour of concrete, the stress–strain relationship proposed by Saenz (1964) was used, and the softening branch was assumed to be linearly decreasing from 23 MPa to 2 MPa (from ε_c = 0.003 to ε_c = 0.01) (Fig. 3.6).

$$\sigma_c = \frac{E_c \varepsilon_c}{1+(R+R_E-2)\left(\frac{\varepsilon_c}{\varepsilon_o}\right)+(2R-1)\left(\frac{\varepsilon_c}{\varepsilon_o}\right)^2+R\left(\frac{\varepsilon_c}{\varepsilon_o}\right)^3} \tag{3.1}$$

Where

$$R=\frac{R_E(R_\sigma-1)}{(R_\varepsilon-1)^2}-\frac{1}{R_\varepsilon}, R_E=\frac{E_c}{E_o}, E_o=\frac{f_c'}{\varepsilon_o} \tag{3.2}$$

and $R_\sigma = 4, R_\varepsilon = 4$.

The tensile strength of concrete is typically 8-15% of its compressive strength. A value of 2.5 MPa measured from the splitting tensile test was used. The softening part of the tensile stress-strain curve is modeled by two lines as shown in Fig. 3.6.

Plasticity parameters were defined in ABAQUS. The damage plasticity model in ABAQUS requires the following parameters to be defined: yield and failure surfaces (Table 3.3.). In Table 3.3, f_{bo} is the biaxial compressive strength, and f_{co} is the uniaxial compressive strength used to define the yield and failure surfaces. K is the ratio of the second stress invariant on the tensile meridian, to that on the compressive meridian. The model also needs damage evolution in terms of plastic strain; this data was obtained from report by Jankowiak et al. (2005). Moreover, it was assumed that concrete recovers 95% of its strength in compression after initial damage.

3.3.1.3 FRP

FRP layers were modeled using membrane elements. FRP was considered to be orthotropic and elastic. Since FRP layers generally behave differently in three orthogonal directions, an orthotropic elastic constitutive model was used. It was also assumed that non-linear behaviour of FRP is negligible. Since no bending was assumed for FRP layers, simple planar membrane elements were used. Bonding between FRP and concrete was simply modeled by constraining membrane elements to brick elements. The material parameters for FRP sheets were obtained from experimental data.

3.3.2 FEM model

Since the RC beams were not symmetric, they had to be modeled over their entire length. Concrete was modeled using ordinary 8-noded solid brick elements with 3×4×50 mesh ties. Steel rebars were modeled using surface elements, while FRPs were modeled by membrane elements. Explicit dynamic approach was selected and the problem was solved in a displacement control manner. In order to simulate quasi-static loading, a one-*cm* displacement was applied in 10 seconds. Since modeling was based on monotonic loading, two beams were modeled for each experimental beam, one for compressive loading and the other for tensile loading (Fig .3.7).

3.4 Results and Discussion

3.4.1 Experimental

In all tests, no major cracks were observed until near the ultimate load. However, as illustrated in Fig. 3.8 the effect of stress concentration at the steel plates contact surface with concrete led to separation of some concrete due to the bearing stress before failure occurred. As expected, failure occurred at the side of the beam with no transverse steel. Beams had lower deflection and higher force for the same amount of actuator displacement in the compression zone with respect to the tension zone. This shows the importance of the shear span ratio and longitudinal rebar effect on the structural behaviour of concrete beams, because except for the longitudinal steel rebar sizes, the beams were symmetric at the top and bottom. Concrete crashed at the compression zone where no steel ties were used, and longitudinal steel rebars did not yield throughout the

experiment. Loading was done using incremental amplitudes of the actuator displacement (±3mm; ±6mm; etc.). Each cycle, except the last one, was repeated thrice to model the effect of repetitive loading. Figure 3.9 shows the cyclic loading pattern versus loading time, while, Fig. 3.10 shows the displacement versus time at the center of all beams during the testing. Figure 3.11 shows the load-deflection (P/δ) hysteretic curves at mid span of the beam specimens. The ductility of all specimens was improved slightly after being retrofitted. The maximum compressive and tensile values of strains at different locations, and load versus deflection values were summarized in Table 3.4.

The control beams without FRP sheets had an average ultimate failure load of 91.6 kN (20.6 kips) in tension, and 145.7 kN (32.1 kips) in compression, respectively (values of the ultimate load capacity of these two beam specimens were comparable with only 5% difference). Shear cracks developed suddenly at the maximum shear span at about 45° inclination, followed by a sudden shear failure in the weak side of the beam specimen as illustrated in Fig. 3.12. Failure occurred at the second cycle of the last amplitude of actuator movement (±12mm). Some small cracks became visible at the first cycle of the last amplitude, but no major cracks were observed.

Various retrofit protocols consisting of four strips of i) carbon/epoxy, ii) carbon-glass/epoxy, and iii) carbon-aramid/epoxy hand layup systems, were applied to the treated shear span concrete surfaces of beams designated as B-I-C, B-П-CG and B-П-CA, respectively. Although the main strengthening material, CFRP, is brittle in nature, previous work has shown that increasing the ductility of RC beams in which CFRP has

been used for strengthening can be achieved [12]. Beam B-I-C failed at the first cycle of the ±15mm actuator load, while beams B-П-CG and B-П-CA failed at the actuator load of ±18mm. Beam B-II-CA achieved the best performance. Its ultimate compression capacity increased by 35% compared to the measured value for the control RC beam specimens. The ultimate failure mode of the retrofitted specimens was a typical concrete crushing. Shear cracks initiated at the un-strengthened areas of the shear span. The failure angle changed from 45 degrees for the control beam to 55 degrees, and the third FRP sheet got separated from the RC beam along with a relatively thick concrete layer. Failure was brittle and accompanied by a loud sound. By comparison of the maximum compression and tension values of strains of beams retrofitted by hybrid FRP sheets (B-II-CG, B-II-CA) with the observed values for beam B-I-C which had only unidirectional carbon fibres, it can be concluded that the hybrid application of FRP sheets increased the chance of rupture at the main fibres and allowed them to contribute more shear capacity. Figure 3.13(a, b) illustrates the failure of beam specimens B-I-C and B-П-CG.

A repair technique consisting of four strips of glass-glass/epoxy hand layup system was applied to the treated shear span concrete surfaces of the beam designated as B-III–GG. Bidirectional glass fibres in the -45° and +45° directions were applied for retrofitting this beam. The ultimate capacity of the repaired beam was 163.8 kN (36.1 kips) in compression and 94.3 kN (20.8 kips) in tension, which indicates that the glass-glass/epoxy hand layup system effectively improved the shear strength of the original beam by up to 12% in compression. The failure angle was approximately 45 degrees and the third FRP sheet ruptured. The lower thickness and strength of glass FRP sheets

compared to that of the carbon FRP sheets used for the other beams allowed fibres to reach their maximum strain capacity and experience rupture instead of de-bonding. Figure 3.13c illustrates the shear failure of the B-III-GG beam specimen.

3.4.2 Numerical model

3.4.2.1 As-built shear beam specimens

The first model predicted cracking load in compression for the original beam was 43.4 kN, which is 1% lower than the corresponding experimental value (44.0 kN). Figure 3.11a shows that in compression the post cracking behaviour, i.e. when cracks propagate in the beam and the beam's response becomes non-linear, is well described by the numerical model, since the numerical values form the envelope for the experimental values and the overall error is negligible. The ultimate load in compression was estimated to be 173 kN, which is 20% larger than the observed value. This appears to be due to fatigue loading and the existence of micro-cracks in the original specimen. These aspects were not considered in the FEM model. The maximum displacement in the tension side was 8.3 mm, which is 11% higher than the experimental value of 7.4 mm. The predicted tensile cracking load was 27.5 kN, which is 10% less than the corresponding experimental value. The predicted ultimate load in tension was 82.3 kN, which is 10% less than the experimental value of 91.6 kN. The cracking pattern in compression is illustrated in Fig. 3.14a which shows that the main cracks are due to shear and appear at 45 degrees in the beam side where there were no ties. Moreover, some flexural cracks appeared, which were small and not visible in Fig. 3.14a.

3.4.2.2 Specimens with CFRP at main direction

Carbon/epoxy repair evaluation Specimen (B-I-C)

In compression, the model prediction is in reasonable agreement with experimental data in the elastic range. The cracking load was 36 kN, which is 15% lower than the observed value. The ultimate load was 173 kN and the maximum displacement was 9.5 mm, which are 4% and 29% larger than the corresponding experimental values (Fig. 3.11b). In tension, the model prediction was in general agreement with the experimental data. The cracking load was 36 kN which is 10% above the measured value. The ultimate load was 86 kN, and sudden collapse was observed when the steel rebars started to yield. Figure 3.14b shows that the cracking pattern was changed compared to that of the As-built beam due to the existence of external FRP sheets and a wider area of concrete has cracked compared to that of the control RC beam, which shows that the external FRP increased the ductility. It can also be observed that the area between the second and third FRP sheets was critical since more cracks were observed in this region.

Carbon/Glass/Epoxy and Carbon-Aramid/Epoxy retrofit scheme (Specimens B-II-CG, B-II-CA)

Model predictions for these beams were in a very good agreement with experimental data in the elastic range. The post cracking trend agrees well with experimental observation in the compression and tension zones (Fig 3.12. (c, d)). It can be observed in Fig 3.14. (c, d)

that, FRP has changed the cracking pattern in the beams compared to that of control beam. FRP increased the cracking area, and the zone between the second and third FRP sheets was critical area and failure happened there. This observation is compatible with experimental observations where the third FRP sheet was debonded from the beam. Moreover, these beams experienced higher maximum strain compared with that of B-I-C. The maximum strain experienced by FRP sheets to retrofit beams B-II-CG and B-II-CA were 28% and 37% higher compared to that of B-I-C at failure. This experimental and numerical observation proves that hybrid application of FRP sheets and application of glass and aramid fibres at transverse direction has significant effect on shear capacity contributed by FRP sheets. Beside shear cracks, some flexural cracks were also observed at the bottom of the beams.

3.4.2.3 Glass-Glass/epoxy repair evaluation (Specimen B-III-GG)

In compression, the model predictions were in a good agreement with the corresponding experimental data in elastic range. The cracking load was 36 kN, which is 16% below the measured value. The post-cracking trend was also compatible with experimental data (Fig. 3.11e). Figure 3.14e shows the strain distribution and crack pattern for beam specimen B-III-GG. The numerical analysis continued beyond experimental observation, considering the stresses induced in the FRP in Fig. 3.15, the beam would have failed at an ultimate load of 198 kN, which is 20% above the corresponding experimental value. The model predicts the rupture of the third FRP sheet at the weak side of the beam, which is compatible with experimental observation. In tension, the model predicted the elastic

behaviour very well; the cracking load was 35 kN, which was the same as the measured experimental value, the post cracking trend was also in excellent agreement with experimental observations. The ultimate load was 86.4 kN, which is 8% below the corresponding experimental value.

3.4.3 Hybrid FRP effect

Debonding of FRP sheets does not allow such sheets to contribute their maximum capacity to the ultimate shear load of RC beams. Generally, the application of most mechanical anchors or bolts to prevent this debonding has not been successful, mainly because of stress concentration effects (Barnes *et al.* 2006). The present study shows that the hybrid application of FRP sheets increases the confinement of fibres in the main direction, and consequently the entire FRP laminate shows better stress-strain behaviour and debonding of the FRP sheets can be postponed.

Research was done by Sakar *et al.* (2009) on the effect of bidirectional CFRP sheets for retrofitting reinforced concrete (RC) beams under cyclic loading. They concluded that adding a horizontal ply in the 0^{o} direction helped to increase the shear friction strength and hindered the crack development at the tension face. Moreover, hybrid application of FRP sheets helped to increase the contribution of the concrete to shear resistance by postponing the crack propagation at the concrete surface.

The ultimate shear resistance of beams with carbon fibres at main direction was compared to the nominal shear resistance predicted by the Colotti model (2004) to clarify the effect of hybrid application of FRP sheets. As expressed before current codes and models ignore effect of fibres at transverse direction. The ultimate shear capacity in compression of all of tested beams at this research with carbon fibres at main direction (B-I-C, B-II-C, B-II-CA) was calculated as 159.8 kN using Colotti model (eq. 2.17 to eq. 2.23). As observed also by Mosallam et al. (2007), the Colotti model gave relatively accurate prediction for the beam retrofitted by unidirectional FRP sheets as external reinforcement (B-I-C) with an error of 4% compared to 166.2 kN experimental observation. While, errors for the beams with hybrid FRP sheets (B-II-CG, B-II-CA) are 12% and 27%, respectively, compared with 178.4 kN and 196.8 kN experimental results.

In addition to ignoring the effect of the transverse fibres, it is not guaranteed that carbon fibres, concrete and/or steel stirrups will make use of their maximum strength at the failure of the beam. Common design codes, however, still use the relative contribution of these materials to calculate the total shear strength. It should be also pointed out that the mechanisms by which concrete, steel and FRP contribute to the overall shear capacity interact with each other.

More recently, Galal *et al.* (2009) proposed a new mechanical anchoring method which is claimed to eliminate the debonding of epoxy-bonded carbon fibre-reinforced polymer (CFRP) sheets, thus utilizing the full capacity of dry carbon fibre sheets. In this method, dry carbon fibre sheets are wrapped around and bonded to two steel rods. Then the rods

are anchored to the corners of the web-flange intersection of a T-beam with mechanical bolts. This makes a U-shaped dry carbon fber jacket around the web, which increases the shear strength of the T-beam using the the higher tensile strength and modulus of elasticity of the dry CF compared to that of the composite CFRP. This method is more labor intensive compared to the application of epoxy for bonding FRP to concrete. Moreover, it is generally applicable for beams with T-sections.

3.5 Concluding Remarks

The objective of the experimental program and numerical analysis in the present study was to evaluate the ultimate shear strengths and to identify the modes of failure of a control RC beam, along with that of unidirectional and hybrid FRP retrofitted beam specimens under quasi-static cyclic loading. The following conclusions can be drawn based on the experimental and numerical work discussed in this chapter:

(i) Hybrid FRP sheets showed a better performance in increasing the ultimate shear capacity of RC beams compared with that of unidirectional carbon fibre-retrofitted beam specimens. The co-existence of other fibres like glass or aramid in the transverse direction allowed carbon fibres in the main direction to get closer to its ultimate strain capacity.

(ii) As shown in previous work (Colotti *et al.* 2005), RC beams with thicker two sides laminated FRP sheet are less likely to undergo failure by rupture of the FRP sheet. Beam B-III-GG, which had glass with lowest thickness as

external FRP, was the only specimen which had FRP rupture at failure. The numerical analysis confirmed this behaviour.

(iii) Design codes and current models need to incorporate provisions that consider the effect of hybrid FRP sheet applications and the interaction between the shear capacity contributed by the FRP sheets and that by concrete.

(iv) The Colotti model provides accurate estimation of the shear capacity of RC beam specimens retrofitted using unidirectional fibres. However, it had a considerable error in calculating the shear capacity of beams retrofitted with hybrid FRP sheets.

(v) Different structural behaviour of RC beams in tension and compression loading confirmed the importance of *a/d* and the longitudinal rebar effect on the shear behaviour of RC beams. This aspect has been generally ignored by several design codes and needs further research.

(vi) Fatigue and repetitive loading affect the ultimate capacity of RC beams through the formation of micro-cracks in concrete and weakening of the bonding layer between concrete and the external FRP sheets. This effect needs to be quantified and accounted for in cyclic loading.

Table 3.1: Details of FRP strengthened RC beam specimens

Specimen	FRP	t_f, mm	E_{f1}, GPa	f_{fu1}, MPa	E_{f2}, GPa	f_{fu2}, MPa	α , degree
B-I-C	Carbon	1.00	87.3	925	3.2	72.4	90°
B-II-CG	Carbon-Glass	1.00	95.8	986	49.3	270.2	0° /90°
B-II-CA	Carbon-Aramid	1.00	72.4	876	61.5	290.3	0° /90°
B-III-GG	Glass-Glass	0.25	19.3	309	19.3	309.0	-45° /+45°

Table 3.2: Details of RC beam specimens

	b, mm	*d*, mm	Tension Steel, mm	ρ	Compression Steel, mm	ρ'	Stirrup, mm	Stirrup, Spacing, mm	ρ_w	*a/d*	FRP
uilt-1	150	220	2φ11	0.003	3φ16	0.009	6	150	0.003	2.5	-
uilt-2	150	220	2φ11	0.003	3φ16	0.009	6	150	0.003	2.5	-
I-C	150	220	2φ11	0.003	3φ16	0.009	6	150	0.003	2.5	90° C
I-CG	150	220	2φ11	0.003	3φ16	0.009	6	150	0.003	2.5	90° /0° C-G
I-CA	150	220	2φ11	0.003	3φ16	0.009	6	150	0.003	2.5	90° /0° C-A
I-GG	150	220	2φ11	0.003	3φ16	0.009	6	150	0.003	2.5	-45° /+45° G-G

* C = carbon, G = glass, A= aramid

Table 3.3: Damage parameters in plasticity model used for concrete

Dilation angle	Eccentricity	f_{bo}/f_{co}	*K*	Viscosity parameter
40	10	1.16	0.667	0

Table 3.4: Experimental results of shear capacity of FRP retrofitted RC beam specimens

nen	Compression					Tension				
	Force, (kN)	Displacement , (mm)	Strain			Force (kN)	Displacement (mm)	Strain		
			0	45	90			0	45	90
ilt	145.7	7.3	-	-	-	91.6	8.2	-	-	-
C	166.2	6.9	0.003	0.010	0.009	88.8	9.82	0.002	0.006	0.005
CG	178.4	9.6	0.005	0.012	0.011	92.8	13.2	0.003	0.005	0.005
CA	196.8	11.9	0.007	0.014	0.012	94.8	16.5	0.003	0.005	0.005
GG	163.8	6.2	0.010	0.017	0.013	94.3	13.4	0.002	0.007	0.006

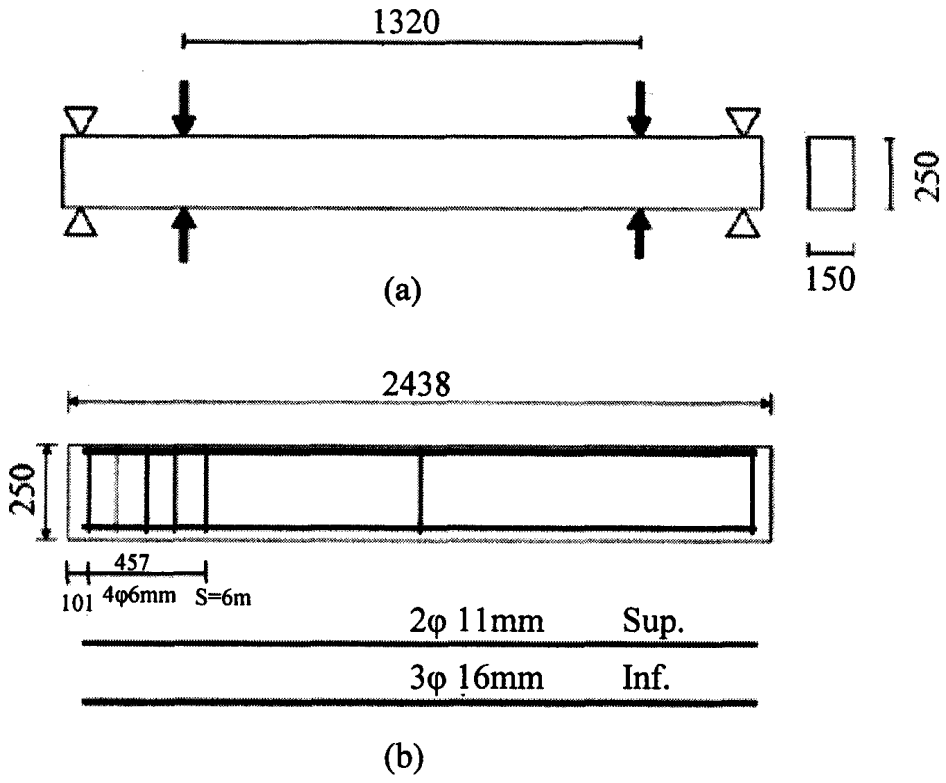

Fig. 3.1: Load scheme and configuration of transverse and longitudinal steel.

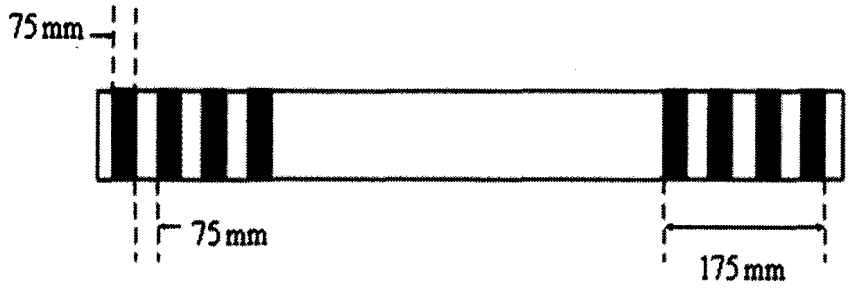

Fig. 3.2: Typical shear strengthening details.

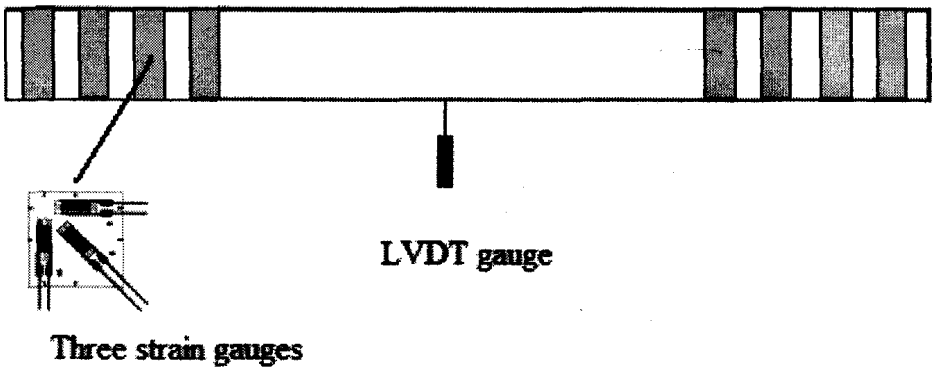

Fig. 3.3: Instrumentation of strain gauges at 0/45/90 degree on the third FRP sheet and location of LVDT gauge.

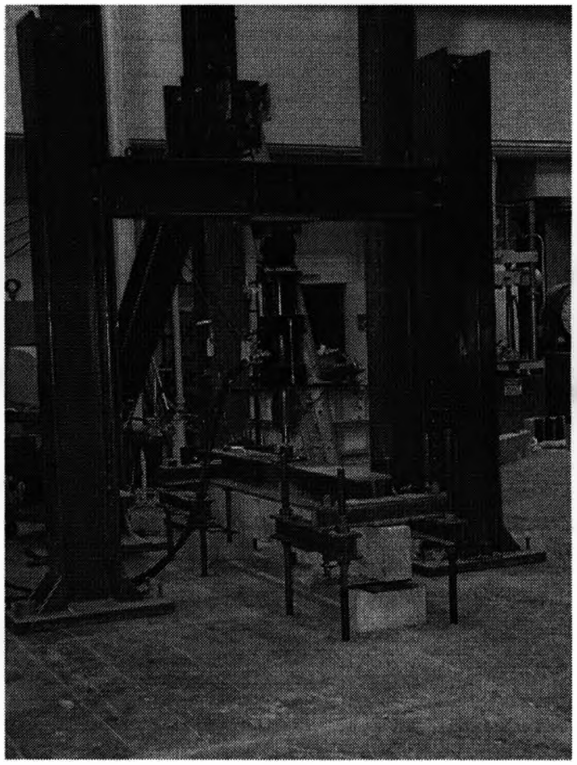

(a)

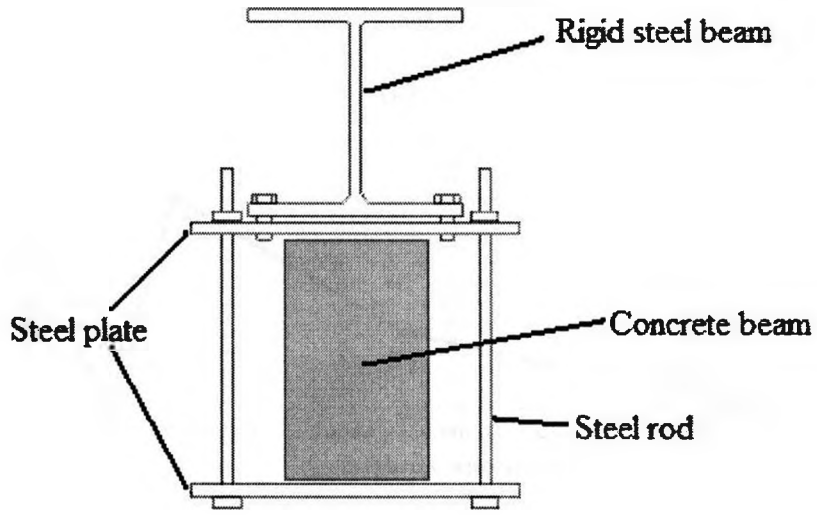

(b)

Fig. 3.4: (a) Experimental set up, and (b) loading cross-section.

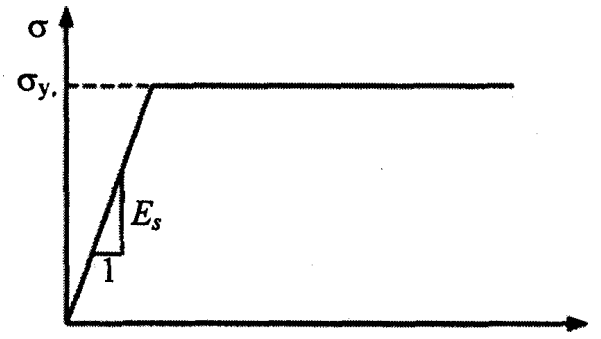

Fig. 3.5: Stress-strain relationship for steel.

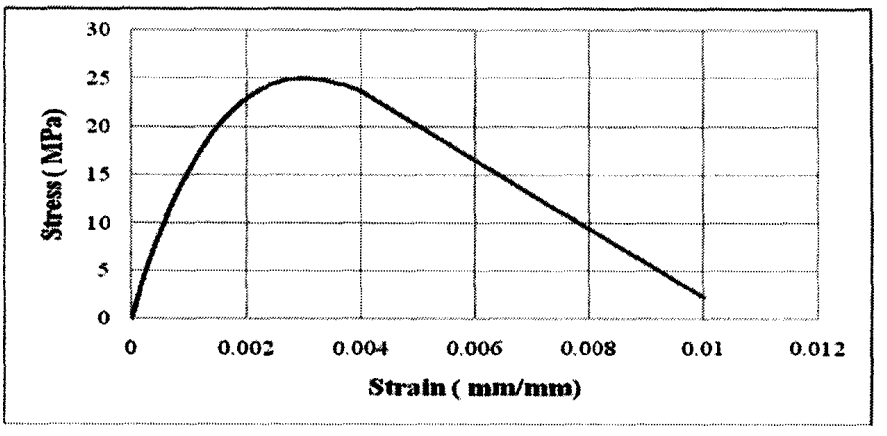

(a)

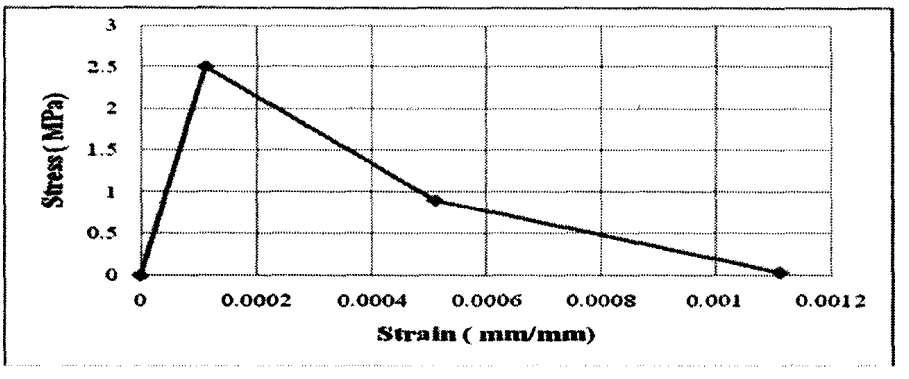

(b)

Fig. 3.6: (a) Compressive behaviour of concrete used in FEM model, and (b) Tensile behaviour of concrete used in FEM model.

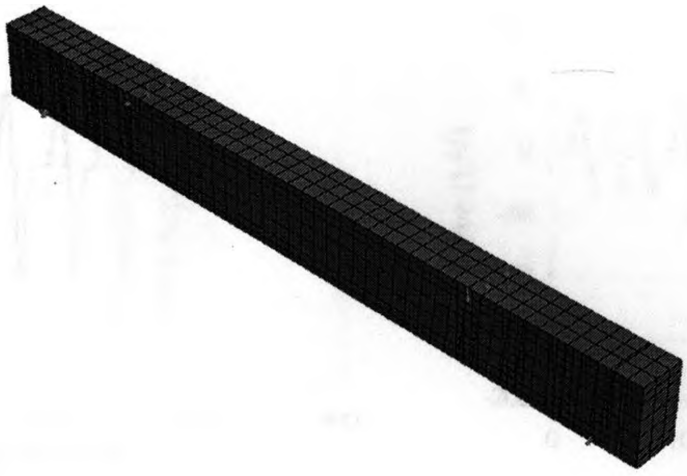

Fig. 3.7: FEM model of RC beam specimens.

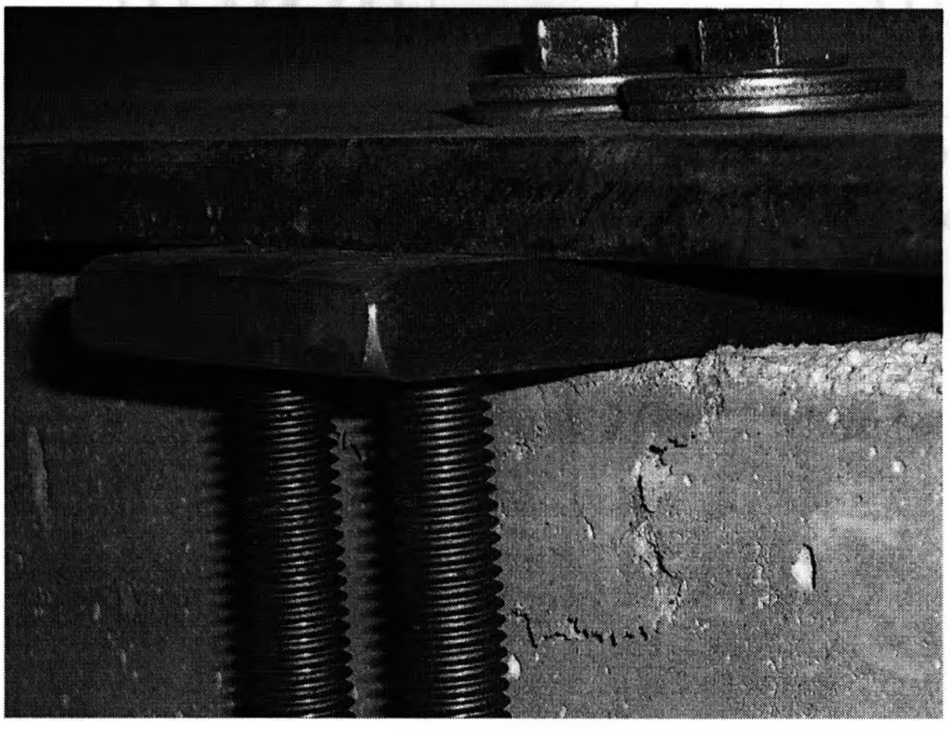

Fig. 3.8: Bearing stress effect on contact surface of steel and concrete.

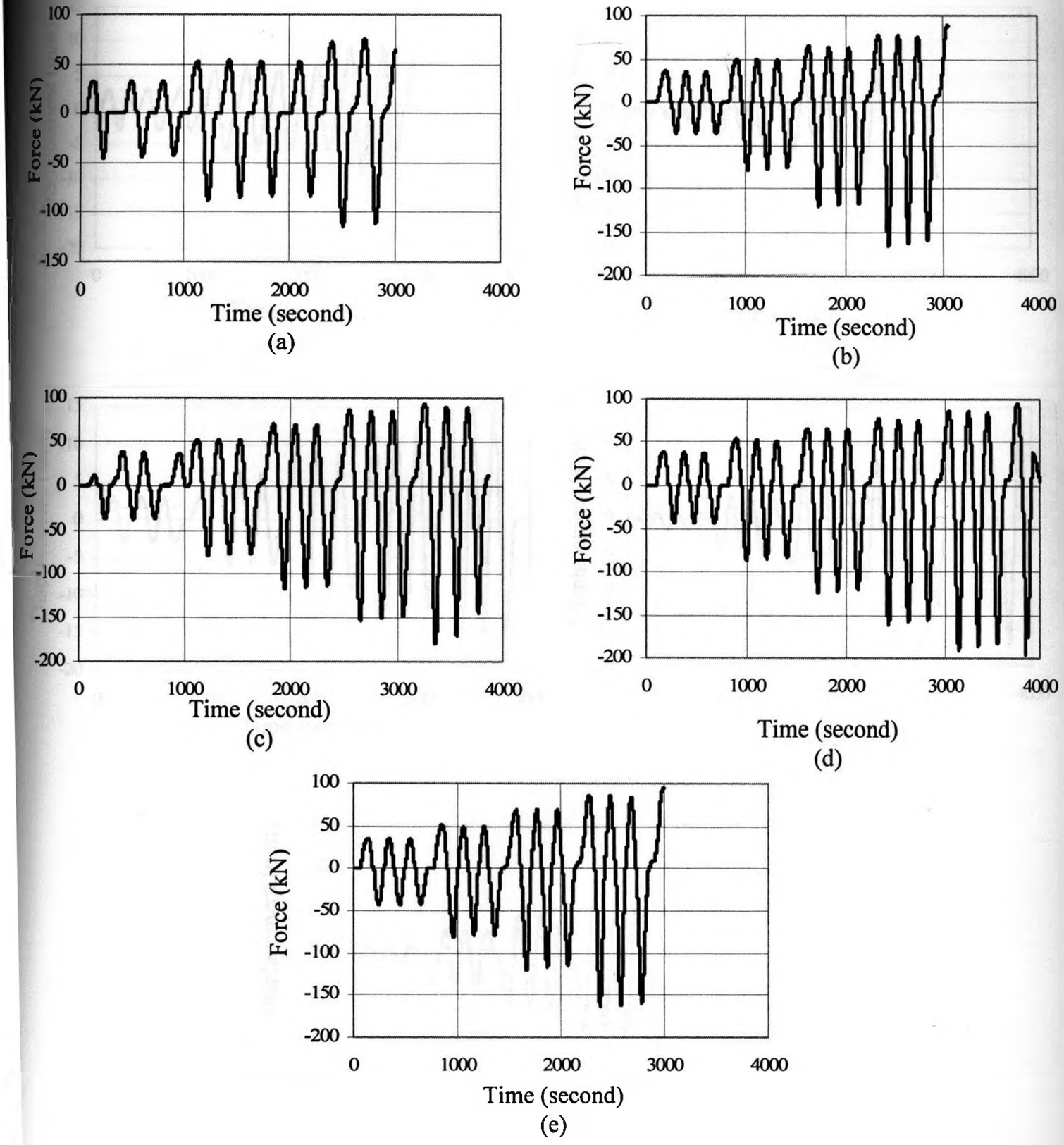

Fig. 3.9: Force – time diagram for (a) control RC beam specimen, (b) B-I-C specimen, (c) B-II-CG specimen, (d) B-II-CA specimen, and (e) B-III-GG specimen, respectively.

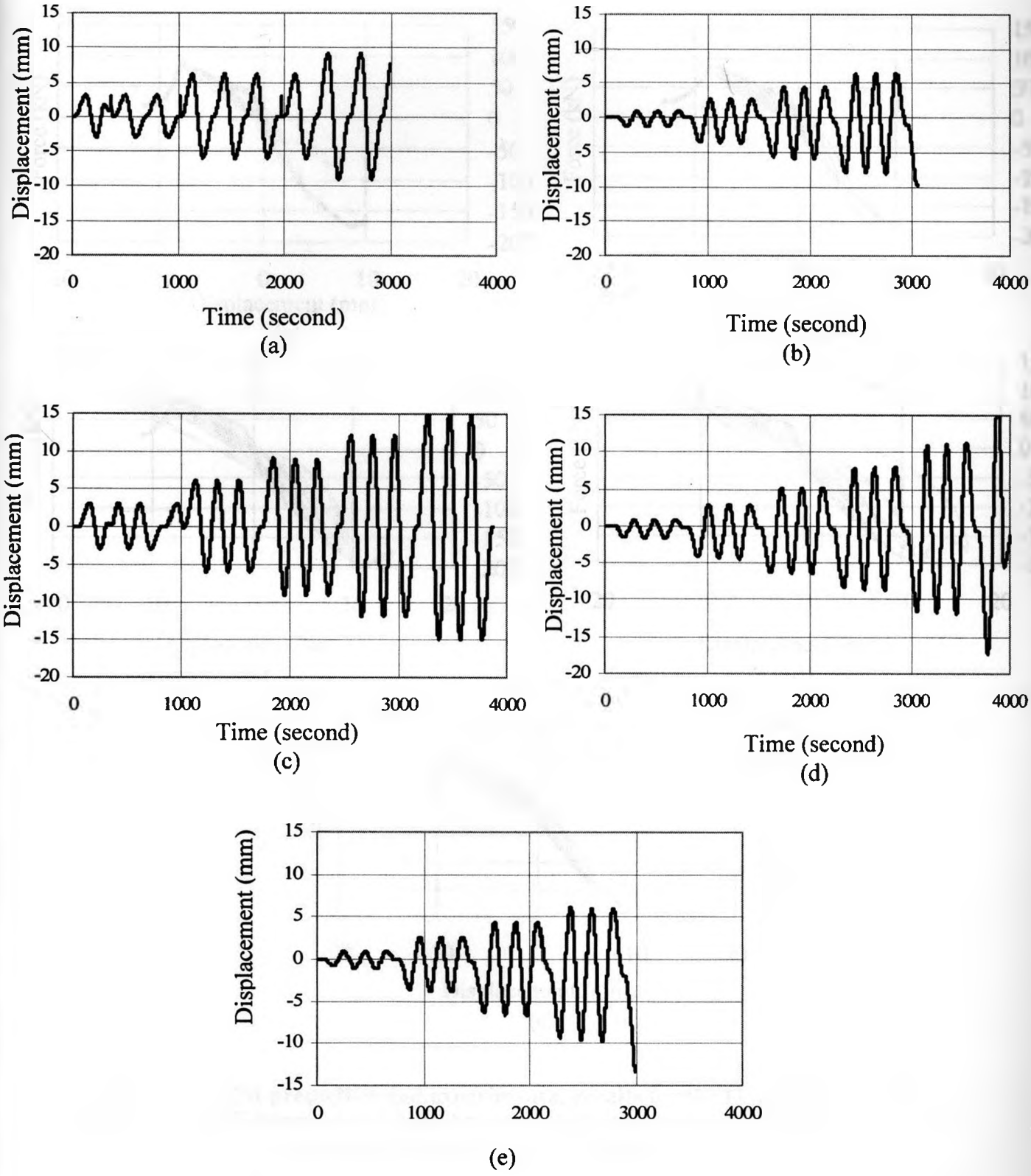

Fig. 3.10: Displacement at the center of the beam versus time diagram for (a) control RC beam specimen, (b) B-I-C specimen, (c) B-II-CG specimen, (d) B-II-CA specimen, and (e) B-III-GG specimen, respectively.

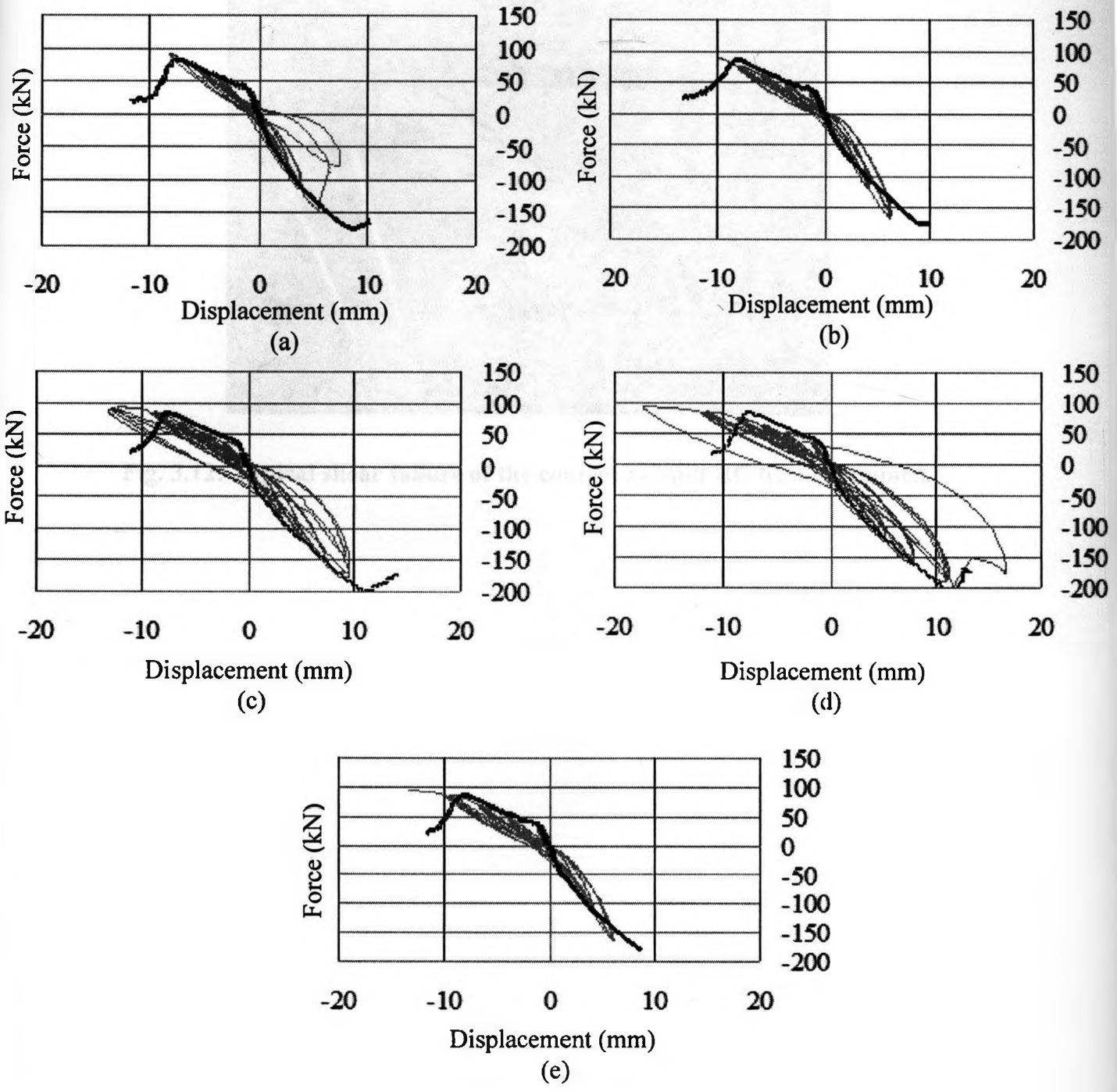

Fig. 3.11: FEM prediction and experimental results for the force-displacement behaviour of RC beams, a) As-built beam, b) B-I-C, c) B-II-CG, d) B-II-CA, and e) B-III-G. (▬▬ Numerical, ____ Experimental).

Fig. 3.12: Typical shear failure of the control as-built RC beam specimen.

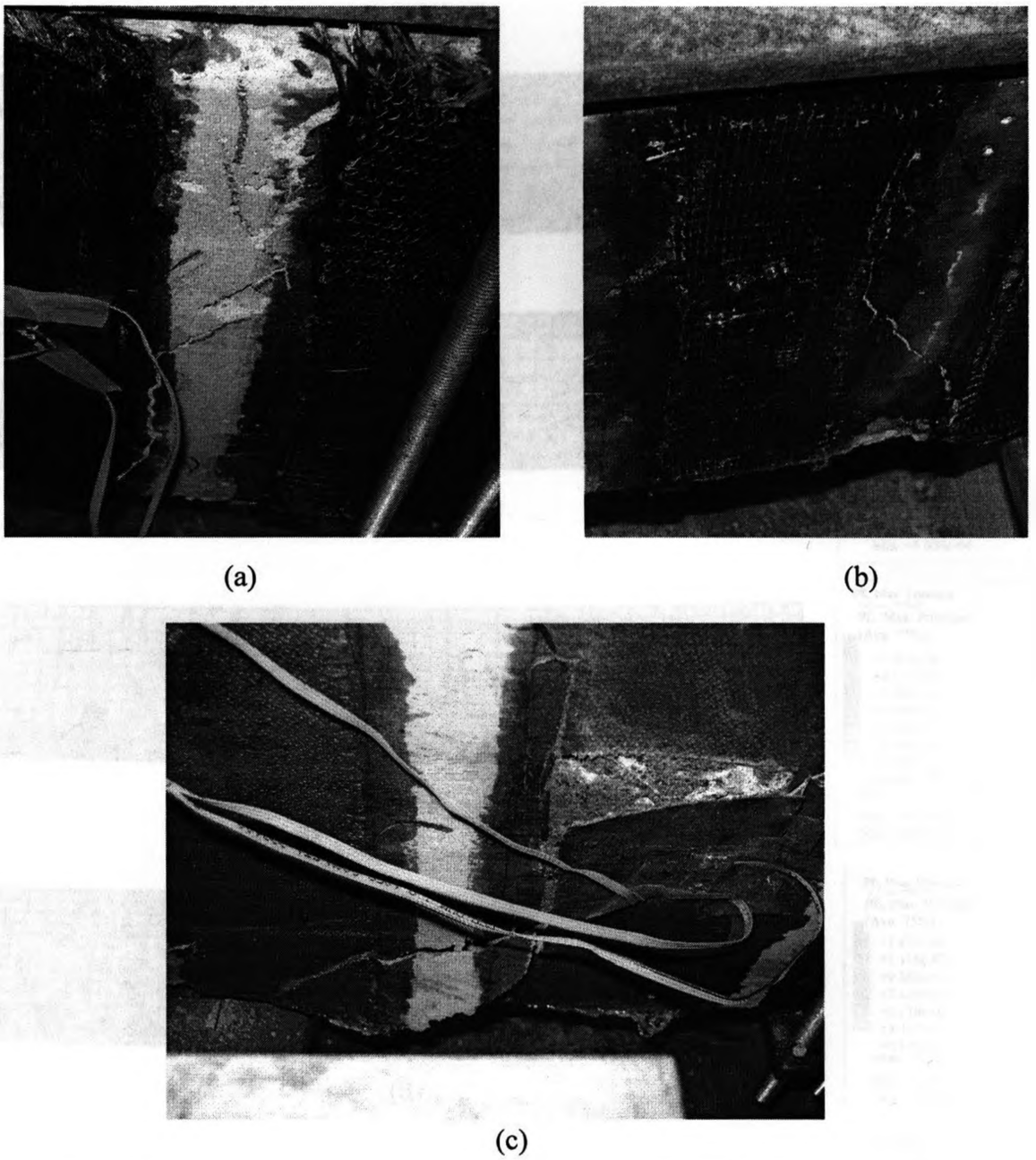

Fig. 3.13: Shear failure and crack pattern for (a) B-I-C specimen, (b) B-П-CG specimen, and (c) B-Ш-GG specimen.

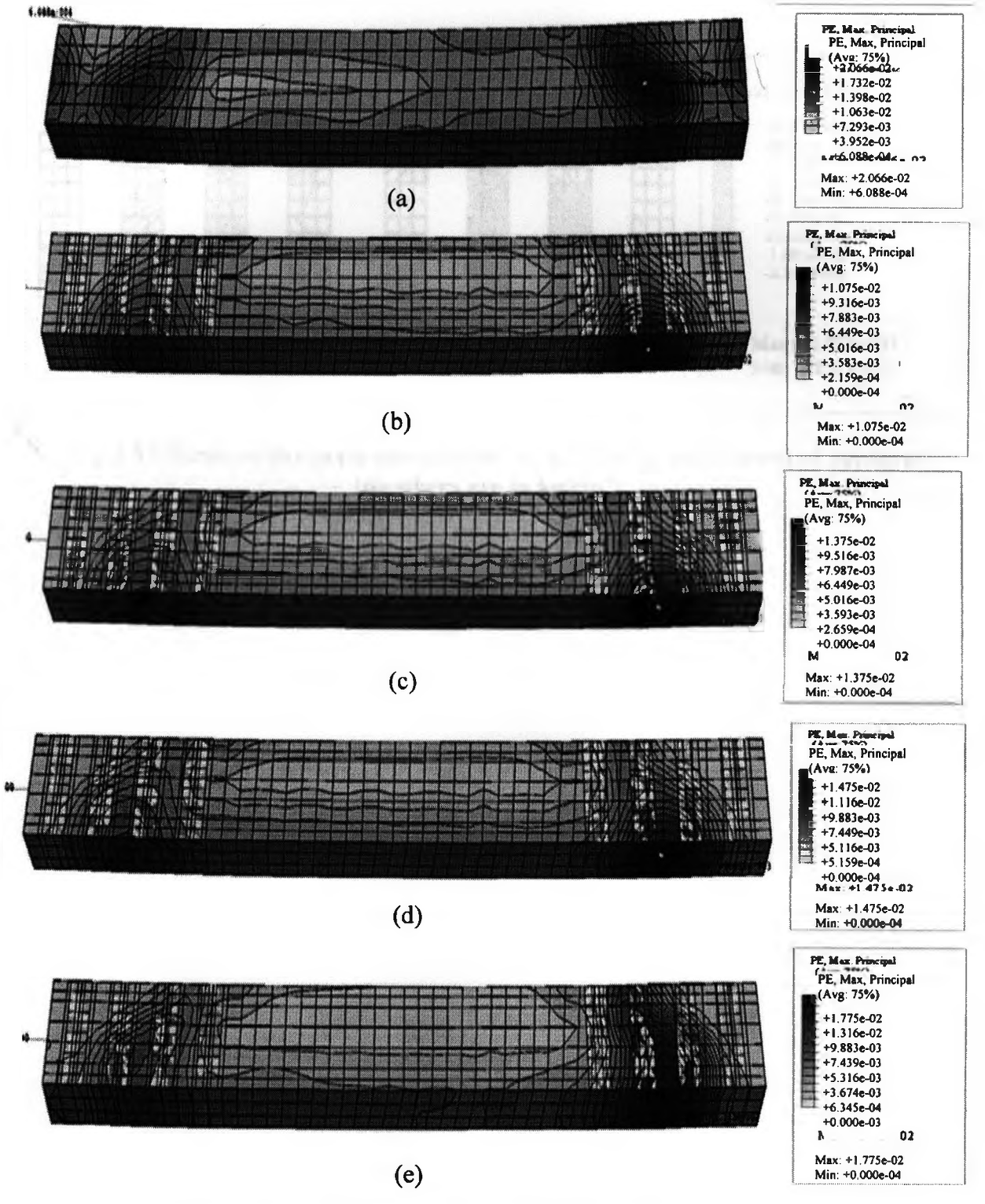

Fig. 3.14: FEM results for the maximum principal plastic strain contour for RC beam specimens, a) as-built beam, b) B-I-C, c) B-II-CG, d) B-II-CA, and e) B-III-G.

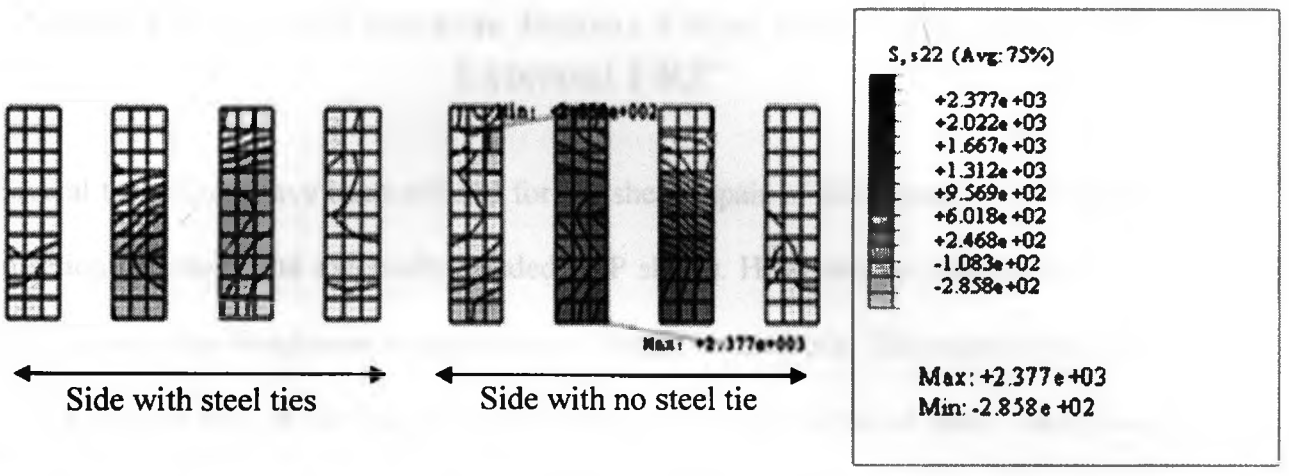

Fig. 3.15:Stress in the main direction of the FRP sheet at the onset of rupture (numbers are in kg/cm^2).

CHAPTER 4

Shear Repair of Concrete Beams Using Epoxy Injection and External FRP[2]

Several techniques have been utilized for the shear repair of RC beams including epoxy injection of cracks and externally bonded FRP sheets. However, not much research has been done on the simultaneous application of these two methods. This experimental study at this chapter aims at investigating performance of beams repaired using simultaneous epoxy injection and external FRP sheets under monotonic loading. Three severely damaged beams were repaired using epoxy injection and unidirectional carbon fibre polymer (CFRP) sheets. The repairing method, FRP type, and wrapping scheme were test variables investigated in this experimental program. Test results show that the repair schemes imparted significant mechanical improvements in terms of ultimate shear capacity and ductility. The simultaneous application of epoxy injection and externally bonded FRP sheets was found to be highly effective repair technique. Failure type of beam is also highly dependent on application scheme of external FRP sheets.

4.1 Introduction

Repair and rehabilitation work for concrete structures can broadly be classified into two main categories: (i) repair in which the damage due to deterioration and cracking is corrected to restore the original structural capacity, and (ii) repair that is necessary to

[2] A version of this chapter has been submitted for review to ACI Materials Journal

strengthen the structural capacity of a member whose load carrying capacity has either been inadequate or whose strength has been severely impaired (Al-Gadhib et al., 2003).

Epoxy resins are commonly used repair materials that generally have very good bonding and durability characteristics (ACI Committee 546R-96, 1996). Calder and Thompson (1998) reported that the overall structural performance of RC slabs repaired using epoxy resin injection performed best compared to other repair materials such as polyester and methyl methacrylate resins. The stiffness of the cracked slabs in this study was about one quarter of that of the un-cracked slabs and the repairs reinstated only about half of the stiffness loss. According to Minoru et al. (2001), the bond between concrete and the injection material is very critical; a good bond may restore the original stiffness of the repaired material and prevent further penetration of chloride ions and water. The crack should also be clean and dry prior to injection. Epoxy injection is not applicable if the cracks are actively leaking or cannot be dried out, unless moisture tolerant epoxies that can flush the moisture from the inner crack surfaces are used.

The American Concrete Institute (ACI) Guide 440.2R-02 (2002), shows that cracks wider than 0.25 mm can move and may affect the performance of externally bonded FRP systems through delamination or fibre crushing. Small cracks exposed to aggressive environments may require resin injection to improve durability performance and delay corrosion of existing steel reinforcement before FRP strengthening.

The present study is undertaken to enhance the understanding of how epoxy injection affects the shear behaviour of reinforced concrete beams with and without CFRP fabrics subjected to four-point static loading. Three of the damaged which were tested on the previous study in chapter three were repaired using epoxy injection into the cracks, two of the beams also had additional new external FRP sheets on its damaged shear span. All three beams were subjected to normal monotonic loading up to failure.

4.2 Experimental Program

In this experimental work, three damaged beams which were tested at previous phase (presented at the chapter three) were repaired using epoxy injection and retested.

4.2.1 Materials properties

Characteristic of concrete, steel, FRP sheets and epoxy used to bind the concrete and external FRP sheets was the same a previous chapter (section 3.2.1).

A two-component epoxy was used to seal crack surfaces in damaged beam specimens and to attach injection ports to the concrete beams. It had a tensile strength of 31.0 MPa, an elongation at break of 0.5%, compressive yield strength of 96.5 MPa determined as the ASTM D-638 "Standard Test Method for Tensile Properties of Plastics" standard provisions. The bond strength between the concrete and this epoxy was 15.9 MPa as

determined following the ASTM C882 "Standard Test Method for Bond Strength of Epoxy-Resin Systems Used with Concrete by Slant Shear" testing procedure.

Another two-component low-viscosity epoxy adhesive (product of BASF chemical company) was used to inject cracks in the damaged concrete beams. It had a tensile strength of 52.0 MPa, an elongation at break of 1.0%, and a compressive yield strength of 76.0 MPa determined following the ASTM D-638, "Standard Test Method for Tensile Properties of Plastics" standard testing guidelines. The bond strength between concrete and this epoxy was 14.0 MPa as per the ASTM C882, "Standard Test Method for Bond Strength of Epoxy-Resin Systems Used with Concrete by Slant Shear" testing recommendations.

4.2.2 Specimens preparation

Three of the damaged beams (presented at chapter three) after quasi-static loading were subsequently repaired using epoxy injection. The As-built-1 control RC beam specimen was repaired using epoxy injection only and labeled "As-built-R". Beam B-I-C, which had unidirectional carbon fibre fabric, was first prepared by removing damaged FRP sheets, repaired using epoxy injection, and then the same scheme of unidirectional carbon fibres was applied. The repaired beam was labeled "B-I-CR1". The As-built-2 control RC beam specimen was also repaired using epoxy injection, and then all shear span surfaces were covered using external unidirectional carbon fibres. The repaired beam was labeled "B-I-CR2". The epoxy injection repair was carried out as follows: first, cracks were

cleaned thoroughly with compressed air. Injection ports were then installed using surface sealing epoxy. The ports were spaced 15 cm apart and were applied on both sides of the beam. Cracks were sealed with epoxy in order to retain the injected epoxy (Fig. 4.1a.). The injection process was started after the sealing epoxy cured. The epoxy injection was initiated at the lowest port until it reached the port above. The lowest port was then capped. The process was repeated until the epoxy completely filled all cracks and all ports were capped. Epoxy injection was done using injection guns (Fig. 4.1b.). After curing of the epoxy, the ports were removed, and the seals were grinded off. After surface preparation, CFRP sheets were applied to the surfaces of beam specimens B-I-CR1 and B-I-CR2 as discussed above. Figure 4.2 shows typical shear strengthening details used in used for B-I-CR1 and B-I-CR2 shear specimens. Table 4.1 shows details of strengthened specimens and FRP sheets used.

4.2.3 Loading apparatus and testing procedure

The same testing set up as presented in previous chapter was used except with difference that bottom plates and connection rods were removed and monotonic loading was applied to the beam specimens. Figure 4.3 shows the loading set up for B-I-CR2. The load was applied using a relatively low displacement rate of 0.5 mm per minute.

4.3 Results and Discussion

4.3.1 Results for repaired beam specimens

Experimental results of ultimate load capacity and displacement obtained on testing repaired beams have been summarized in Table 4.2. The load versus mid-span displacement for repaired beams is presented in Fig. 4.4.

4.3.1.1 "As-built-R" shear beam specimen

This beam specimen was only repaired using epoxy injection into cracks. It exhibited an ultimate load capacity of 176.4 kN, which was 21% higher than the ultimate capacity of the "As-built" control beams. The final displacement of the specimen was 13 mm, which was 78% greater than that of the "As-built" control beam. This indicates that the epoxy injection repair protocol was very effective both in terms of load capacity and ductility improvements. Also, in the linear part of the deflection-force graph, higher stiffness was observed compared to that of the control beam. This could be explained by the bond-strength to concrete of the low viscosity injection material which was higher than the tensile strength of the concrete itself. Hence, new cracks formed next to the injected ones at the weakened locations. The beam failed by concrete crushing at the side of the beam which had no stirrups. However, major cracks were also observed at the side with transverse steel rebars. Figure 4.5a shows the "As-built-R" repaired specimen crack pattern at failure.

4.3.1.2 B-I-CR1 beam specimen

In addition to repairing cracks with epoxy injection, this beam specimen had four unidirectional CFRP laminates on each of its shear spans. There was a free space between subsequent laminates equal to the width of each laminate (75 mm) (Fig. 4.2a.). The beam had an ultimate load capacity of 233.0 kN, which is 33% higher than that of the repaired specimen "As-built-R" and 40% higher than that of the retrofitted specimen B-I-C presented earlier. Again, this can be due to the higher bond strength between the concrete and the injected epoxy compared to the tensile strength of the concrete. The final midspan displacement of the beam was 7.7 mm, which is 41% lower than that of the repaired "As-built-R" beam, but 19% higher than that of the retrofitted specimen B-I-C tested in the previous phase. Comparing the ultimate deflection of the this beam with that of the repaired specimen "As-built-R" indicates that some FRP repair schemes can increase the ultimate shear capacity but reduce ductility. Higher ductility of this specimen compared to that of the retrofitted specimen B-I-C can be justified by the formation of a plastic hinge at the injected epoxy location.

This beam behaved almost linearly up to its brittle failure. The beam specimen with epoxy crack injection had a higher initial stiffness than that of the counterpart specimen without epoxy injection. Major cracks were also observed at the side of the beam having transverse steel ties. However, the beam failed at the side with no transverse steel as expected. Contrary to the behaviour observed in the previous phase, FRP sheets ruptured

in the repaired beam specimen and the crack angle was almost 45°. The crack pattern at failure for beam B-I-CR1 is illustrated in Fig. 4.5b.

4.3.1.3 B-I-CR2 beam specimen

In this beam, all shear spans were completely covered using unidirectional CFRP sheets (Fig. 4.2b.) subsequent to low epoxy injection of cracks. There was a significant improvement in the mechanical behaviour of this specimen, particularly in its ultimate midspan displacement capacity and much enhanced ductile behaviour. The ultimate capacity of the B-I-CR2 beam specimen was 192.5 kN, which is 9% higher than that of the "As-Built-R" specimen. The ultimate midspan deflection of the beam at failure was 29.3 mm, which is 125% higher than that of the "As-Built-R" specimen. Comparing the ultimate deflections of beams B-I-CR1 and B-I-CR2 shows that a ductile or brittle behaviour of the repaired beams is highly dependent on the scheme used for external FRP rehabilitation, which can shift a very brittle failure to a ductile one.

First major cracks during the loading of this specimen occurred at the end of the FRP sheets on the concrete surface where both shear and moment loads are considerably high while no retrofit or repair protocol was applied at that location. As observed in Fig. 4.4, at the initial elastic zone, the beam showed similar behaviour to that of the "As-Built-R" beam specimen with approximately the same stiffness. However, it could undergo much higher deflection at the plastic zone with an almost constant load of 190 kN. A crash of concrete occurred in the shear span of the beam at the beam side having no transverse

steel reinforcement, which led to debonding of the attached FRP laminate. The crack pattern and failure of beam B-I-CR2 is illustrated in Fig. 4.5c. It can be argued that epoxy injection of cracks aided in limiting crack opening. Moreover, epoxy injection combined with externally bonded FRP sheets was very effective for the structural repair of shear deficient RC beams.

4.3.2 Comparison with conventional repair methods

Historically, intact concrete members have been retrofitted by post-tension or jacketing with new concrete in conjunction with a surface adhesive (Klaiber, 1987). Since the mid 1960's, epoxy bonded the steel plates have been used in Europe and South Africa to retrofit concrete members (Dussek, 1987). Steel plates have a durability problem unique to this application, because corrosion may occur along the adhesive interface. This type of corrosion adversely affects the bond at steel plate-concrete interface and is difficult to monitor during routine inspections. Additionally, special equipment is necessary to install the heavy plates. As a result of these problems new materials have been sought by engineers. Unidirectional or woven FRP laminates have proven to be a promising alternative for retrofitting exiting RC structures. However, results of the first phase of the presented experimental study showed that the application of hybrid FRP sheets has a considerable effect on improving the mechanical behaviour of the retrofitted beams in terms of ultimate shear capacity and ductility improvements compared to that of unidirectional FRP.

Several methods have also been used for repairing cracks in damaged RC beams, including, (i) routing and sealing, (ii) drilling and plugging, and (iii) stitching which can be performed by drilling holes on both sides of the cracks and grouting a U-shaped steel stitch with epoxy. The main disadvantage of the routing and sealing method is that not much load capacity can be reinstated in the structural member, while the main difficulty in using the drilling and plugging or stitching technique is that they are more labor intensive. Moreover, a high amount of stress concentration usually occurs at the concrete surface using these methods (Hamoush, 1997). The application of epoxy injection generally eliminates such problems.

The simultaneous application of epoxy injection and externally bonded FRP sheets for repairing damaged RC beams was observed to be highly effective. Repairing cracks using epoxy injection improve not only the short term, but also the long term behaviour of damaged beams by reducing chloride ion and moisture migration to longitudinal rebars. Moreover, the injected epoxy can have better mechanical characteristics than concrete, such as higher tensile and better elongation strength than original concrete. Simultaneous application of FRP sheets with epoxy injection increases the confinement of the concrete section, and has demonstrated effectiveness in the shear repair of RC beams in the present study.

4.4 Concluding Remarks

The objective of this experimental study was to evaluate the ultimate shear strength and to identify the modes of failure of re-retrofitted beams using epoxy injection or epoxy injection combined with externally bonded CFRP laminates. The following conclusions can be drawn based on the experimental results discussed in this chapter:

(vii) Crack injection using low viscosity epoxy provided an increase of stiffness in the linear region of the load-displacement curves of all repaired RC beams tested in the second phase of the testing program.

(viii) An increase in the ultimate strength of all beams was observed in the second phase of testing compared to their counterparts in the first phase. This is likely due to the stronger epoxy to concrete bond-line strength compared to the tensile strength of concrete.

(ix) Whether to observe ductile or brittle behaviour of RC beams repaired with epoxy injection and external FRP sheets is highly dependent of the scheme and type of the attached FRP laminates.

Table 4.1: Details of strengthened specimens and FRP sheets used

Specimen	FRP	t_f, mm	E_{f1}, GPa	f_{fu1}, MPa	E_{f2}, GPa	f_{fu2}, MPa	α, degree
B-I-CR1*	Carbon	1.00	87.3	925	3.2	72.4	90°
B-I-CR2	Carbon	1.00	87.3	925	3.2	72.4	90°

*Shear span surfaces were totally covered by CFRP in B-I-CR2 while half of the surface area was covered in B-I-CR1

Table 4.2: Experimental results of shear capacity of retrofitted beam specimens

Specimen	Loading	Results	
		Force, (kN)	Displacement, (mm)
As-Built-R	Monotonic	176.4	13.0
B - I- CR1	Monotonic	233.0	7.7
B - I- CR2	Monotonic	192.5	29.3
As-Built	Cyclic	145.7	7.3
B - I- C	Cyclic	166.2	6.9

(a) (b)

Fig. 4.1: (a) Sealed surface and installed injection ports for the second phase of testing repaired beams, and (b) injection of epoxy into the cracks using an injection gun.

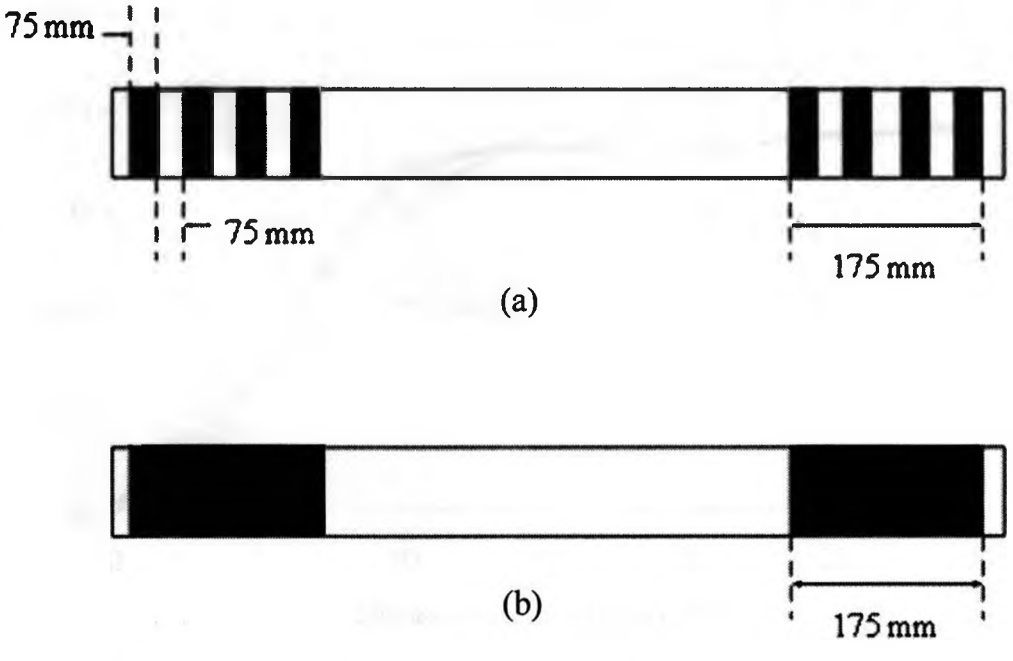

Fig. 4.2: Typical shear strengthening details used in, (a) B-I-CR1, and (b) B-I-CR1 shear specimen.

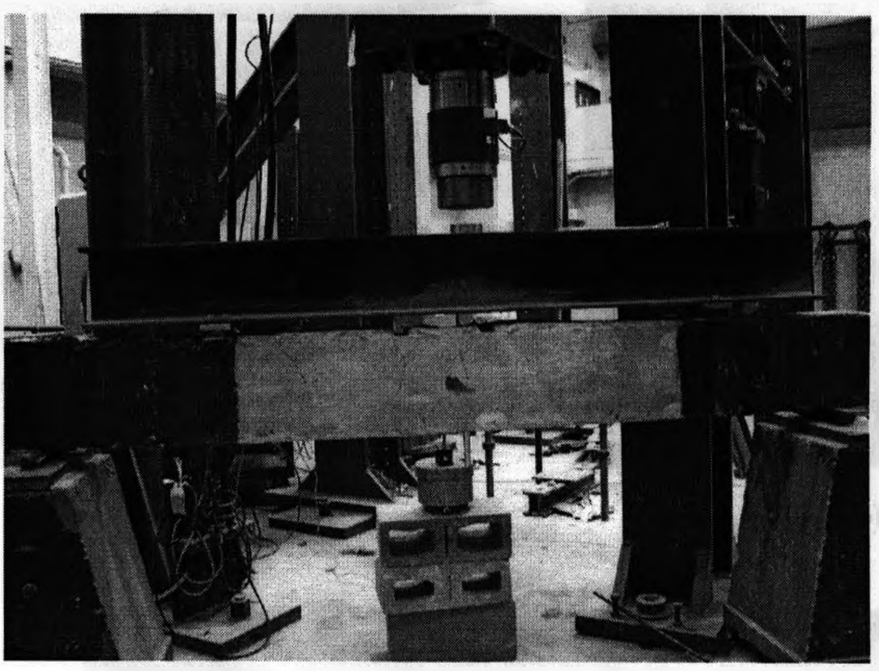

Fig. 4.3: Experimental set-up used in second experimental phase on repaired RC beams.

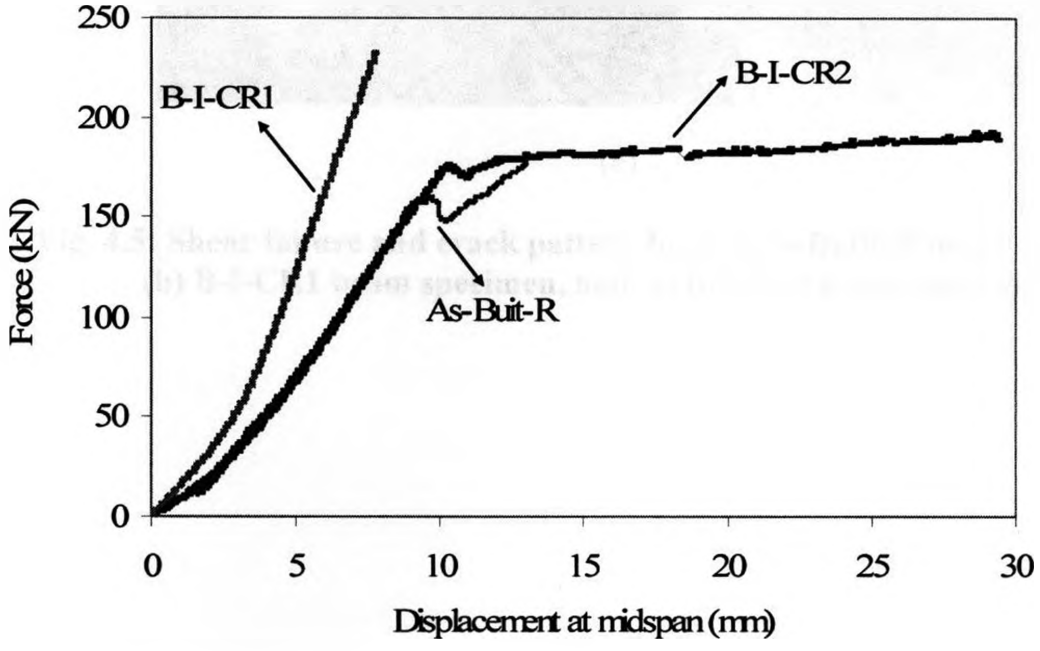

Fig. 4.4: Experimental results for force versus displacement at the midspan of the beams at the second phase of testing.

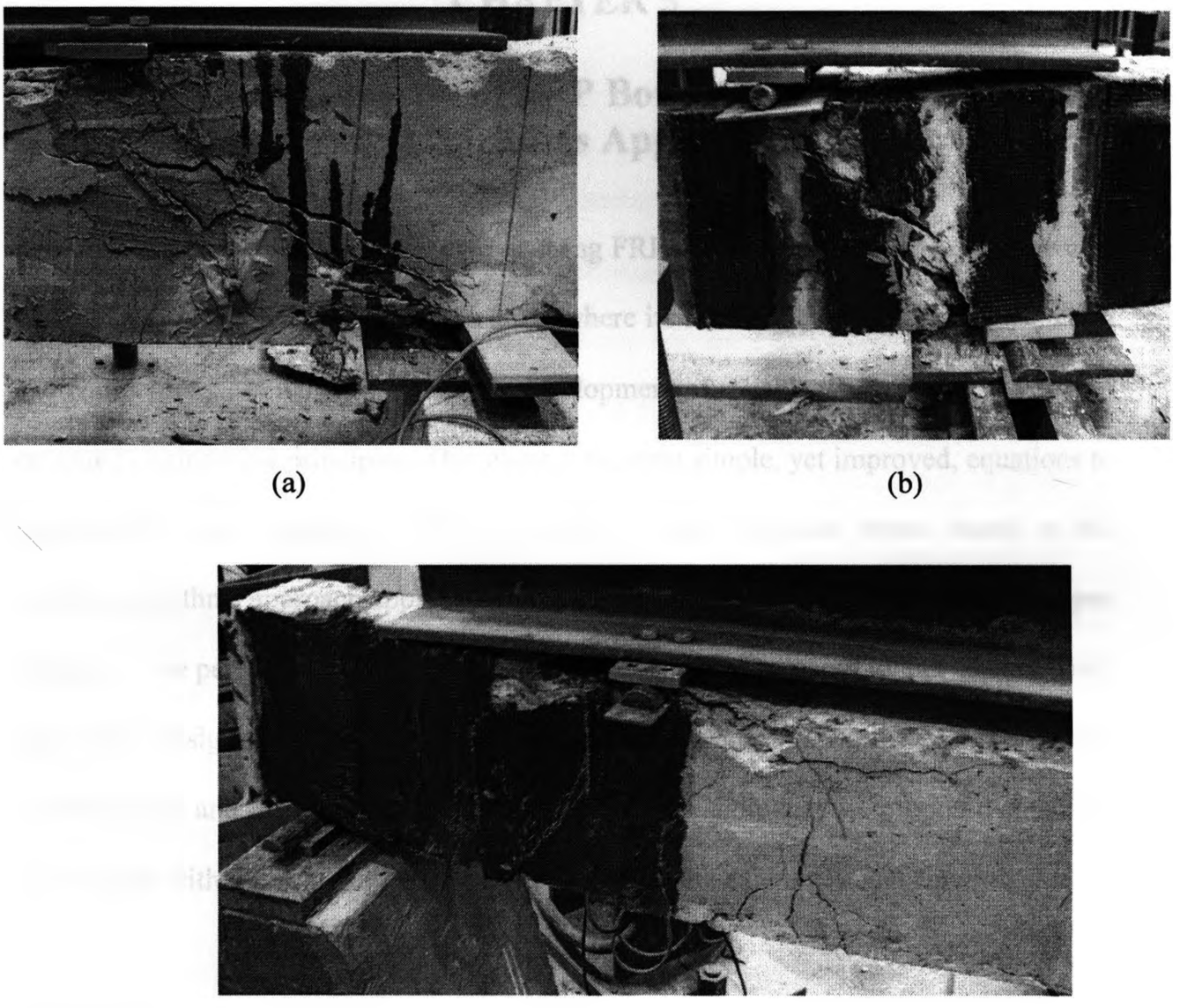

Fig. 4.5: Shear failure and crack pattern for, (a) As-Built-R beam specimen, (b) B-I-CR1 beam specimen, and (c) B-I-CR2 beam specimen.

CHAPTER 5

Modeling Shear Capacity of FRP Bonded-Reinforced Concrete Beams Using Genetic Algorithms Approach[3]

Although a variety of on-site applications using FRP materials have been realized world-wide, this technology is currently at a stage where its future wide-spread implementation and competitiveness will depend on the development of reliable design guidelines based on sound engineering principles. This chapter presents simple, yet improved, equations to calculate the shear capacity of FRP bonded-reinforced concrete beams based on the genetic algorithms approach applied to 212 experimental data points available in the open literature. The performance of the proposed equations was compared to that of commonly used shear design methods, namely the ACI 440, Eurocode (EC2), the Matthys Model, Colotti model and the ISIS Canada guidelines. Results show that the proposed equations better agree with the available experimental data than the existing models investigated.

5.1 Introduction

Previous studies (e.g. Mosallam *et al.* 2007) concluded that current design guidelines are highly conservative and underestimate the shear capacity of FRP-bonded RC beams. Accordingly, the objective of this study is to develop simple, yet accurate, shear design equations for FRP- bonded RC beams with and without stirrups for different kinds of FRP laminates and variable configurations. The proposed equations account for the effect of common shear design parameters and have been developed based on the genetic

[3] A version of this chapter has been submitted for review to Journal of Materials and Structures.

algorithms approach using the ultimate shear capacity results of 212 FRP- strengthened RC beams available in the open literature.

This work aims at improving the understanding of the complex mechanisms that characterize the ultimate shear capacity of continuous and simply supported RC members with transverse steel reinforcement and externally bonded FRP sheets. In particular, the mechanisms of interaction between the external FRP strengthening and the internal steel shear reinforcement and concrete strength are investigated. This interaction is generally not considered in design code provisions and in most existing shear design models, which generally assume that FRP strengthening does not change the shear resistance contributed by concrete and/or steel.

5.2 Genetic Algorithms Methodology

Genetic algorithms (GAs) are used in computing both exact and approximate solutions to optimization and search problems. Categorized as a global search experience-based technique, GAs are a particular class of evolutionary algorithms that use techniques inspired by evolutionary biology, including inheritance, mutation, selection, and crossover to solve problems. GAs have become increasingly useful in the nonlinear programming field as a result of their strong search capabilities.

GA is case dependent and the appropriate selection of its key parameters is essential for its successful development and acceptable performance. These key parameters include

the selection method and pressure, recombination type and rate, mutation rate and number of individuals. The selection method and pressure are critical in directing the search and arriving at an appropriate solution. Their operation depends on the nature and difficulty of the problem to be solved. The value of the recombination and mutation rates is essential to the convergence and stability of the solution. A high value of the crossover rate gives larger space for exploring possible solutions, allowing for the optimum solution to be found and reducing the possibility of the solution converging to a local optimum. One negative aspect is that a recombination rate that is too high may lead to a search of less-promising regions, delaying the convergence of a solution. A high mutation rate leads to more random alterations in which offspring start losing their resemblance to their parents. In contrast, a low mutation rate may cause the solution to try fewer individuals who would otherwise have been useful to the solution. More information about this issue is discussed by Goldberg (1989).

The genetic algorithms approach has several applications in engineering practice; however, the GA has not been used in concrete materials and structural research until recently. Ramasamy and Rajasekaran (1996) investigated the potential for using expert systems, artificial neural networks, and genetic algorithms, in order to construct an empirical model for the shear strength of reinforced concrete deep beams. Nehdi (2007) used the GA method to calculate the shear capacity of RC beams that are internally reinforced with FRP rebars. Genetic algorithms were also used in modeling the compressive strength of cement mortar (Akkurt *et al.* 2003) and in the design of the mixture proportions of high-strength concrete (Lim and Yoon 2004).

5.3 Experimental Database

In this study, the ultimate shear capacity for 212 RC beams were collected from published literature (Mosallam *et al.* 2007, Khalifa *et al.* 1999, Cao *et al.* 2005, Abdel-Jaber *et al.* 2003, Kachlakev *et al.* 1999, Kage *et al.* 1997, Mitsui *et al.* 1998, Sato *et al.* 1996, Triantafillou 1998, Uji 1992, Huthchinson *et al.* 1999, Taerwe *et al.* 1997, Taljsten *et al.* 1999, Michael *et al.* 1995, Carolin *et al.* 2005, Pellegrino *et al.* 2006, Hadi 2003, Monti *et al.* 2006, Matthys 2000, Spadea *et al.* 1998, Swamy *et al.* 1996, Norris *et al.* 1997, Umezu *et al.* 1997, Araki *et al.* 1997, Swamy *et al.* 1999, Chajes *et al.* 1995, Al-Sulaimani *et al.* 1994). A total of 132 data points had CFRP, 58 had GFRP and 22 had AFRP as externally bonded reinforcement. The database was complied in a patterned format. Each pattern consists of an input vector containing the geometrical and mechanical properties of the retrofitted RC beam, and an output vector containing the corresponding shear capacity. Table 5.1 shows the range of shear design parameters and ultimate shear capacity of beams used in the database.

5.4 Proposed Design Equation Based on Genetic Algorithms Model

In most of the previous empirical models, the following equation was adopted

$$V_{f,exp} = V_{u,exp} - V_{u,base} \tag{5.1}$$

Where, $V_{u,base}$ is the ultimate shear capacity of a similar beam but without any external FRP laminates. It has been shown by Pellegrino (2006) that there is considerable nteraction between steel stirrups and external FRP laminates and that it is possible at

failure, whether in de-bonding or rupture, stresses in the steel stirrups be much lower than the yield stress.

The genetic algorithms approach has been used herein as an optimization technique to develop equations for the shear design of externally bonded FRP reinforced concrete beams with or without shear reinforcement. Thus, an original form of the equation defining the overall shear bahaviour and including the main shear design parameters that influence the shear capacity of concrete beams is required. The original form of the shear equations considered in the GA optimization are as follows:

$$V_n = (C_1\sqrt{f_c'} + C_2\frac{\rho_l}{\frac{a}{d}})b_w d + \frac{A_v f_{steel} d}{s} + \frac{A_f E_f \varepsilon_{fe} d_f}{s_f}(\sin\alpha + \cos\alpha) \quad (5.2)$$

$$\varepsilon_{fe} = C_3 \Gamma_f^{C_4} \varepsilon_u \quad (5.3)$$

$$\Gamma_f = \frac{E_f \rho_f}{f_c^{\frac{2}{3}}(a/d)} \quad (5.4)$$

$$\rho_f = \frac{A_f}{b s_f} \quad (5.5)$$

$$f_{steel} = \min(\varepsilon_{fe} E_s ; f_y) \quad (5.6)$$

where C_1, C_2, , C_3, C_4= unknown coefficients of the model that need calibration. The first part of equation 5.2 is similar to the ACI code guideline, but the constant values in the ACI code are assumed to be unknown coefficients in the GA model. The second part of Eq. 5.2 is also similar to the ACI code, but it is assumed in the ACI code that the stress at

failure in the transverse stirrups is always f_y, which is not always a true assumption. Stress can be much lower in transverse stirrups when cracks initiate in fibre-reinforced polymer sheets. For selecting the format of the third part of the object function, different functions were tested. Equation 5.1 was used and ε_{fe} was calculated using equation 2.5. The results show that a power function best describes the effective strain at failure for different kinds of FRP materials and mechanisms of their attachment (Fig. 5.1). Knowing the general form of the predictive equation, the model was optimized using the Genetic Algorithms toolbox in a Matlab environment.

In previous works, calibration of codes is based on Eq. 5.1, where V_f represents the shear capacity which is added to the ultimate shear capacity of a beam without FRP sheet attachments. The strong nonlinear capability of the genetic algorithms approach makes it possible to optimize all factors simultaneously and to consider the interaction of the shear capacity provided by concrete, FRP and/or steel. In the present model, the predictive equation was solved directly by using the ultimate shear capacity in the GA target points.

5.5 Results and Discussion

5.5.1 *Optimization of coefficients C_1 and C_2*

Table 5.2 shows the results for optimizing C_1, which is mostly related to the aggregate interlock effect. Previous works generally suggest a constant value of C_1 for different configurations and material types of FRP laminates used in rehabilitation systems.

However, the present study shows that there is a significant difference between the value of C_1 for different FRP materials and application schemes. Because the failure of the concrete element and the rupture or debonding of the FRP laminates do not occur simultaneously, especially for two or there sided laminate applications, it is likely that FRP laminates will fail well below the point at which concrete reaches its load capacity. After failure of the FRP sheets, all the stress will suddenly be transmitted to the concrete and steel.

Results show that using CFRP in a four-sides bonded scheme leads to better performance, and generally in a completely wrapped scheme, the C_1 coefficient is 16% greater than that for two or three-sides bonded application for carbon fibre-reinforced polymers, and 26% greater for glass fibre-reinforced polymers, respectively. There was not sufficient data available in the open literature on two or three-sides bonded beams with Aramid (Kevlar) FRP RC beams.

Table 5.2 also shows the results for optimizing the C_2 coefficient. This factor mainly shows the effect of longitudinal rebars on the ultimate shear capacity. It can be observed that the C_2 coefficient has a higher value for completely wrapped systems. It can be concluded that the completely wrapped scheme is a better choice not only because FRP sheets will undergo higher strain before failure, but also because other elements (concrete and steel) can reach their maximum capacity before failure.

5.5.2 *Optimization of coefficients C_3 and C_4*

The coefficients C_3 and C_4 relate to the final strain level in the FRP sheets ε_{fe} and are shown in Table 2. It can be observed that generally, in the completely wrapped scheme, the strain level in the FRP laminate will generally be closer to the ultimate strain than that for two- or three-sides bonded application, and that CFRP provides better results because it has the highest C_3, and the lowest C_4 coefficients compared to that of GFRP and AFRP. This means that it is more likely that CFRP sheets reach its maximum capacity than in the case of other FRPs.

The performance of the proposed genetic algorithm-based equations and that provided by other existing models was investigated using the testing experimental database described earlier, based on both the ratio of the experimental to the corresponding calculated shear strength (V_{exp}/V_{cal}), and the average absolute error (AAE) calculated using Eq. (5.7)

$$AAE = \frac{1}{n}\sum \frac{\left|V_{\exp} - V_{cal}\right|}{V_{cal}} \times 100 \tag{5.7}$$

The average, standard deviation (SD), and coefficient of variation (COV) for V_{exp}/V_{cal} and AAE for all shear design models investigated are listed in Table 5.3. Figure 5.2 shows the bar chart of the error associated with each code or model.

5.5.3 *Performance of ACI 440, CSA 860 and ISIS equations*

The ACI 440 code does not consider the interaction between the shear capacity contributed by the concrete, steel and FRP sheets. It does not also consider the effect of the shear span-to-depth ratio on the effective strain level in the FRP sheets at failure. Moreover, the second modification factor K_2 (in Eq. 2.9), sometimes becomes negative, especially for two sided laminated applications, which does not have any physical significance. The ACI 440 model has often underestimated shear capacity results with an average $V_{\text{experimental}}/V_{\text{predicted}}$ ratio of 1.62, and a coefficient of variation of 33%, which is considerably high. The CSA and ISIS codes use the same methodology as ACI guidelines and do not consider the effect of the shear span-to-depth ratio, *a/d*, on the effective strain of FRP sheets at failure. They also underestimated the ultimate shear capacity of FRP-bonded reinforced concrete beams with an average $V_{\text{experimental}}/V_{\text{predicted}}$ ratio of 1.56 and 1.43, respectively, which is also too high.

5.5.4 *Performance of EC2 model*

The EC2 model does neither consider the effect of the shear span-to-depth ratio, *a/d*, on the effective strain of FRP sheets at failure, nor the interaction between concrete, steel and FRP sheets. The EC2 model has often overestimated results with an average $V_{\text{experimental}}/V_{\text{predicted}}$ ratio of 0.91, and a coefficient of variation of 22.4%.

5.5.5 *Performance of Matthys model*

The Matthys model does not consider the interactions between concrete, steel and FRP sheets, but takes into account the effect of the shear span-to-depth ratio. The Matthys model generally overestimated the ultimate shear capacity of FRP-bonded concrete beams with an average $V_{experimental}/V_{predicted}$ ratio of 0.94, and a coefficient of variation of 26.2%. This performance is comparable to that the Eurocode EC2.

5.5.6 *Performance of Colotti model*

The Colotti model also does not consider the interactions between the shear capacity contributed by concrete, steel and FRP sheets and ignores the effect of the shear span-to-depth ratio. It uses several formulas to identify the failure type and to predict the ultimate shear capacity of FRP bonded reinforced concrete beams. The Colotti model provides reasonable results with an average $V_{experimental}/V_{predicted}$ ratio of 1.08, and coefficient of variation of 18%, yet it needs several parameters that are not always available.

5.5.7 *Performance proposed GA model*

The shear equation optimized using the genetic algorithms approach outperformed other existing design methods and models. It has lower *AAE* (16.5%) and *COV* (15.0%) than that of the other existing models, and estimated the ultimate shear capacity of fibre-reinforced polymer bonded concrete beams more accurately.

5.6 Sensitivity Analysis of Effect of Shear Span-to-Depth Ratio

This study showed that the shear span-to-depth ratio not only affects the shear capacity provided by concrete, but also the shear capacity provided by the steel and external FRP sheets. In this section of this chapter, the effect of the shear span-to-depth ratio was investigated using an example. Figure 5.3 shows the characteristics of the selected retrofitted RC beam. All variables were assumed to be constant except the FRP sheets used to retrofit the beam and the shear span-to-depth ratio of the beam which were variable. To ensure shear failure in all cases, the longitudinal reinforcement ratio was selected to be 0.04, which is relatively high, and a large spacing between stirrups was used (#3 steel stirrups spaced at 150 mm). The nominal compressive strength of the concrete was assumed to be 25 MPa and the specified yield strength of both the transverse and longitudinal steel was assumed to be 460 MPa. Table 5.4 summarizes the selected values for the thickness, Young's modulus along the major axis, and the design rupture strain for the different materials used. This example was solved for both two and three sides bonded (using CFRP or GFRP) beam, and completely wrapped retrofitting schemes (using CFRP or GFRP). The effects of the shear span-to-depth ratio on the shear capacity contributed by concrete, effective strain in the FRP sheets and effective stress in the transverse steel are discussed here.

a) *Shear capacity provided by concrete*

Figure 5.4 shows results for the shear capacity provided by concrete. As expected, increasing the shear span-to-depth ratio slightly decreased the ultimate shear capacity. It

can also be observed that the shear capacity provided by the concrete is not independent of the selection of the FRP type and reinforcement scheme. This interaction effect has been ignored in most previous models. In this example, completely wrapped CFRP sheets showed a better performance, while two or three sides bonded GFRP was less adequate in terms of interaction with concrete.

b) ***Effective strain in FRP sheet***

Figure 5.5 shows the GA model results for the effect of the shear span-to-depth ratio on the effective ultimate strain in FRP sheets. Increasing the shear span-to-depth ratio, *a/d* generally decreases the effective ultimate strain in the FRP sheets. Completely wrapped reinforcement schemes were more likely to experience rupture or to de-bond in stress levels closer to the design ultimate strain.

c) ***Effective stress in transverse steel***

Figure 5.6 shows predicted results for the effect of the shear span-to-depth ratio on the effective stress in the transverse steel. It is shown that the effective stress in the transverse steel can be significantly lower than the yield stress of steel. Previous models generally ignore the interaction effect between concrete, steel and FRP sheets. For instance, the ACI 440 model overestimates the stress level in the transverse steel by assuming that f_y is constant and independent of the shear span-to-depth ratio. Hence, it overestimates the shear capacity provided by the transverse steel and underestimates the shear capacity

provided by the FRP. However, when FRP sheets are about to fail (rupture or de-bonding), it is possible that the stress level in the steel be much lower than f_y. Once the FRP sheets fail, all applied loads have to be carried by the steel and concrete. Thus, the stress level in steel will increase suddenly and overall failure occurs.

5.7 Concluding Remarks

This study proposed shear design equations for RC beams reinforced with externally bonded FRP sheets based on the genetic algorithms method applied to an experimental database of 212 beams collected from the literature. Existing models for this problem are based on regression analysis done separately for the shear capacity contributed by steel, concrete and FRP sheets. Thus, such models are generally unable to consider interaction mechanisms between steel stirrups, concrete and FRP laminates. The following conclusions can be drawn from this work:

(i) The genetic algorithms approach can be used as an effective tool to optimize equations for the shear design of externally bonded FRP reinforced concrete beams. The shear equation optimized using the genetic algorithms approach outperformed other existing design methods and models.

(ii) The stress in steel stirrups at failure can be less than the yield stress, f_y which has not been considered in previous equations and models.

(iii) The ACI 440 method does not consider the effect of the shear span-to-depth ratio on the effective shear strain in FRP laminates, and assumes a linear relationship between the thickness of FRP laminates and the shear capacity contributed by these

FRP laminates, which is not always true. The second modification factor of the ACI code, k_2, sometimes becomes negative, which does not have any physical meaning. This formula often underestimates the shear capacity of FRP retrofitted RC beams.

(iv) The Matthys model considers the effect of the *a/d* ratio on the effective strain of FRP sheets, but is only applicable to CFRP sheets and does not consider the interaction mechanisms between concrete, steel and FRP laminates.

(v) The Colotti model also does not consider the effect of the *a/d* ratio and the interaction mechanisms between concrete, steel and FRP laminates. This model uses several formulas involving parameters that are not always provided in experimental studies, therefore it is not generally simple use.

(vi) It was shown that the completely wrapped scheme provides better results for the shear retrofitting of RC beams compared to other schemes by increasing the confinement of the concrete beam section and consequently the aggregate interlock. On the other hand, the completely wrapped scheme provides better bonding behaviour between concrete and FRP. It was shown that CFRP materials provide better shear capacity in retrofitting RC beams compared to GFRP or AFRP.

(vii) The shear design equations proposed in this study consider both the interaction between concrete, steel stirrups and FRP laminates, and the effect of the shear span-to-depth ratio. Hence, it provided more accurate shear predictions compared to results of the other models considered in this study. RC beams with lower shear span-to-depth ratio are more likely to fail by rupture of FRP sheets. Moreover, concrete and transverse steel rebars in such beams can contribute more shear capacity compared to beams with higher shear span-to-depth ratio.

Table 5.1: Range of design parameters used in experimental database

	a/d	f_c'	b	d	ε_{fu}	Γ_f	V_n
Minimum	1.1	13.3	64	100	0.0095	0.05	18.75
Maximum	4.0	71.9	600	499	0.0370	12.69	662.00
Average	2.6	39.2	171	254	0.0174	2.16	205.83
***COV* (%)**	25.0	37.0	50	46	39.4	103.2	77.25

Table 5.2: C_1, C_2, C_3 and C_4 coefficients estimated by the GA model

Coefficient	FRP type	Two or three sides bonded	Completely wrapped
C_1	CFRP	0.24	0.28
	GFRP	0.20	0.26
	AFRP	*	0.23
C_2	CFRP	12	14
	GFRP	11	12
	AFRP	*	15
C_3	CFRP	0.23	0.32
	GFRP	0.15	0.27
	AFRP	*	0.15
C_4	CFRP	0.66	0.17
	GFRP	0.92	0.39
	AFRP	*	0.44

* No sufficient data were available for two or three sides AFRP bonded concrete beams in shear testing.

Table 5.3: Performance of shear design equations

Method	*AAE* (%)	*Vexp/Vcal*		
		Average	*SD*	*COV* (%)
ACI-440. 2R-02	59.8	1.62	0.52	33.0
CSA S806-02	52.5	1.56	0.43	27.0
ISIS Canada	46.3	1.43	0.38	27.0
Eurocode (EC2)	27.2	0.91	0.20	22.4
Matthys	29.3	0.94	0.24	26.2
Colotti	22.3	1.08	0.18	17.0
Proposed Equation	16.5	1.00	0.15	15.0

Table 5.4: Properties of FRP sheets selected to investigate the effect of shear span to depth ratio

Material	Thickness t_f, (mm)	Major modulus of elasticity E_f, (MPa)	Design rupture strain, ε_{fu} (mm/mm)
CFRP	0.10	90	0.015
GFRP	0.25	20	0.020

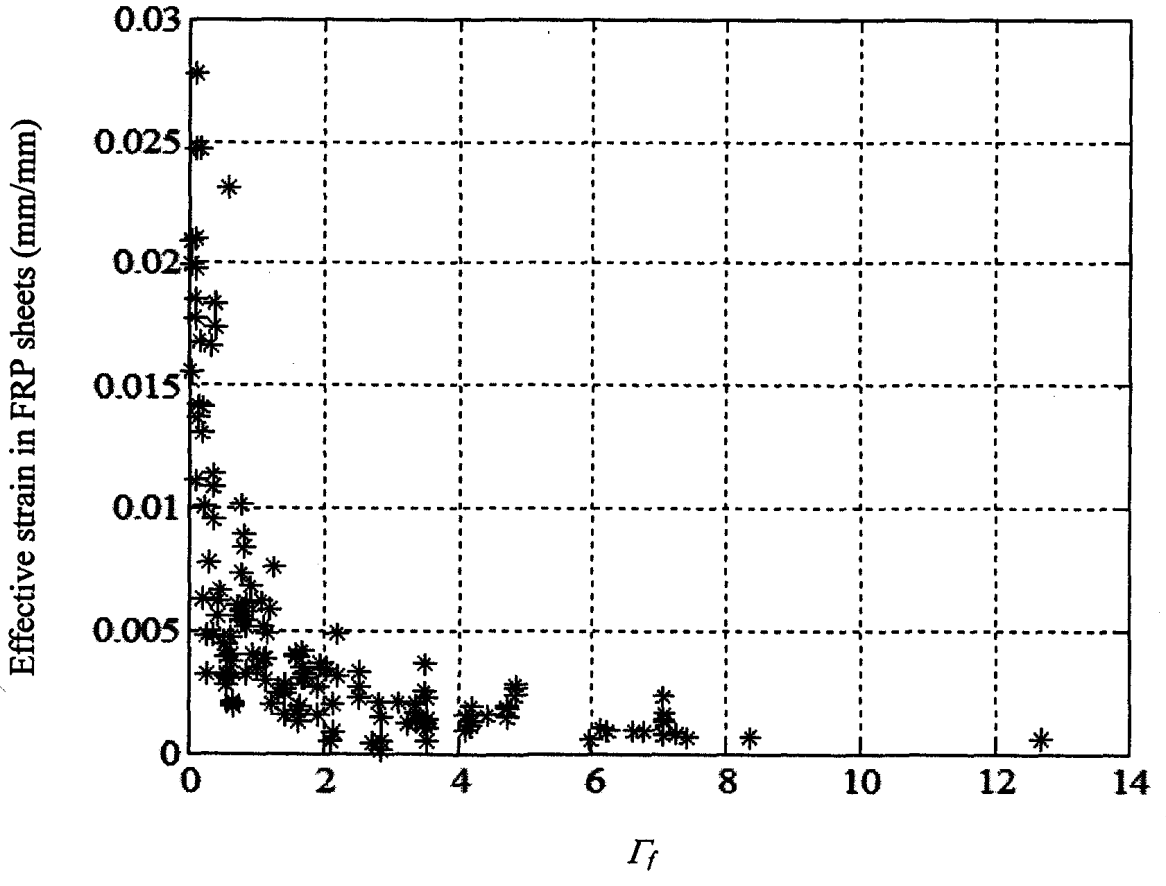

Fig. 5.1: Effective strain in FRP in terms of Γ_f.

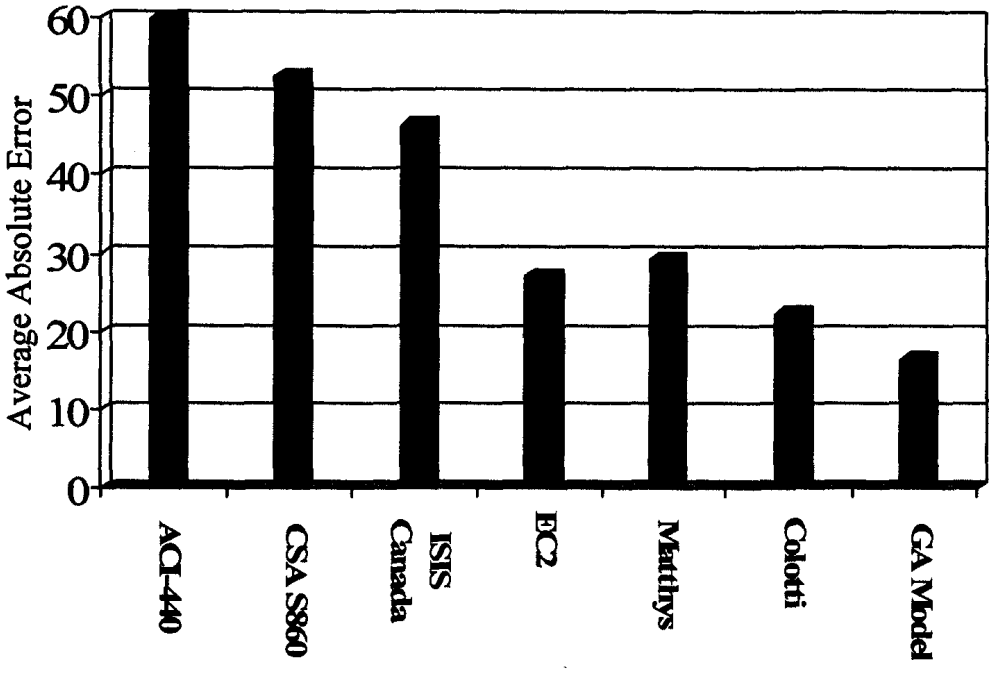

Fig. 5.2: Average Absolute Error (*AAE*) for prediction of shear codes (ACI 440, CSA S860, ISIS Canada and EC2) and models (Matthys, Colotti and GA).

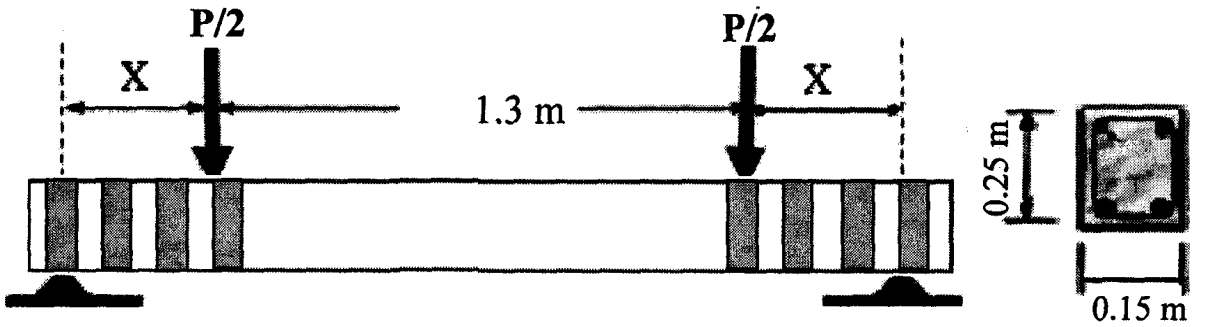

Fig. 5.3: Geometrical characteristics of the selected beam.

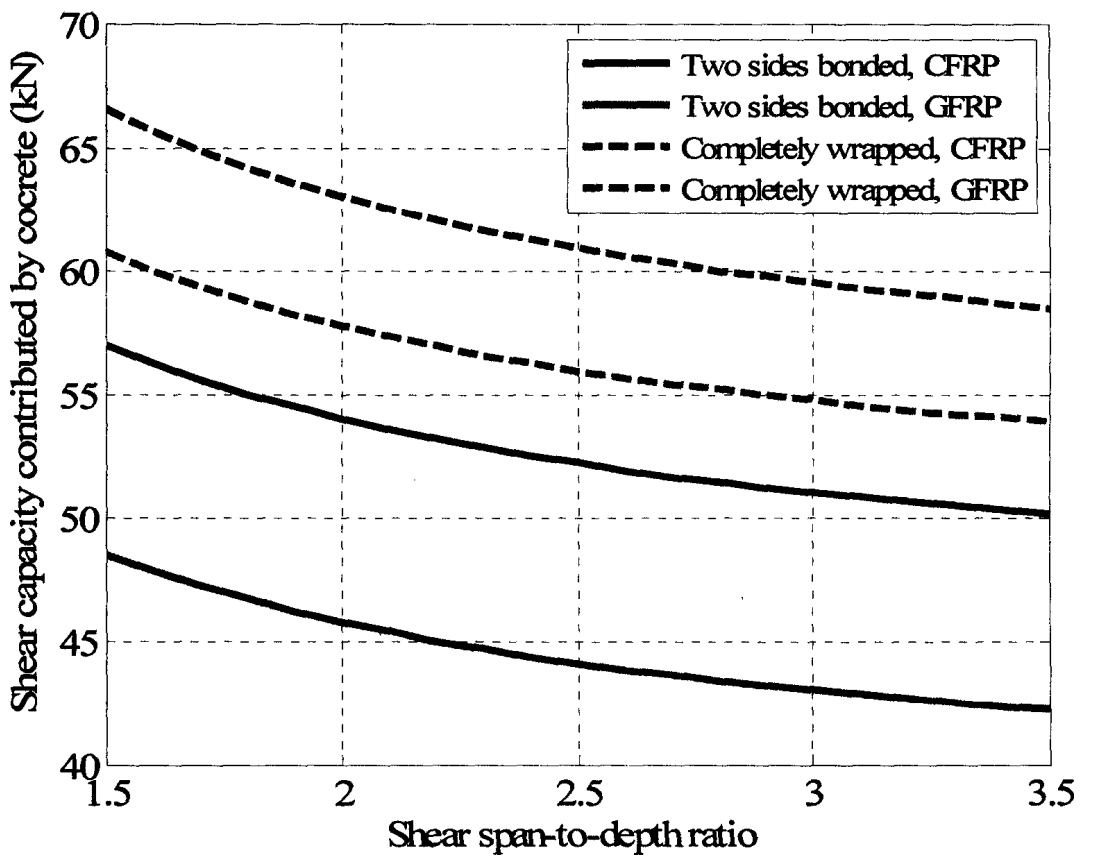

Fig. 5.4: Effect of shear span-to-depth ratio on shear capacity provided by concrete.

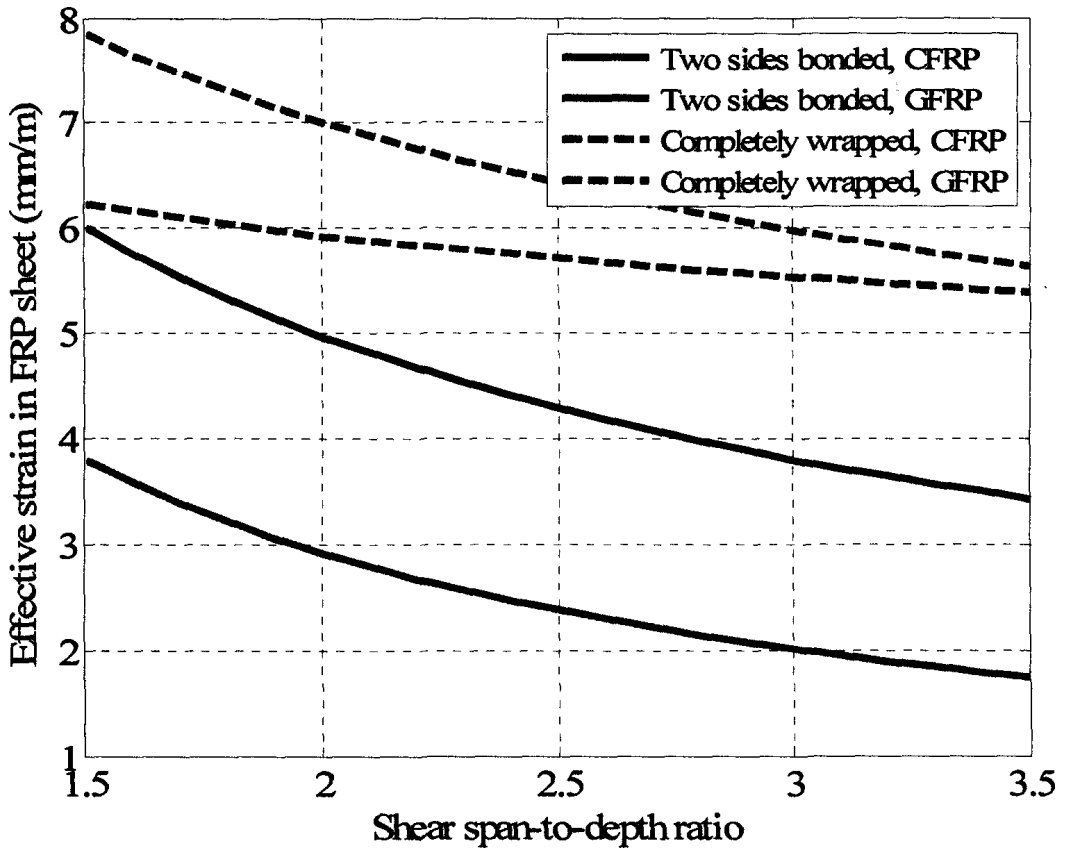

Fig. 5.5: Effect of shear span-to-depth ratio on effective ultimate strain in FRP sheets.

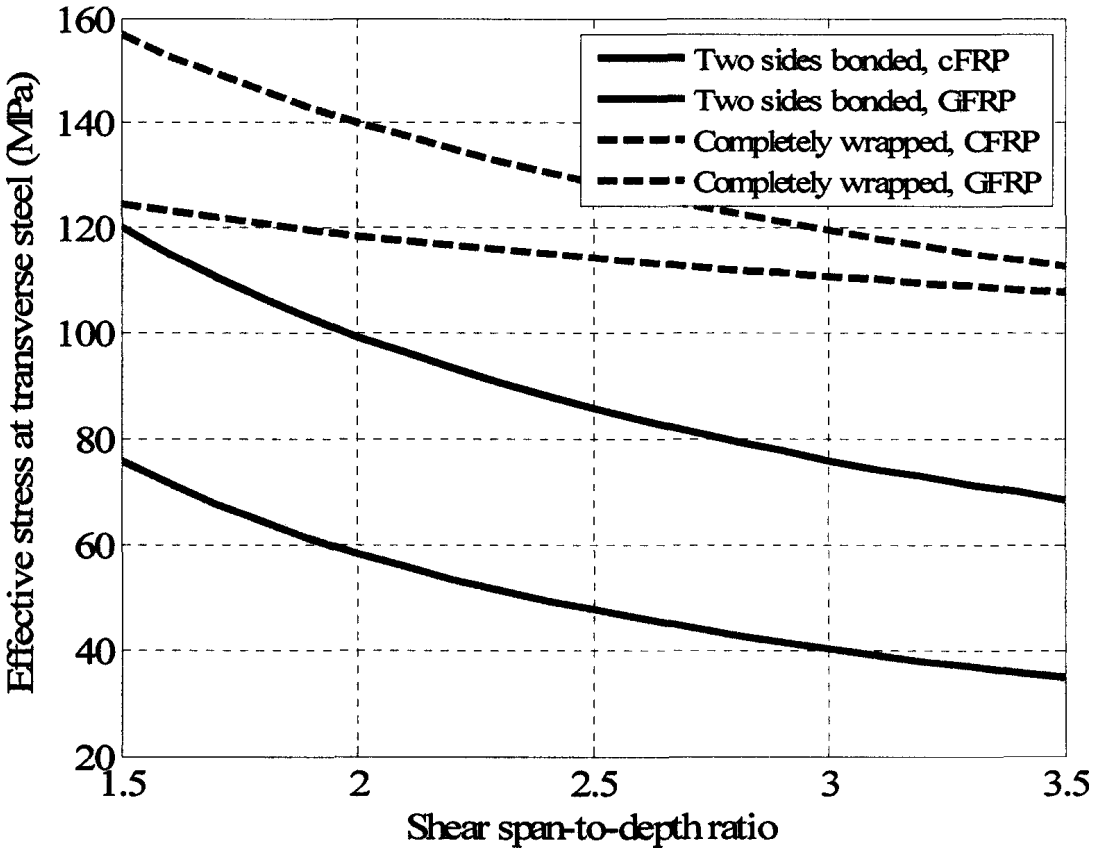

Fig. 5.6: Effect of shear span-to-depth ratio on effective ultimate stress in transverse steel.

CHAPTER 6

Summary, Conclusions, and Future Research

6.1 Summary

The objective of this study was to investigate the shear behaviour of externally FRP-bonded reinforced concrete (RC) beams using unidirectional or hybrid FRP sheets, under quasi-static or monotonic loading. Moreover, the aim was to study the behaviour of damaged beams repaired using epoxy injection along with externally bonded FRP sheets. First, a literature review on previous research on FRP-bonded reinforced concrete beams and current models for predicting the ultimate shear capacity of such beams was conducted. The experimental investigation carried out in this study included the ultimate load capacity, deflection, crack pattern and mode of failure of FRP-bonded reinforced concrete beams. In the fist phase of the experimental study, hybrid and unidirectional fibres were used to retrofit beams. These beams were tested using quasi-static loading. The experimental results of this phase of research were predicted using a numerical modeled based on the Finite Elements Method (FEM) developed in this thesis. In the second phase of the experimental work, cracks in the damaged RC beams were repaired using the epoxy injection method. Unidirectional CFRP sheets were also used to cover the shear span of three of the beams in different schemes. The effect of different parameters such as the retrofitting protocol, shear span-to-depth ratio and application scheme of FRP on shear behaviour of externally FRP-bonded reinforced concrete beams

were investigated. New equations were proposed to calculate the shear capacity of FRP bonded-reinforced concrete beams based on the genetic algorithms approach applied to 212 experimental data points collected from the open literature. The performance of the proposed equations was compared to that of commonly used shear design methods and models namely the ACI 440, Eurocode (EC2), the Matthys Model, Colotti model, CSA and the ISIS Canada guidelines.

6.2 Conclusions

FRP sheets have a great potential for retrofitting concrete structures. The main advantages of FRP sheets are their ease of application and ability to mitigate corrosion problems while having a high strength-to-weight ratio. Research on the application of externally bonded unidirectional FRP sheets for reinforced concrete (RC) beams under monotonic loading is well established, and several analytical and empirical models are available for predicting the ultimate shear capacity of such beams. However, these models generally do not consider the interaction between the internal shear reinforcement and the shear capacity imparted by the FRP. Moreover, these models are generally not applicable for hybrid or bidirectional applications of FRP sheets.

Epoxy injection was found to be a powerful and simple method for repairing cracks in damaged concrete structural members compared to conventional methods such as stitching, drilling and plugging, and routing and sealing. Data on the simultaneous application of epoxy injection and externally bonded FRP sheets is scarce.

The present experimental study showed that hybrid FRP sheets have a better performance in increasing the ultimate shear capacity of RC beams compared with that of unidirectional carbon fibre-retrofitted beam specimens. The co-existence of other fibres like glass or aramid in the transverse direction allow carbon fibres in the main direction to get closer to their ultimate strain capacity by increasing the confinement of FRP laminates and postponing the development of cracks in the concrete surface. RC beams with thicker and stronger FRP sheets are less likely to undergo failure by rupture of the FRP sheet. The FEM model developed in this study gave predictions that confirm with the results above.

Fatigue and repetitive loading affect the ultimate load capacity of RC beams through the formation of micro-cracks in concrete and weakening of the bonding layer between concrete and the external FRP sheets. This effect needs to be quantified and accounted for in cyclic loading. The failure mode is also dependent on the FRP retrofitting scheme, type, internal steel arrangement, and type and position of the applied load. Although GFRP and CFRP are brittle in nature, increasing the ductility of RC beam specimens can be achieved by proper application and retrofitting scheme using such materials.

Crack injection using low viscosity epoxy provides an increase of stiffness in the linear region of the load-displacement curves of repaired RC beams. Moreover, considerable increase in the ultimate strength of repaired RC beams can be achieved by the simultaneous application of epoxy injection and externally bonded FRP. This is likely due to the stronger bond-line of epoxy to concrete strength compared to the tensile

strength of concrete. Whether to observe ductile or brittle behaviour of RC beams repaired with epoxy injection and external FRP sheets is highly dependent of the scheme and type of the attached FRP laminates.

A set of equations was proposed in this study to predict ultimate shear capacity of externally FRP bonded beams under monotonic loading based of Genetic Algorithms Approach. It was concluded that the genetic algorithms approach can be used as an effective tool to optimize equations for the shear design of externally bonded FRP reinforced concrete beams. The shear equations optimized using the genetic algorithms approach outperformed other existing design methods. Due to the strong nonlinear curve fitting abilities of GAs, the interactions between the shear capacity contribution of concrete, steel and FRP are considered in the proposed equations. It was concluded that the stress at failure in steel stirrups can be less than the yield stress, f_y which has not been considered in previous models. Failure of the concrete element and the rupture or debonding of the FRP laminates may not occur simultaneously, especially for two or there sides laminate applications. Hence, it is likely that FRP laminates will fail well below the point at which concrete reaches its load capacity. After failure of the FRP sheets, all the stress will suddenly be transmitted to the concrete and steel.

It was shown that the completely wrapped scheme provides better results for the shear retrofitting of RC beams compared to other schemes by increasing the confinement of the concrete beam section and consequently the aggregate interlock. On the other hand, the completely wrapped scheme provides better bonding behaviour between the concrete and

FRP. It was shown that CFRP materials provide better shear capacity in retrofitting RC beams compared to GFRP or AFRP.

It was also found that current design codes generally underestimate the ultimate shear capacity of externally FRP bonded RC beams. All of the models investigated in this study except, the Matthys, model ignore the effect of the *a/d*. This study showed that the shear span-to-depth ratio has a considerable effect on the shear capacity contributed by concrete, the effective strain in FRP sheets, and the effective stress in the transverse steel. Generally, beams with a lower shear span-to-depth ratio are more likely to experience a shear failure due to the rupture of the FRP sheets. Moreover, steel stirrups in such beams have higher stress at failure, and are therefore more likely to yield compared to RC beams with a higher shear span-to-depth ratio.

6.3 Proposed Future Research

This study focused on the effect of the main experimental parameters that influence the shear behaviour of FRP bonded-reinforced concrete beams. However, various issues related to this subject need further research as follows:

(i) More experimental data are needed to build a comprehensive database for FRP bonded-reinforced concrete beams under cyclic loading.

(ii) More research is still needed to investigate long-term behaviour of FRP bonded reinforced concrete beams.

(iii) More data is needed on the effect of different external FRP reinforcement scheme in the transverse direction.

(iv) More reliable equations can be proposed based on an extended FEM database including more design parameters.

(v) More innovative techniques should be proposed for bonding FRP to the concrete surface.

(vi) The effect of environmental factors such as temperature, moisture and ions penetrations need to be investigated.

(vii) Data on aramid fibre reinforced polymers (AFRP) bonded RC beams, especially on two or three sides bonded schemes, is very limited. Particularly, more research should be done on the seismic behaviour of beams retrofitted with AFRP sheets since AFRP has a better damping behaviour compared to that of CFRP or GFRP.

(viii) Other artificial intelligence techniques such as neural networks or fuzzy logic methods can be applied to extend the numerical and/or experimental database on experimentally FRP bonded-reinforced concrete beams.

REFRENCES

ABAQUS 6.6 User's Manual, ABAQUS Inc., Providence, RI, USA, 2006.

Abdel-Jaber, M.S., Walker, P.R., Hutchinson, A.R., 2003, Shear Strengthening of Reinforced Concrete Beams Using Different Configurations of Externally Bonded Carbon Fibre Reinforced Plates, Materials and Structures , **36**:291-301.

ACI Committee 224R-80. Control of Cracking in Concrete Structures, American Concrete Institute; 1980, Farmington Hills, MI.

ACI Committee 224.1R-93. Causes, Evaluation, and Repair of Cracks in Concrete Structures, American Concrete Institute, 1993, Farmington Hills, MI.

ACI Committee 318R-05. Code Requirement for Structural Concrete and Commentary, American Concrete Institute; 2005, Farmington Hills, MI.

ACI Committee 440.2R-02. Guide for the Design and Construction of Externally Bonded FRP Systems for Strengthening Concrete Structures, American Concrete Institute; 2002, Farmington Hills, MI.

ACI Committee 546R-96. Concrete Repair Guide, American Concrete Institute; 1996, Farmington Hills, MI.

Akkurt, S., Ozdemir, S., Tayfur, G., Akyol, B., 2003, The Use of GA-ANNs in Modeling of Compressive Strength of Cement Mortar, Cement and Concrete, **33**:973-979.

Al-Gadhib, A.H., 2003, Repair and Retrofitting of Deteriorated Reinforced Concrete structures-Three Case Studies, Proceedings of the 6th Saudi Engineering Conference ,Vol. 3, Dhahran:KFUPM:147-56.

Al-Sulaimani, G.J., Sharif, A.M., Basunbul, I.A., Baluch, M.H., Ghaleb, B.N., 1994, Shear Repair for Reinforced Concrete by Fibreglass Plate Bonding, Structural Journal, **91**:458-64

Altin, S., Anil, O., Kara, M., 2005, Improving Shear Capacity of Existing RC Beams Using External Bonding of Steel Plates, Engineering Structures, **27**:781-91.

Araki, N., Matsuzaki, Y., Nakano, K., Kataoka, T., Fukuyama, H., 1997, Shear Capacity of Retrofitted RC Members with Continues Fibre Sheets, Proceedings of the third international symposium on non-metallic (FRP) reinforcement for concrete structures, Japan Concrete Institute, Tokyo, Japan, pp. 515-522.

Bennett, S.C., Johnson, D.J., 1978, Structural Heterogeneity in Carbon Fibers, Proceedings of the fifth London carbon and graphite conference, London, UK, pp.377-86.

Bousselham, A., Chaallal, O., 2006, Shear Behaviour of Reinforced Concrete T-Beams Strengthened in Shear with Carbon Fibre-Reinforced Polymer-An Experimental Study, Structural Journal, **103**: 339-47.

Burgoyne, C., 1999, Advanced Composites in Civil Engineering in Europe, Journal of the International Association for Bridge and Structural Engineering, **9**: 267-73.

Calder, A.J.J., Thompson D.M., 1998, Repair of Cracked Reinforced Concrete: Assessment of Corrosion Protection, Crowthorne, Berkshire, Bridges Division, Transport and Road Research Laboratory, Research Report 150.

Canadian Standards Association (CSA). 2002, Design and Construction of Building Components with Fibre-Reinforced Polymers, Canadian Standards S806-02, Rexdale, Ontario, Canada.

Cao, A.Y., Chen, J.F., Teng, J.G., Hao, Z., Chen, J., 2005, Debonding in RC Beams Shear Strengthened with Complete FRP Wrap, Composites for Construction, **9**: 417-428.

Carolin, A., Taljesten, B., 2005, Experimental Study of Strengthening for Increased Shear Bearing Capacity, Composites for Construction, **9**:488-496.

Carolin, A., Taljesten, B., 2005, Theoretical Study of Strengthening for Increased Shear Bearing Capacity, Composites for Construction, **9**:497-506.

Chajes, M.J., Januszka, T.F., Mertz, D.R., Thomson, T.A., William, J., 1995, Shear Strengthening of Reinforced Concrete Beams Using Externally Applied Composite Fabrics, Structural Journal, **92**:295-302.

Chen, J.F., Teng, J.G., 2003, Shear Capacity of FRP-Strengthened RC beams: FRP debonding, Construction and Building Materials, **17**:27-41.

Colotti, V., Spadea, G., 2001, Shear Strength of RC Beams Strengthened with Bonded Steel or FRP Plates, Structural Engineering, **127**:367-373.

Colotti, V., Spadea, G., Swamy, N., 2005, Analytical Model to Evaluate Failure behaviour of Plated Reinforced Concrete Beams Strengthened for Shear, Structural Journal, **101**:755-65.

Dussek, I., 1987, Strengthening of Bridge Beams and Similar Structures by Means of Epoxy-Resin-Bonded External Reinforcement , Transp. Res. Rec. No. 785, Transp. Res. Board, Washington, D.C., 21-24.

EC2-Eurocode 1. 1992, Design of Concrete Structures, European Committee for Standardization, Lausanne, Switzerland.

Ekenel, M., Myers, J.J., 2007, Durability Performance of RC Beams strengthened with Epoxy Injection and CFRP Fabrics, Construction and Building Materials **21**:1182-87.

Goldberg, D.E., 1989, Genetic Algorithm in search, Optimization, and Machine Learning, Addison-Wesley, Reading, Mass.

Guadagnini, M., Pilakoutas, K., Waldron, P., 2006, Shear Resistance of FRP RC Beams: Experimental Study, Composites for Construction, **10**: 464-473.

Hadi, M.N.S., 2003, Retrofitting of Shear Failed Reinforced Concrete Beams, Composite Structures, **62**:1-6.

Hamoush, S., Ahmad, S.H., 1997, Concrete Crack Repair by Stitches, Materials and Structures, **30**:418-423

Holland, J.H., 1975, Adaptation in Natural and Artificial Systems, University of Michigan Press, Ann Arbor, Mich.

Hull, D., Clyne, T.W, An Introduction to Composite Materials, Cambridge University Press, New York, New York, 1996.

Huthchinson, R.L., Rizkalla, S.H., 1999, Shear Strengthening of AASHTO Bridge Girders Using Carbon Fibre Reinforced Polymer Sheets, Proceedings of the fourth international symposium on fibre reinforced polymer reinforcement for Reinforced concrete structures, ACI Publications SP-188, pp.945-56.

ISIS Canada. 2001, Strengthening Reinforced Concrete Structures with Externally-Bonded Fibre Reinforced Polymers, Design Manual No. 4, Zukewich, J., ed., The Canadian Network of Centers of Excellence on Intelligent Sensing for Innovative Structures, University of Manitoba, Winnipeg, Canada.

Islam, M.R., Mansur, M.A., Maalej, M., 2005, Shear Strengthening of RC Deep Beams Using Externally Bonded FRP Systems , Cement and Concrete Composites, **27**:413-20.

Jankowiak, T., Lodygowski, T., Identification of Parameters of Concrete Damage Plasticity Constitutive Model, Publishing House of Poznan University of Technology, 2005; ISSN 1642-9303.

Kachlakev, D.I., Barnes, W.A.1999, Flexural and Shear Performance of Concrete Beams Strengthened with Fibre Reinforced Polymer Laminates. Proceeding of the fourth international symposium on fibre reinforced polymer reinforcement for reinforced concrete structures, ACI Publications SP-188, pp.959-71.

Kachlakev, D., McCurry, D.D., 2000, Behaviour of Full-Scale Reinforced Concrete Beams Retrofitted for Shear and Flexural with FRP Laminates, Journal of Composites, **31**: 445-52.

Kage, T., Abe, M., Lee, H.S., Tomosawa, F., 1997, Effect of CFRP Sheets on Shear Strengthening of RC Beams Damaged by Corrosion of Stirrup. Non-Metallic (FRP) Reinforcement for Concrete Structures, Proceeding of the third international symposium, Sapporo, Japan, pp.443-50.

Khalifa, A., Tumialan, G., Nanni, A., Belarbi, A., 1999, Shear Strengthening of Continuous Reinforced Carbon Fibre Reinforced Beam Using Externally Bonded Carbon Fibre Polymer sheets, Proceeding of the fourth international symposium on fibre reinforced polymer reinforcement for reinforced concrete structures, ACI Publications SP-188, pp.995-1008.

Khalifa, A., Nanni, A. 2000, Improving Shear Capacity of Existing RC T-Sections Beams Using CFRP Composites, Cement & Concrete Composites, **22**:165-74.

Klaiber, F.W., Dunker, K.F., Wipf, T.J., Sanders, W.W., 1987, Methods of Strengthening Existing Highway Bridges , Nat. Cooperative Hwy. Res. Program Rep. No. 293, Transp. Res. Board, Washington, D.C.

Labossiere, P., 2000, Fibre Reinforced Polymer Strengthening of the Sainte-Emelie-de-l'Energie Bridge: Design, Instrumentation, and Field Testing, Canadian Journal of Civil Engineering, **27**:916-27.

Li, A., Diagana, C., Delmas, Y., 2002, Shear Strengthening Effect by Bonded Composite Fabrics on RC Beams, Journal of Composite, **33**:225-39.

Li, L.J., Guo, Y.C., Liu, F., Bungey, J.H. 2005, Efficiency of Hybrid FRP Sheets in Strengthening Concrete beams, Proceedings of the International Conference on Repair and Renovation of Concrete Structures, 343-350.

Li, J., Samali, B., Ye, L., Bakoss, S., 2002, Behaviour of Concrete Beam-Column Connections Reinforced with Hybrid FRP Sheet, Composite Structures, **57**:357-365.

Lim, C.H, Youn, Y.S., 2004, Genetic Algorithm in Mix Proportioning of High-Strengthened Concrete, Cement and Concrete, **34**: 409-20.

Maalej, M., Leong, K.S., 2005, Effect of Beam Size and FRP Thickness on Interfacial Shear Stress Concentration and Failure Mode of FRP-Strengthened Beams, Composites Science and Technology, **65**:1148-58.

Malek, A.M., Saadatmanesh, H., 1998, Analytical Study of Reinforced Concrete Beams Strengthened with Web-Bonded Fibre Reinforced Plates or Fabric, Structural Journal, **95**: 343-51.

Matthys, A.M.S., 2000, Structural Behaviour and Design of Concrete Members Strengthened with Externally Bonded FRP Reinforcement, PhD dissertation, Department of Structural Engineering, Faculty of Applied Science, Ghent University, Belgium.

Michael, J., Januszka, T.F., Mertz, D.R., Thomson, T.A., Finch, W.W., 1995, Shear Strengthening of Reinforced Concrete Beams Using Externally Applied Composite Fabrics, Structural Journal, **92**:295-303.

Minoru, K., Toshiro, K., Yuichi U., Keitetsu, R. 2001, Evaluation of Bond Properties in Concrete Repair Materials, ASCE Journal of Materials in Civil Engineering, **13**:98-105.

Mitsui, Y., Murakami, K., Takeda, K., Sakai, H., 1998, A Study on Shear Reinforcement of Reinforced Concrete Beams Externally Bonded with Carbon Fibres Sheets, Compos Interface, **5**:285-95.

Monti, G., Liotta, M.A., 2006, Holistic Design of RC Beams and Slabs Strengthened with Externally Bonded FRP Laminates, Cement and Concrete Composites, **28**:832-844.

Monti, G., Liotta, M.A., 2007, Tests and Design Equations for FRP-Strengthening in Shear, Construction and Building Materials, **21**:799-809.

Mosallam, A., Banerjee, S., 2007, Shear Enhancement of Reinforced Concrete Beams Strengthened with FRP Composite Laminate, Composites Journal Part B, **38**:781-793.

Nehdi, M., El Chabib, H., Said, A. 2007, Proposed Shear Design Equations for FRP-Reinforced Concrete Beams Based on Genetic Algorithms Approach, ASCE Journal of Materials in Civil Engineering **19**:1033-42.

Norris, T., Saadatmanesh, H., Ehsani, M.R., 1997, Shear and Flexural Strengthening of R/C Beams with Carbon Fibre Sheets, Structural Engineering, **123**:903-911.

Pellegrino, C., Modena, C., 2006, Fibre-Reinforced Polymer Shear Strengthening of Reinforced Concrete Beams: Experimental Study and Analytical Modeling, Structural Journal, **103**:720-28.

Ramasamy, J.V., Rajasekaran, S., 1996, Artificial Neural Network and Genetic Algorithm for the Design of Industrial Roofs - a Comparison, Composite Structure, **58**:747-55.

Rita, S., Wong, Y., Frank, J. 2003, Toward Shear Modeling of Reinforced Concrete Members with Externally Bonded Fibre-Reinforced Polymer Composites, Structural Journal, **100**: 47-55.

Saenz, L.P. 1964, Discussion of "Equation for the stress–strain curve of concrete" by Desayi P., Krishnan S., ACI Structural Journal, **61**:1229–35.

Sakar, G., Tanarslan, H.M., Alku, O.Z., 2009, An Experimental Study on Shear Strengthening of RC T-Section Beams with CFRP Plates Subjected to Cyclic Load , Concrete Research, **61**:43-55.

Sato, Y., Ueda, T., Kakuta, Y., Tanaka, T.1996, Shear Reinforcing Effect of Carbon Fibre Sheets Attached to Side of Reinforced Concrete Beams. In: El-Badry MM, editor, Advanced Composite materials in Bridges and Structures, pp. 621-7.

Sato, Y., Ueda, T., Kakuta, Y., Ono, S.1997, Ultimate shear capacity of reinforced concrete beams with carbon fibre sheets, Non-Metallic (FRP) Reinforcement for concrete Structures, Proceedings of the Third Symposium, vol. 1, Japan, pp.499-505.

Shah, S.P., Swartz, S.E., and Ouyang, C., Fracture Mechanics of Concrete, John Wiley & Sons, Inc., New York, New York, 1995.

Shash, A.A., 2005, Repair of concrete beams—a Case Study, Construction and Building Materials, **19**:75-79.

Shin, Y.S., Lee, C., 2003, Flexural Behavior of Reinforced Concrete Beams Strengthened with Carbon Fiber-Reinforced Polymer Laminates at Different Levels of Sustaining Load, ACI Structural Journal, **100**:231-39.

Spadea, G., Bencaridino, F., Swamy, R. N., 1998, Structural Behaviour of Composite RC Beams with Externally Bonded CFRP, Composites for Construction, **2**:132-137.

Swamy, R.N., Jones, R., Charif, A.N., 1996, Contribution of Externally Bonded Steel Plate Reinforcement to the Shear Resistance of Concrete Beams, Repair and Strengthening of Concrete Members with Adhesive Bonded Plates, SP-165, R.N., American Concrete Institute, Farmington Hills, Mich., pp.1-24.

Swamy, R.N., Mukhopadhyaya, P., Lynsdale, C.J., 1999, Strengthening for Shear of RC Beams by External Plate Bonding, The Structural Engineer, **77**:19-30.

Taerwe, L., Matthys, S., 2000, Concrete Slabs Reinforced with FRP Grids. II: Punching Resistance, Composites for Construction, **4**:154-61.

Taljsten, B., 2003, Strengthening Concrete Beams for Shear with CFRP Sheets, Construction and Building Materials, **17**:15-26.

Taljsten, B., Elfgren, L., 2000, Strengthening Concrete Beams for Shear Using CFRP-Materials: Evaluation of Different Application Methods, Composite: Part B, **31**:87-96.

Triantafillou, T.C.1998, Shear Strengthening of Reinforced Concrete Beams Using Epoxy-Bonded FRP Composites, Structural Journal, **95**:107-15.

Tsisatas, G., Robinson, J., 1994, Durability Evaluation of Concrete Cracks Repair Systems, Transportation Research Record 1795, Paper No 02-3596:82-87.

Uji, K., 1992, Improving Shear Capacity of Existing Reinforced Concrete Members by Applying Carbon Fibre Sheets, Trans Japan Concrete Institute, **14**:253-66.

Umezu, K. et al., 1997, Shear Behaviour of RC Beams with Aramid Fibre Sheet. Non-Metallic (FRP) Reinforcement for Concrete Structures, Proceeding of the third international symposium, Sapporo, Japan, pp.491-98.

Wu, G., Wu, Z.S., Lu, Z.T., Ando, Y.B., 2008, Structural Performance of Concrete Confined with Hybrid FRP Composites, Reinforced Plastics and Composites, **27**:1323-48.

CHAPTER 1

GENERAL INTRODUCTION

CHAPTER 1

1.1 INTRODUCTION

1.1.1 Brassinosteroids: historical background

The involvement of several plant hormones in the process of reproduction led plant scientists to believe that pollen could be a rich source of phytohormones. A search for novel plant hormones in pollen led to the discovery of 'Brassin' in rape (*Brassica napus*) pollen, which elicited strong growth-promoting activity in the bean second internode assay (Mitchell et al., 1970). Later, in a major coordinated effort involving several United States Department of Agriculture (USDA) laboratories, the active component of Brassin was isolated in minute quantities (4 mg from 227 kg of bee-collected rape pollen). X-ray crystallographic studies identified the substance to be a steroidal lactone, which was named as brassinolide (BL) (Grove et al., 1979). BL is the first characterized brassinosteroid (BR) and since then about 60 additional BRs have been identified from various plant species, indicating that BRs are ubiquitous in the plant kingdom (Bajguz and Tretyn, 2003). Although BRs are found in all plant organs, their endogenous levels are quite low. Pollen and immature seeds are the richest sources of BRs with levels ranging between 1-100 ng g^{-1} fresh weight. Shoots and leaves usually have lower amounts in the range of 0.01-0.1 ng g^{-1} fresh weight (Bajguz and Tretyn, 2003).

The structure of BL, the most active BR, is shown in Figure 1.1A. BRs show structural variations and fall into seven categories depending on the side chain structure derived from their parent sterols (Figure 1.1B). There are also differences in the number of hydroxyl groups with varying configurations at the C-2 and C-3 positions in the A ring and the presence of either a ketone or a lactone moiety at C-6 and C-7 in the B ring (Figure 1.1C and D). Certain structural features are common to all active BRs. The A and B rings are always in *trans* configuration, which is determined by an α hydrogen at C-5; the B ring contains a 6-oxo or a 6-oxo-7-oxa group (Figure 1.1D); and the hydroxyl groups at C-2 and C-3 are *cis* oriented (Choe, 2004). These structural features are deemed to be essential for the activity of BRs. The growth-promoting activities of BR were first noted by exogenous application of BRs at nanomolar to micromolar concentrations to

Figure 1.1 Structural variations in brassinosteroids. **A)** Structure of brassinolide. **B)** sic
chain structural variations. **C)** variations in the A ring. **D)** variations in the B ring (Cho
2004).

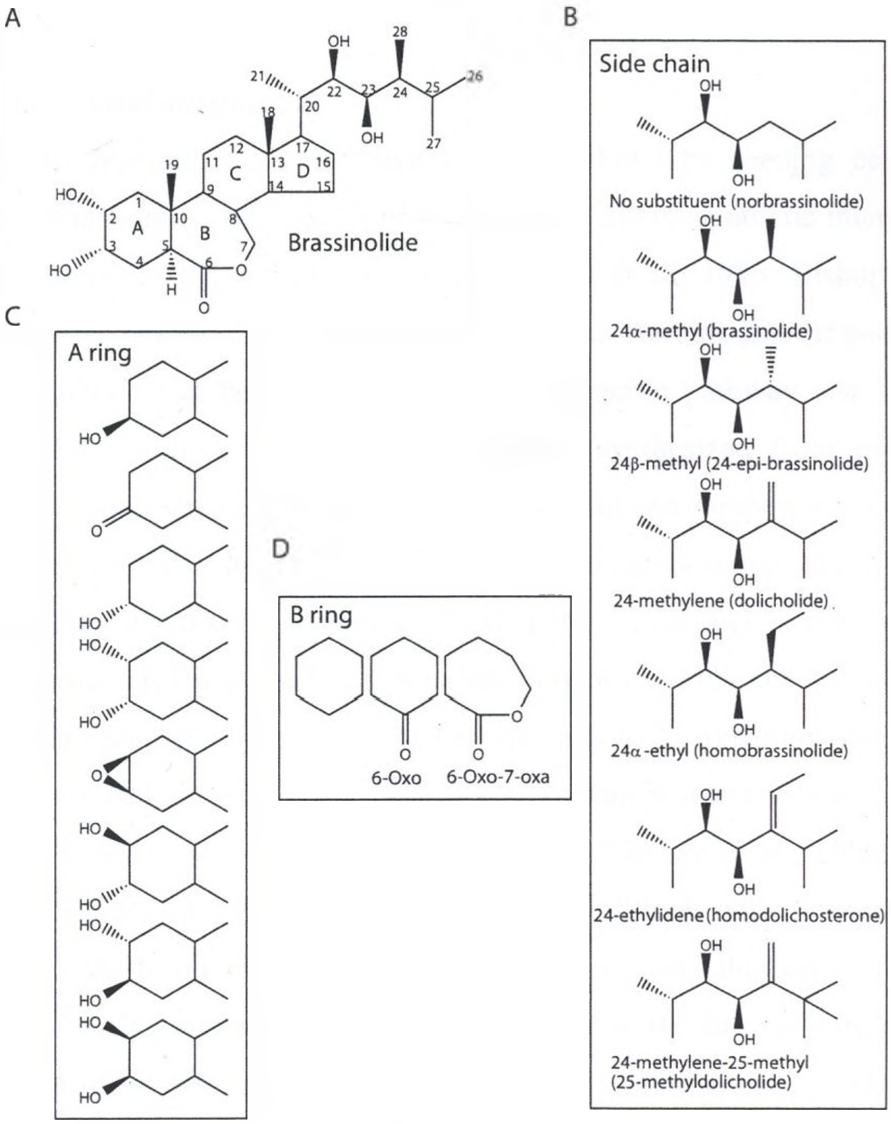
A
Brassinolide
B
Side chain
No substituent (norbrassinolide)
24α-methyl (brassinolide)
24β-methyl (24-epi-brassinolide)
24-methylene (dolicholide)
24α -ethyl (homobrassinolide)
24-ethylidene (homodolichosterone)
24-methylene-25-methyl
(25-methyldolicholide)
C
A ring
D
B ring
6-Oxo
6-Oxo-7-oxa

plants, which induced a wide spectrum of physiological effects such as cell elongation, vascular differentiation, ethylene biosynthesis, and retardation of abscission (Mandava, 1988). Studies of BR-deficient and BR-insensitive Arabidopsis mutants in the mid 1990s provided convincing evidence for an essential role of BRs in plant development (Clouse and Sasse, 1998; Clouse, 2002). For this reason BRs now have the status of phytohormone.

1.1.2 Brassinosteroid biosynthesis

The BR biosynthetic steps have been elucidated by feeding cell suspension cultures of *Catharanthus roseus* with isotope-labeled BR biosynthetic intermediates and by genetic analysis of BR-deficient mutants (Fujioka et al., 1995; Bishop and Yokota, 2001; Fujioka and Yokota, 2003). BRs are derived from steroids and the pathway leading to their biosynthesis can be divided into a sterol-specific pathway and a BR-specific pathway. In the sterol specific pathway, squalene synthesized from mevalonic acid (MVA) is converted to two major plant sterols, sitosterol and campesterol. Campesterol is the precursor of C_{28} BRs and is initially converted to campestanol. Stepwise metabolic experiments have revealed the presence of two parallel pathways from campestanol to castasterone termed as early and late C-6 oxidation pathways (Figure 1.2; Noguchi et al., 2000). Another branching pathway termed as the early C-22 oxidation pathway (Fujioka et al., 2002), as well as a shortcut pathway from campesterol to 6-deoxytyphasterol involving C-23 oxidation, have also been described (Ohnishi et al., 2006). In the final steps, castasterone is converted to BL by lactonization of the B ring.

The isolation and characterization of dwarf mutants that are defective in BR biosynthesis was also instrumental in understanding the BR biosynthetic pathway. The Arabidopsis BR-deficient mutants are characterized by short robust stature, dark-green, round and curly leaves, reduced fertility and prolonged life span (Kwon and Choe, 2005). In addition, when grown in the dark, severe BR dwarfs often display abnormal etiolation patterns including reduction in hypocotyl length, open cotyledons, and absence of apical hook (Choe et al., 2000). Exogenous application of BR can recover BR-deficient mutants to the wild-type (WT) phenotype (Szekeres et al., 1996; Clouse and Sasse, 1998). Several genes encoding BR biosynthetic enzymes have been characterized using BR biosynthesis

mutants of Arabidopsis, pea, tomato and rice (Kwon and Choe, 2005). The dwarf mutant *de-etiolated2* (*det2*) was identified in a study of light-regulated development in Arabidopsis (Chory et al., 1991). The *DET2* gene encodes a steroid 5α-reductase, which is involved in the conversion of 22-OH-4-en-3-one to 22-OH-3-one (Noguchi et al., 1999). The oxidation steps of BR biosynthesis are catalyzed by cytochrome P450 monooxygenases. The C-22 and C-23 hydroxylation reactions are mediated by the P450s DWF4 (DWARF4) and CPD (CONSTITUTIVE PHOTOMORPHOGENESIS AND DWARFISM), respectively (Choe et al., 1998; Szekeres et al., 1996), and the C-6 oxidation is catalyzed by BR-6-oxidases (BR6ox) (Figure 1.2; Shimada et al., 2001). The C-22 hydroxylation step catalyzed by DWF4 is considered a rate-determining step in the BR biosynthetic pathways. The *DWF4* gene encodes a cytochrome P450 monooxygenase (CYP90B1) that catalyzes conversion of cathasterone to 6-deoxocathasterone in the late C-6 oxidation pathway and of 6-oxocampestanol to cathasterone in the early C-6 oxidation pathway (Figure 1.2; Choe et al., 1998). The Arabidopsis *dwf4* mutants are severely dwarf displaying typical BR-deficient phenotypes (Choe et al,. 1998). The C-23 hydroxylation is catalyzed by CPD, another cytochrome P450 enzyme belonging to the CYP90 family (CYP90A1). The *cpd* mutant is an extreme dwarf and can be rescued only by 23α-hydroxylated BRs, indicating that CPD acts as a C-23 steroid hydroxylase (Szekeres et al., 1996). A genetic defect similar to *cpd* has also been found in the tomato *dpy (dumpy)* mutant, which can also be rescued only by C-23 hydroxylated BRs (Koka et al., 2000). Two other members of the CYP90 family, CYP90C1/ROTUNDIFOLIA3 and CYP90D1, act as functionally redundant C-23 hydroxylases in BR biosynthesis (Ohnishi et al., 2006). The gene responsible for C-6 oxidation was first identified in tomato. Analysis of the tomato *DWARF* gene, whose encoded product shares high amino acid similarity with mammalian steroid hydroxylases, revealed that the C-6 oxidation of 6-deoxoBRs to 6-oxoBRs is mediated by the cytochrome P450, CYP85 (Bishop et al., 1999). The Arabidopsis genome has two copies of the tomato *DWARF* homologs: *AtBR6ox1 (CYP85A1)* and *AtBR6ox2 (CYP85A2)*. Shimada et al. (2003) showed that both genes converted 6-deoxocathasterone, 6-deoxoteasterone, 6-deoxotyphasterol and 6-deoxocastasterone to their respective 6-oxidized forms (Figure 1.2).

Figure 1.2 A simplified illustration of the BR biosynthesis pathway (Divi and Krishna, 2009b).

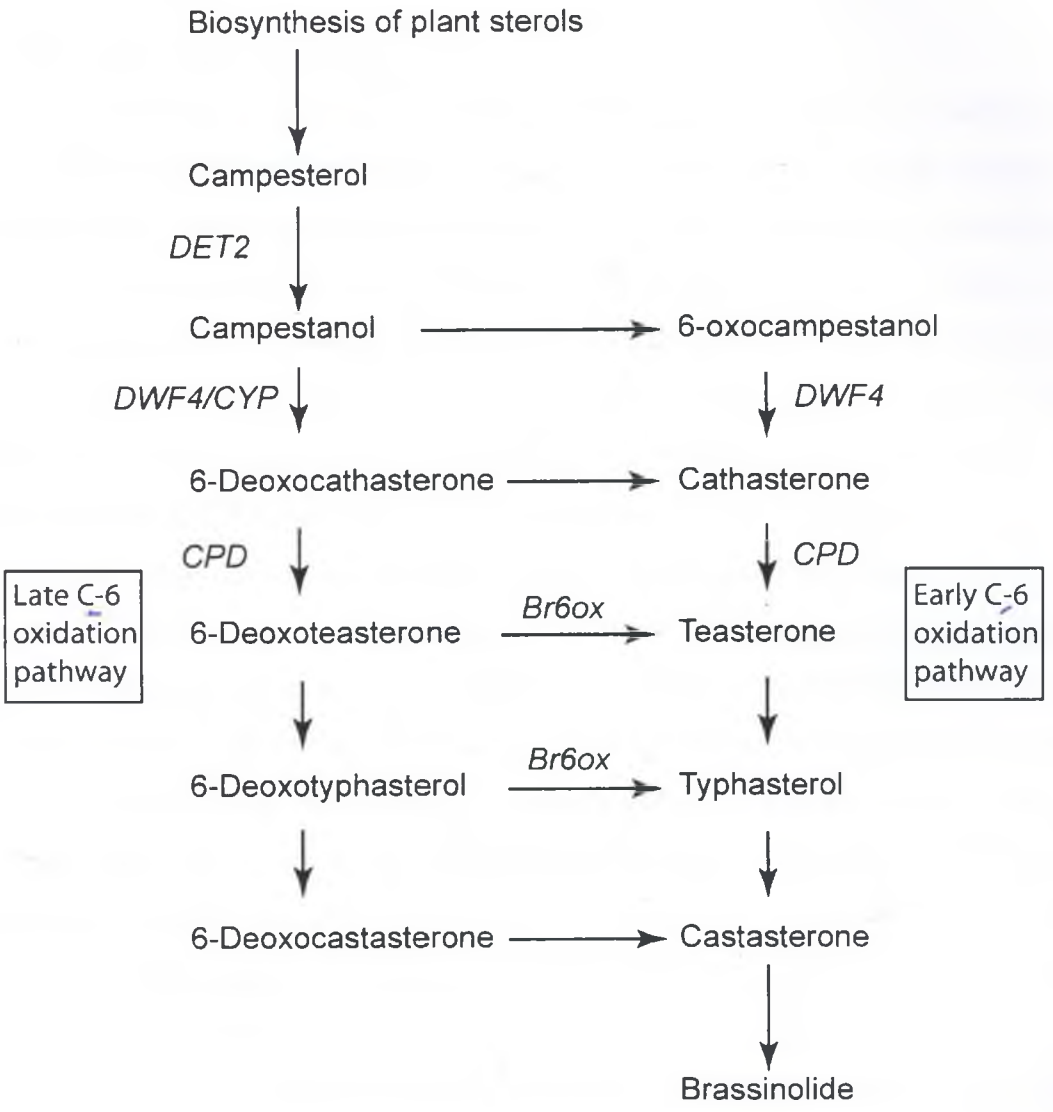
Biosynthesis of plant sterols
Campesterol
DET2
Campestanol
6-oxocampestanol
DWF4/CYP
DWF4
6-Deoxocathasterone
Cathasterone
CPD
CPD
Late C-6 oxidation pathway
6-Deoxoteasterone
Br6ox
Teasterone
Early C-6 oxidation pathway
Br6ox
6-Deoxotyphasterol
Typhasterol
6-Deoxocastasterone
Castasterone
Brassinolide

The Arabidopsis BR biosynthetic P450 genes are under negative feedback regulation by BRs and require BR signaling for this auto-regulation (Bancos et al., 2002; Tanaka et al., 2005). Thus, the C-22 and C-23 hydroxylation and the C-6 oxidation reactions are key regulatory steps in BR biosynthesis, and hence the P450 enzymes catalyzing these reactions are potential targets for biotechnological intervention to modulate endogenous BR levels for enhanced plant traits.

1.1.3 Brassinosteroid signaling

A current model of BR signaling is illustrated in Figure 1.3. Unlike animal steroids that are perceived by nuclear receptors, BRs are perceived at the cell surface by BRI1 (BRASSINOSTEROID-INSENSITIVE 1), a plasma membrane localized leucine-rich repeat receptor-like kinase (LRR-RLK) (He et al., 2000). BR binding to BRI1 induces a series of biochemical events, such as autophosphorylation of BRI1 in its C-terminal domain, dissociation of an inhibitory protein, BKI1 (BRI1 KINASE INHIBITOR 1), and association of BRI1 with another LRR-RLK, BAK1 (BRI1-ASSOCIATED RECEPTOR KINASE 1) (Nam and Li, 2002; Wang and Chory, 2006), which likely enhances signaling output through reciprocal BRI1 transphosphorylation (Wang et al., 2008). Other known components of the BR signaling pathway include the glycogen synthase kinase-3, BIN2 (BRASSINOSTEROID-INSENSITIVE 2), which negatively regulates the transcription factors BZR1 (BRASSINAZOLE-RESISTANT 1) and BES1 (*bri1*-EMS-SUPPRESSOR 1) by phosphorylating them (Li and Nam, 2002; Vert and Chory, 2006), while the phosphatase BSU1 (*bri1* SUPPRESSOR 1) positively regulates BR signaling possibly by dephosphorylating BZR1 and BES1 (Mora-Garcia et al., 2004). BIN2-catalyzed phosphorylation likely inhibits BZR1 and BES1 functions through several modes, such as targeted degradation, reduced DNA binding, and cytoplasmic retention through interaction with 14-3-3 proteins (Gampala et al., 2007). In summary, BRI1 binding to BR inactivates BIN2 and activates BSU1, resulting in the activation and nuclear accumulation of BZR1 and BES1. Activated BZR1 and BES1 directly bind the promoters of BR-regulated genes to affect their expression (He et al., 2005; Yin et al., 2005). Neither BIN2 nor BSU1 has been shown to interact with BRI1; thus, how BR signal is transmitted to these downstream proteins is currently not known.

The recently identified BR signaling kinase BSK3 functions downstream of BRI1 (Tang et al., 2008), but it remains to be seen if BIN2 is a direct downstream target of BSK3 or its relatives.

Numerous BR-regulated genes have been identified by genome wide microarray analyses (Goda et al., 2002; Müssig et al., 2002; Vert et al., 2005). The majority of the known BR-regulated genes are associated with plant growth and development processes, such as cell wall modification, cytoskeleton formation, and hormone synthesis (Vert et al., 2005). The modes of action of BZR1 and BES1 are currently known for only a limited set of BR-responsive genes. BZR1 binds to the CGTG(T/C)G motif found in the promoters of BR biosynthetic genes, *CPD* and *DWF4,* to suppress their expression (He et al., 2005), while BES1 binds to the CANNTG motif (E-box) in the *SAUR-AC1* promoter to activate gene expression (Yin et al., 2005). In view of the number of physiological processes regulated by BR, it was hypothesized that BZR1 and BES1 heterodimerize with other transcriptional factors to regulate transcriptional processes. Indeed, BES1 has been demonstrated to interact with BIMs (BES1-INTERACTING MYC-LIKE PROTEINS), leading to enhanced binding of BES1 to the *SAUR-AC1* promoter (Yin et al., 2005), MYB30 (MYB DOMAIN PROTEIN 30), a transcription factor that acts as a positive regulator of the hypersensitive cell-death response (Li et al., 2009), and the jumonji (Jmj) domain-containing proteins ELF6 (EARLY FLOWERING 6) and REF6 (RELATIVE OF EARLY FLOWERING 6) that are involved in regulating flowering time (Yu et al., 2008). Since Jmj domain-containing histone demethylases are involved in many developmental processes and diseases, it is possible that recruitment of these proteins by BES1 is one of the ways by which BR affects diverse biological processes. Similarly, MYB30 and BES1 bind to a conserved MYB-binding site and E-box sequences, respectively, in the promoters of genes that are regulated by both BRs and AtMYB30, promoting the expression of a subset of BR target genes (Li et al., 2009).

1.1.4 Brassinosteroid-regulated genes

The best characterized direct BR effects are the early transcriptional changes in response to BR treatment (Müssig et al., 2002; Müssig and Altmann, 2003; Vert et al.,

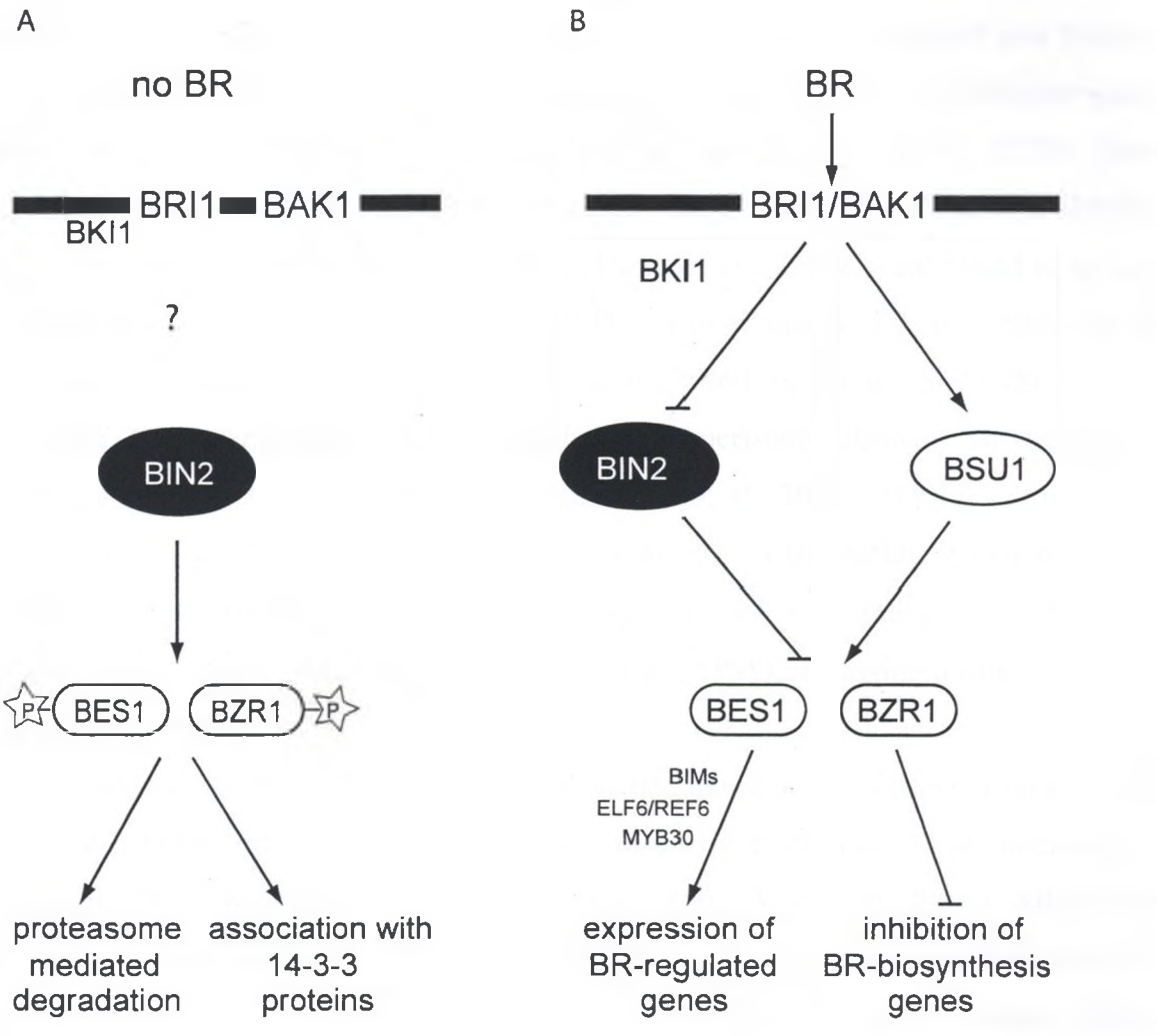
A
no BR
BRI1
BAK1
BKI1
?
BIN2
BES1
BZR1
P
P
proteasome mediated degradation
association with 14-3-3 proteins
B
BR
BRI1/BAK1
BKI1
BIN2
BSU1
BES1
BZR1
BIMs
ELF6/REF6
MYB30
expression of BR-regulated genes
inhibition of BR-biosynthesis genes

2005). BR-regulated genes encode enzymes and proteins involved in diverse physiological processes including cell wall loosening (Müssig and Altmann, 2003), regulation of cell division (Hu et al., 2000), carbohydrate metabolism (Goetz et al., 2000), ethylene (ET) (Yi et al., 1999) and jasmonic acid (JA) biosynthesis (Müssig et al., 2000), protein translation (Jiang and Clouse, 2001; Dhaubhadel et al., 2002), and other physiologic processes (Müssig et al., 2006). Cell wall modifying enzymes, such as xyloglucan endotransglucosylase/hydrolases (XTHs) and expansins were among the first to be identified as BR-regulated. XTHs are known to be involved in cell wall loosening to facilitate wall expansion and in biogenesis of cell wall material (Campbell and Braam, 1999; Rose et al., 2002). The transcript levels of several XTHs from different plant species, such as *BRU1* from *Glycine max* (Zurek and Clouse, 1994), *TCH4* from Arabidopsis (Xu et al., 1995), *LeBRI1* from *Lycopersicon esculentum* (Koka et al., 2000), and *OsXTR1* and *OsXTR3* from *Oryza sativa* (Uozu et al., 2000), were found to be up-regulated by BR treatment. *CYCD3 (CYCLIN D3)*, a gene involved in the regulation of cell division, is another BR-induced gene (Hu et al., 2000). In tomato, *SUS4 (SUCROSE SYNTHASE 4)* transcripts accumulate throughout the meristem following BR treatment, indicating a role for BRs in carbon metabolism (Pien et al., 2001). The expression of β-tubulin gene, *TUB1,* is reduced in *dim (diminuto/dwarf1),* a BR-deficient mutant in rice (Takahashi et al., 1995). Accordingly, the expression of a β-tubulin gene of *Cicer arietinum* is induced by exogenous BRs (Munoz et al., 1998), indicating a role for BRs in microtubule formation.

In addition to the small scale studies on BR genomic responses, several recent studies have identified genome wide BR responses by employing DNA microarrays (Goda et al., 2002; Müssig et al., 2002; Yin et al., 2002; Vert et al., 2005). All studies thus far have focused on the effects of short-term BR treatment of plants and an important outcome of these studies is that BR responses are modest by nature. About 80% of genes consistently detected in these studies showed estimated expression changes of < 2-fold (Vert et al., 2005). BR-regulated genes consist of those that are specifically regulated by BRs, as well as those that show regulation in response to additional phytohormones, such as auxins, gibberellic acid (GA), ethylene (ET) and jasmonic acid (JA), indicating cross-talk of BR with other plant hormones.

1.1.5 Interaction of Brassinosteroids with other phytohormones

BRs interact with other plant hormones in mediating developmental responses (Khripach et al., 1999). Experimental evidence points to interactions of BR with auxin (Mouchel et al., 2006; Hardtke et al., 2007), GA (Bouquin et al., 2001; Shimada et al., 2006), abscisic acid (ABA) (Steber and McCourt, 2001; Abrahám et al., 2003), ET (Yi et al., 1999; Arteca and Arteca., 2001) and JA (Kitanaga et al., 2006; Müssig et al., 2006), primarily in plant growth regulatory processes. With the exception of BR-auxin interaction, little is known in terms of genes how BR interacts with other hormones. Recent progress made towards understanding BR-auxin interaction can serve as a paradigm for how two hormones could interact at multi-levels. Auxin and BR share a number of target genes, many of which are involved in growth related processes (Hardtke et al., 2007). Since promoter regions in BR-responsive genes are enriched in Auxin Response Factor (ARF)-binding sites, and binding sites of BES1 are over-represented in genes regulated by both hormones, regulatory elements in gene promoters represent a point of cross-talk between auxin and BR (Nemhauser et al., 2004). Recently, the BR-regulated BIN2 kinase was demonstrated to phosphorylate ARF2, a member of the ARF family of transcriptional regulators, leading to loss of ARF2 DNA binding and repression activities (Vert et al., 2008). Thus, in this model ARF2 links BR and auxin signaling pathways. In addition to gene coregulation, BR can also promote auxin transport (Li et al., 2005), and optimal auxin action is dependent on BR levels (Mouchel et al., 2006).

The role of BR in plant responses to abiotic stress has become well established over the last decade (Divi and Krishna, 2009a), but there are very few reports indicating how BR interacts with other stress related hormones and their signaling pathways in conferring stress tolerance. While there exists evidence to indicate that BR increases ET and JA levels under normal growth conditions (Arteca and Arteca, 2001; Kitanaga et al., 2006), there appears to be only one report linking BR with increase in ABA levels in the lower plant *Chlorella vulgaris* under stress condition (Bajguz, 2009). Very recently it has been demonstrated that ABA inhibits BR signaling through phosphorylation of BES1 (Zhang et al., 2009). Currently there are no studies at the genetic level as to how BR interacts with other hormones under stress conditions.

1.1.6 Brassinosteroid-mediated stress tolerance

Similar to the growth promoting effects of BR, the stress protective properties of BRs had also been noticed prior to the time research on BR caught the interest of the larger plant community. However, these preliminary studies manifested considerable variability in the efficacy of BRs to promote stress tolerance, which likely contributed to the relatively slower pace of progress made in this direction. It is believed that the mode of BR application (seed soak, root soak or foliar spray), as well as the developmental stages at which BR was applied, were the primary reasons for the inconsistency in the results of earlier studies (Krishna, 2003; Divi and Krishna, 2009a). Recent attempts to study BR effects on plant stress responses under standardized conditions have indeed yielded reproducible effects. These studies have largely contributed towards understanding BR effects on diverse processes that converge into producing enhanced tolerance to a broad range of stresses (Figure 1.4; Divi and Krishna, 2009a).

TEMPERATURE STRESS

The effects of BR on plant's ability to cope with high and low temperatures have been evaluated in several studies. Positive consequences of BRs in combating chilling stress were reported in maize, cucumber, tomato and rice (He et al., 1991; Katsumi, 1991; Kamuro and Takatsuto, 1991). A general conclusion that can be derived from these studies is that the BR effects on growth and yield are more pronounced during cold stress conditions than under normal conditions. More recently, the regulatory relationship between BR and chilling was investigated in a proteomic study using mung bean epicotyls. Treatment with 24-epibrassinolde (EBR), a BR, could partly recover the elongation of mung bean epicotyls after initial suppression of growth by chilling conditions (Huang et al., 2006). Concomitantly, 17 proteins observed to be down-regulated by chilling stress were up-regulated by EBR. These up-regulated proteins were functionally linked with methionine assimilation, ATP synthesis, cell wall construction, and stress response (Huang et al., 2006).

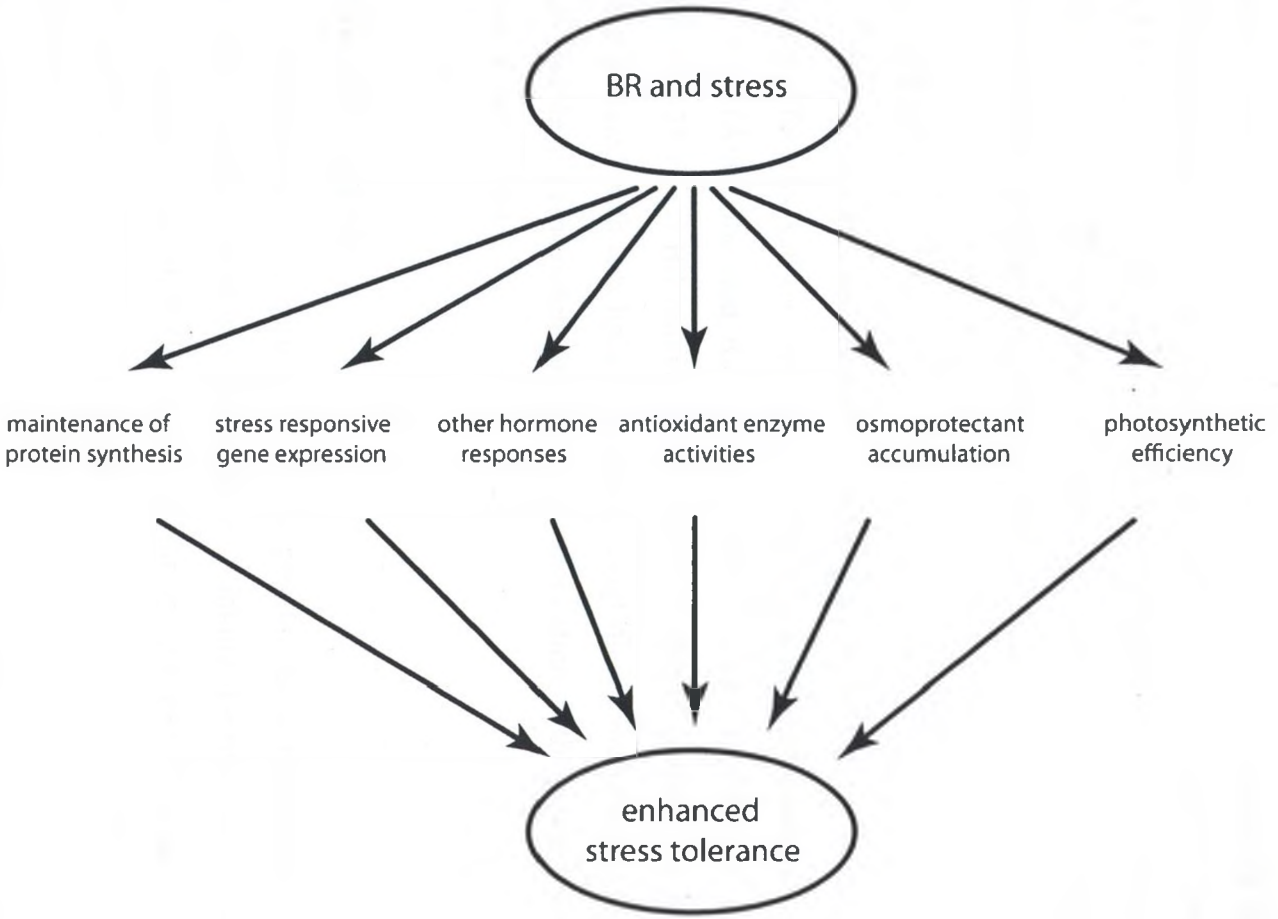
BR and stress
maintenance of protein synthesis
stress responsive gene expression
other hormone responses
antioxidant enzyme activities
osmoprotectant accumulation
photosynthetic efficiency
enhanced stress tolerance

The positive effects of BR under high temperature conditions were noted in tomato, as better photosynthetic efficiency, *in vitro* pollen germination and pollen tube growth, and reduction in pollen bursting as compared to untreated plants. These effects correlated with higher accumulation of mitochondrial small heat shock proteins (Singh and Shono, 2005), reduction in total hydrogen peroxide and malonaldehyde contents, and increases in the activities of antioxidant enzymes such as superoxide dismutase (SOD), ascorbate peroxidase (APX), guaiacol peroxidase (GPOD), and catalase (CAT) in BR-treated tomato plants (Ogweno et al., 2007). This BR-mediated increase in carboxylation efficiency and antioxidant enzyme activities must contribute to mitigating the detrimental effects of high temperatures on plant growth.

SALT STRESS

Salinity stress inhibits seed germination and plant growth. BR reduced the inhibitory effects of salt on seed germination in *Eucalyptus camaldulensis* (Sasse et al., 1995), rice (Anuradha and Rao, 2001), and *B. napus* (Kagale et al., 2007). In salt sensitive IR-28 rice, EBR reduced the extent of oxidative damage incurred by salt stress, which correlated with less lipid peroxidation, significant increase in the activity of APX, higher soluble protein content and higher accumulation of the protective osmolyte proline (Ozdemir et al., 2004).

DROUGHT STRESS

Measurements of both growth and physiological parameters suggest that BRs diminish the negative effects of water stress. Soaking the roots of *Robinia pseudoacacia* L. seedlings in brassinolide (BL) prior to planting increased the survival and growth of seedlings under simulated drought conditions (Li et al., 2007). BL-treated seedlings accumulated higher levels of osmolytes like proline and soluble sugars, had higher leaf water content and greater increases in the activities of antioxidant enzymes SOD, peroxidase (POD) and CAT as compared to untreated seedlings. Also, the stress-induced reduction in the transpiration rate, stomatal conductance and malondialdehyde content was less severe in BL-treated seedlings as compared to untreated seedlings (Li et al.,

2007). A drought susceptible variety of French bean was less affected in nodule number, nodulated root mass and root length under drought stress in response to EBR treatment (Upreti and Murti, 2004).

PATHOGEN ATTACK

The potential of BR to induce resistance to a broad range of pathogens, including fungus, bacteria and virus, was demonstrated in tobacco and rice (Nakashita et al., 2003). Tobacco plants treated with BL exhibited enhanced resistance to the viral pathogen tobacco mosaic virus (TMV), the bacterial pathogen *Pseudomonas syringae*, and the fungal pathogen *Oidium* sp. Similarly, BL-treated rice plants were resistant against rice blast and bacterial blight caused by *Magnaporthe oryzae* and *Xanthomonas oryzae,* respectively. Application of brassinazole (Brz), a BR biosynthesis inhibitor, had a suppressive effect in a dose dependent manner on the defense response of tobacco against TMV, indicating that endogenous BR is involved in disease resistance (Nakashita et al., 2003). Interestingly, in this study BL treatment had no affect on endogenous salicylic acid (SA) levels or the expression of pathogenesis-related (*PR*) genes, suggesting that BR-mediated disease resistance is distinct from the SA-induced systemic acquired resistance (SAR). In contrast to these findings, higher *PR* gene expression in response to BR treatment had been noted in a few studies. The BR-deficient mutant *cpd* showed remarkably lower expression of *PR-1*, *PR-2*, and *PR-5* as compared to WT, but overexpression of the *CPD* cDNA resulted in a significant induction of these genes in the complemented lines (Szekeres et al., 1996). Short-term treatment (1 h and 6 h) of Arabidopsis seedlings with BL also induced the expression of *PR-1* and *PR-2* genes (Seo et al., 2008). These results together make a case for *PR* genes to be primary response genes of BR. Surely then, the mechanism by which BR induces their expression warrants exploration in the future.

OTHER STRESSES

The involvement of BR in signaling events during UV-B stress (280-315 nm) was investigated in Arabidopsis BR-deficient (*det2, dim1, cpd*) and BR-insensitive (*bri1*) mutants (Sävenstrand et al., 2004). These mutants showed reduced expression of a set of UV-B responsive defense genes [chalcone synthase (*CHS*), *PYROA*, *PR-5*, and a gene

regulated by very low levels of UV-B, *MEB5.2*] as compared to WT. Interestingly, the expression of *PR-5* transcripts was most affected by BR-deficiency. Overall, these results indicate that a complete BR pathway is required for proper UV-B dependent gene expression in Arabidopsis (Sävenstrand et al., 2004).

A few studies have demonstrated that BR treatment can protect against the toxic effects of heavy metals (Hasan et al., 2008), as well as block the uptake and accumulation of heavy metals (Sharma and Bhardwaj, 2007). While earlier studies suggested that BRs can protect plants from chemical damage caused by pesticides and insecticides (Cutler, 1991) these effects have not been substantiated in recent studies.

GENETIC EVIDENCE FOR THE ROLE OF BR IN PLANT STRESS RESPONSES

Although numerous studies described so far have suggested a role for BR in plant stress responses, only a few genetic studies have been conducted to confirm this property. The most convincing evidence comes from the analysis of knockout (KO) mutants of *OsGSK1*, the rice ortholog of *BIN2,* a negative regulator of BR signaling (Koh et al., 2007). The *OsGSK1* KO mutants obtained by T-DNA insertion showed enhanced tolerance to cold, heat, salt, and drought stresses when compared with non-transgenic (NT) segregants. For example, the wilting ratios for KO mutants were about 20, 26 and 36% lower as compared with NT plants after cold, heat, and salt stress, respectively. Furthermore, higher expression of abiotic stress-responsive genes was observed in the KO plants under different abiotic stress conditions. The strong likeness of these results with those obtained in the systemic studies carried out in our laboratory using BR-treated *B. napus* and Arabidopsis (Dhaubhadel et al., 1999; Kagale et al., 2007), strongly suggest that BR has roles in plant stress responses.

SYSTEMATIC STUDY TO DISSECT THE ROLE OF BR IN ABIOTIC STRESS TOLERANCE

To systematically dissect the mechanisms involved in BR-mediated tolerance to abiotic stresses, first it was established that BR treatment could consistently increase the freezing, heat and drought tolerance of plants (Wilen et al., 1995; Dhaubhadel et al., 1999; Kagale et al., 2007). Next, the effect of BR on the expression of prototype genes

up-regulated in response to heat, cold and drought stress were studied in *B. napus* and Arabidopsis. Interestingly, while BR-treated *B. napus* seedlings accumulated significantly higher levels of heat shock proteins (hsps) in response to heat stress (HS) (Dhaubhadel et al., 1999), there was little to no difference in hsp levels in BR-treated Arabidopsis seedlings as compared to untreated seedlings (Kagale et al., 2007). In response to cold stress, transcript levels of structural genes involved in cold and dehydration tolerance (*RD29A*, an ortholog of *BN115* and *COR47*) were observed at much higher levels in BR-treated Arabidopsis seedlings as compared to untreated seedlings. By contrast, there were no noticeable differences between untreated and treated *B. napus* seedlings in the expression of regulatory genes *BNCBF5* and *BNDREB*, and structural genes *BN115, BN28*, and *hsp90* (Kagale et al., 2007). While these results indicate that BR-mediated stress-responsive gene expression profiles are somewhat different in *B. napus* and Arabidopsis, it is also clear that, in general, there is higher induction of stress-responsive genes in BR-treated *vs.* untreated seedlings.

Further investigation of why BR-treated *B. napus* seedlings accumulate higher levels of hsps indicated that BR treatment both limits the loss of the components of the translational apparatus during heat stress, and increases their levels during recovery, which correlate with higher hsp synthesis during stress, more rapid resumption of cellular protein synthesis following HS and a higher survival rate (Dhaubhadel et al., 2002). To identify additional BR-induced gene expression changes in *B. napus* seedlings, the differential display–reverse transcription PCR technique was used. Substantial changes were identified in the expression levels of genes encoding a mitochondrial transcription termination factor (mTERF)-related protein, glycine-rich protein 22 (GRP22), myrosinase, and 3-ketoacyl-CoA thiolase (Dhaubhadel and Krishna, 2008). Transcripts of mTERF-related protein, *GRP22*, and myrosinase were present at approximately 2-, 4-, and 6-fold higher levels, respectively, in treated seedlings before HS, whereas those of 3-ketoacyl-CoA thiolase rose to higher levels in treated seedlings during exposure to HS. These results indicate that BR treatment in *B. napus* leads to substantial changes in the expression levels of genes involved in a variety of physiologic responses, either before or during stress exposure.

1.1.7 Objectives and significance of the present research

The potential of BRs to increase plant resistance to a range of stresses has been established in several studies. BR has also been shown to induce the expression of stress-responsive genes, however, our understanding of the mechanisms by which BR induces stress tolerance is still in its infancy. A systematic and thorough investigation of the molecular mechanism of BR-mediated stress tolerance in model plant systems is important from the standpoint of basic research as well as commercial applications of BR to agriculture.

The objectives of the present study are:

1. to study the effects of exogenous application of BR on dehydration stress in Arabidopsis and to establish conditions under which these effects can be studied in a reproducible manner at the morphological and molecular level,
2. to study the interactions of BR with other plant hormones in mediating stress responses by using various hormone biosynthesis and signaling mutants of Arabidopsis,
3. to identify genes differentially expressed in BR-treated *vs.* untreated Arabidopsis seedlings under no-stress and HS conditions by use of DNA microarrays, and to carry out knockout mutant analysis on a subset of genes for stress-related functions, and
4. to overexpress a BR biosynthetic enzyme AtDWF4 in Arabidopsis seeds and analyze the resulting transgenic plants for stress tolerance.

The results of the present study will shed light on a macro scale on how BR promotes stress tolerance in plants, as well as how BR-mediated regulation of stress responses is integrated with its effects on plant growth and development. Such an understanding is important when contemplating changes of plant architecture, productivity or sustainability through manipulation of BR levels.

1.2 REFERENCES

Abraham, E., Rigo, G., Szekely, G., Nagy, R., Koncz, C., and Szabados, L. (2003). Light dependent induction of proline biosynthesis by abscisic acid and salt stress is inhibited by brassinosteroid in Arabidopsis. Plant Mol. Biol. **51,** 363-372.

Anuradha, S., and Rao, S.S.R. (2001). Effect of brassinosteroids on salinity stress induced inhibition of seed germination and seedling growth of rice (*Oryza sativa* L.). Plant Growth Regul. **33,** 151-153.

Arteca, J.M, and Arteca, R.N. (2001). Brassinosteroid-induced exaggerated growth in hydroponically grown Arabidopsis plants. Physiol. Plant **112,** 104-112.

Bajguz, A. (2009). Brassinosteroid enhanced the level of abscisic acid in chlorella vulgaris subjected to short-term heat stress. J. Plant Physiol. **166,** 882-886.

Bajguz, A., and Tretyn, A. (2003). The chemical characteristic and distribution of brassinosteroids in plants. Phytochemistry **62,** 1027-1046.

Bancos, S., Nomura, T., Sato, T., Molnar, G., Bishop, G., Koncz, C., Yokota, T., Nagy, F. and Szekeres, M. (2002). Regulation of transcript levels of the arabidopsis cytochrome P450 genes involved in brassinosteroid biosynthesis. Plant Physiol. **130,** 504-513.

Bishop, G.J., and Yokota, T. (2001). Plants steroid hormones, brassinosteroids: current highlights of molecular aspects on their synthesis/metabolism, transport, perception and response. Plant Cell Physiol. **42,** 114-120.

Bishop, G.J., Nomura, T., Yokota, T., Harrison, K., Noguchi, T., Fujioka, S., Takatsuto, S., Jones, J.D., and Kamiya, Y. (1999). The tomato DWARF enzyme catalyses C-6 oxidation in brassinosteroid biosynthesis. Proc. Natl. Acad. Sci. USA **96,** 1761-1766.

Bouquin, T., Meier, C., Foster, R., Nielsen, M.E., and Mundy, J. (2001). Control of specific gene expression by gibberellin and brassinosteroid. Plant Physiol. 127, 450-458.

Campbell, P., and Braam, J. (1999). Xyloglucan endotransglycosylases: diversity of genes, enzymes and potential wall-modifying functions. Trends. Plant Sci. **4,** 361-366.

Choe, S. (2004). Brassinosteroid biosynthesis and metabolism. In Plant Hormones: Biosynthesis, Signal Transduction and Action, P.J. Davies, ed (Dordrecht: Kluwer), pp. 156–178

Choe, S., Dilkes, B.P., Fujioka, S., Takatsuto, S., Sakurai, A., and Feldmann, K.A. (1998). The DWF4 gene of Arabidopsis encodes a cytochrome P450 that mediates

multiple 22alpha-hydroxylation steps in brassinosteroid biosynthesis. Plant Cell **10,** 231-243.

Choe, S., Tanaka, A., Noguchi, T., Fujioka, S., Takatsuto, S., Ross, A., Tax, F., Yoshida, S. and Feldmann, K. (2000). Lesions in the sterol Δ^7 reductase gene of arabidopsis cause dwarfism due to a block in brassinosteroid biosynthesis. Plant J. **21,** 431-443.

Chory, J., Nagpal, P., and Peto, C. (1991). Phenotypic and genetic analysis of *det*2, a new mutant that affects light-regulated seedling development in Arabidopsis. Plant Cell **3,** 445-459.

Clouse, S., and Sasse, J. (1998). Brassinosteroids: Essential regulators of plant growth and development. Annu. Rev. Plant Physiol. Plant Mol. Biol. **49,** 427-451.

Clouse, S.D. (2002). Brassinosteroid signal transduction: clarifying the pathway from ligand perception to gene expression. Mol. Cell **10,** 973-982.

Cutler, G. (1991). Brassinosteroids through the looking glass: an appraisal. In Brassinosteroids: Chemistry, Bioactivity and Applications, H.G. Cutler, T. Yokota, and G. Adam, eds (Washington: ACS Symp Ser 47, American Chemical Society), pp. 334-345.

Dhaubhadel, S. and Krishna, P. (2008). Identification of differentially expressed genes in brassinosteroid-treated brassica napus seedlings. J. Plant Growth. Regul. **27,** 297-308.

Dhaubhadel, S., Browning, K., Gallie, D. and Krishna, P. (2002). Brassinosteroid functions to protect the translational machinery and heat-shock protein synthesis following thermal stress. Plant J. **29,** 681-691.

Dhaubhadel, S., Chaudhary, S., Dobinson, K.F., and Krishna, P. (1999). Treatment with 24-epibrassinolide, a brassinosteroid, increases the basic thermotolerance of *Brassica napus* and tomato seedlings. Plant Mol. Biol. **40,** 333-342.

Divi, U.K., and Krishna, P. (2009a). Brassinosteroids confer stress tolerance. In Plant stress biology: Genomics goes systems biology, H. Hirt, ed (Weinheim: Wiley-VCH), pp. 119-135.

Divi, U.K., and Krishna, P. (2009b). Brassinosteroid: a biotechnological target for enhancing crop yield and stress tolerance. N Biotechnol. (doi:10.1016/j.nbt.2009.07.006).

Fujioka, S., and Yokota, T. (2003). Biosynthesis and metabolism of brassinosteroids. Annu. Rev. Plant Biol. **54,** 137-164.

Fujioka, S., Inoue, T., Takatsuto, S., Yanagisawa, T., Yokota, T., and Sakurai A. (1995). Identification of a new brassinosteroid, cathasterone, in cultured cells of

Catharanthus roseus as a biosynthetic precursor of teasterone. Biosci. Biotechnol. Biochem. **59,** 1543–1547.

Fujioka, S., Takatsuto, S., and Yoshida, S. (2002). An early C-22 oxidation branch in the brassinosteroid biosynthetic pathway. Plant Physiol. **130,** 930-939.

Gampala, S.S., Kim, T., He, J., Tang, W., Deng, Z., Bai, M., Guan, S., Lalonde, S., Sun, Y., and Gendron, J.M. (2007). An essential role for 14-3-3 proteins in brassinosteroid signal transduction in *Arabidopsis*. Dev. Cell **13,** 177-189.

Goda, H., Shimada, Y., Asami, T., Fujioka, S., and Yoshida, S. (2002). Microarray analysis of brassinosteroid-regulated genes in arabidopsis. Plant Physiol. **130,** 1319-1334.

Grove, M. D., Spencer, G. F., Rohwedder, W. K., Mandava, N., Worley, J. F., Warthen, J. D., Steffens, G. L., Flippen-Anderson, J. L., and Cook, J. C. (1979). Brassinolide, a plant growth-promoting steroid isolated from brassica napus pollen. Nature **281**, 216-217.

Hardtke, C. (2007). Transcriptional auxin-brassinosteroid crosstalk: Who's talking?. Bioessays **29,** 1115-1123.

Hasan, S. A., Hayat, S., Ali, B., and Ahmad, A. (2008). 28-homobrassinolide protects chickpea (*Cicer arietinum*) from cadmium toxicity by stimulating antioxidants. Environ. Pollut. **151**, 60-66.

He, J., Gendron, J., Sun, Y., Gampala, S., Gendron, N., Sun, C. and Wang, Z. (2005). BZR1 is a transcriptional repressor with dual roles in brassinosteroid homeostasis and growth responses. Science **307,** 1634-1638.

He, R.Y., Wang, G.J., and Wang, X.S. (1991). Effects of brassinolide on growth and chilling resistance of maize seedlings. In Brassinosteroids: Chemistry, Bioactivity and Applications, H.G. Cutler, T. Yokota, and G. Adam, eds (Washington: ACS Symp Ser 47, American Chemical Society), pp. 220-230.

He, Z., Wang, Z., Li, J., Zhu, Q., Lamb, C., Ronald, P., and Chory, J. (2000). Perception of brassinosteroids by the extracellular domain of the receptor kinase BRI1. Science **288,** 2360-2363.

Hu, Y., Bao, F., and Li, J. (2000). Promotive effect of brassinosteroids on cell division involves a distinct CycD3-induction pathway in Arabidopsis. Plant J. **24,** 693-701.

Huang, B., Chu, C.H., Chen, S.L., Juan, H.F., and Chen, Y.M. (2006). A proteomics study of the mung bean epicotyl regulated by brassinosteroids under conditions of chilling stress. Cell Mol. Biol. Lett. **11,** 264-278.

Jiang, J., and Clouse, S.D. (2001). Expression of a plant gene with sequence similarity to animal TGF-beta receptor interacting protein is regulated by brassinosteroids and required for normal plant development. Plant J. **26,** 35-45.

Kamuro, Y., and Takatsuto, S. (1991). Capability for and problems of practical uses of brassinosteroids. In Brassinosteroids: Chemistry, Bioactivity and Applications, H.G. Cutler, T. Yokota, and G. Adam, eds (Washington: ACS Symp Ser 47, American Chemical Society), pp. 292-297.

Katsumi, M. (1991). Physiological modes of brassinolide action in cucumber hypocotyl growth. In Brassinosteroids: Chemistry, Bioactivity and Applications, H.G. Cutler, T. Yokota, and G. Adam, eds (Washington: ACS Symp Ser 47, American Chemical Society), pp. 246-254.

Khripach, V., Zhabinski V., and de Groot A. (1999). Brassinosteroids: A new class of phytohormones. (San Diego: Academic Press), pp. 236.

Kitanaga, Y., Jian, C., Hasegawa, M., Yazaki, J., Kishimoto, N., Kikuchi, S., Nakamura, H., Ichikawa, H., Asami, T., and Yoshida, S. (2006). Sequential regulation of gibberellin, brassinosteroid, and jasmonic acid biosynthesis occurs in rice coleoptiles to control the transcript levels of anti-microbial thionin genes. Biosci. Biotechnol. Biochem. **70**, 2410-2419.

Koh, S., Lee, S.C., Kim, M.K., Koh, J.H., Lee, S., An, G., Choe, S., and Kim, S.R. (2007). T-DNA tagged knockout mutation of rice *OsGSK1*, an orthologue of Arabidopsis *BIN2*, with enhanced tolerance to various abiotic stresses. Plant Mol. Biol. **65,** 453-466.

Koka, C.V., Cerny, R.E., Gardner, R.G., Noguchi, T., Fujioka, S., Takatsuto, S., Yoshida, S., and Clouse, S.D. (2000). A putative role for the tomato genes DUMPY and CURL-3 in brassinosteroid biosynthesis and response. Plant. Physiol. 122, 85-98.

Krishna, P. (2003). Brassinosteroid-mediated stress responses. J. Plant Growth. Regul. **22,** 289-297.

Kwon, M., and Choe, S. (2005) Brassinosteroid biosynthesis and dwarf mutants. J. Plant Biol. **48,** 1-15.

Li, J., and Nam, K. (2002). Regulation of brassinosteroid signaling by a GSK3/SHAGGY-like kinase. Science **295**, 1299-1301.

Li, L., Xu, J., Xu, Z., and Xue, H. (2005). Brassinosteroids stimulate plant tropisms through modulation of polar auxin transport in brassica and arabidopsis. Plant Cell 17, 2738-2753.

Li, L., Yu, X., Thompson, A., Guo, M., Yoshida, S., Asami, T., Chory, J., and Yin, Y. (2009). Arabidopsis MYB30 is a direct target of BES1 and cooperates with BES1 to regulate brassinosteroid-induced gene expression. Plant J. 58, 275-286.

Mandava, N.B. (1988). Plant growth-promoting brassinosteroids. Ann. Rev. Plant Physiol. Plant. Mol. Biol. **39,** 23-52.

Mitchell, J.W., Mandava, N.B., Worley, J.F., Plimmer, J.R., and Smith, M.V. (1970). Brassins: a new family of plant hormones from rape pollen. Nature **225,** 1065-1066.

Mora-Garcia, S., Vert, G., Yin, Y., Cano-Delgado, A., Cheong, H., and Chory, J. (2004). Nuclear protein phosphatases with Kelch-repeat domains modulate the response to brassinosteroids in Arabidopsis. Genes Dev. 18, 448-460.

Mouchel, C.F., Osmont, K.S., and Hardtke, C.S. (2006). BRX mediates feedback between brassinosteroid levels and auxin signalling in root growth. Nature **443,** 458-461.

Munoz, F.J., Labrador, E., and Dopico, B. (1998). Brassinolides promote the expression of a new *Cicer arietinum* beta-tubulin gene involved in the epicotyl elongation. Plant Mol. Biol. **37**, 807-817.

Müssig, C., and Altmann, T. (2003). Genomic brassinosteroid effects. J. Plant Growth Regul. **22,** 313-324.

Müssig, C., Biesgen, C., Lisso, J., Uwer, U., Weiler, E.W. and Altmann, T. (2000). A novel stress-inducible 12-oxophytodienoate reductase from *Arabidopsis thaliana* provides a potential link between brassinosteroid action and jasmonic-acid synthesis. J. Plant Physiol. **157,** 143-152.

Müssig, C., Fischer, S., and Altmann, T. (2002). Brassinosteroid-regulated gene expression. Plant Physiol. 129, 1241-1251.

Müssig, C., Lisso, J., Coll-Garcia, D., and Altmann, T. (2006). Molecular analysis of brassinosteroid action. Plant Biol. **8,** 291-296.

Nakashita, H., Yasuda, M., Nitta, T., Asami, T., Fujioka, S., Arai, Y., Sekimata, K., Takatsuto, S., Yamaguchi, I., and Yoshida, S. (2003). Brassinosteroid functions in a broad range of disease resistance in tobacco and rice. Plant. J. **33,** 887-898.

Nemhauser, J., Mockler, T., and Chory, J. (2004). Interdependency of brassinosteroid and auxin signaling in arabidopsis. PLoS Biol. 2, e258.

Noguchi, T., Fujioka, S., Choe, S., Takatsuto, S., Tax, F.E., and Feldmann, K.A. (2000). Biosynthetic pahways of brassinolide in Arabidopsis. Plant Physiol. **124,** 201-209.

Noguchi, T., Fujioka, S., Takatsuto, S., Sakurai, A., Yoshida, S., Li, J., and Chory, J. (1999). Arabidopsis *det2* is defective in the conversion of (24R)-24-methylcholest-4-En-3-one to (24R)-24-methyl-5alpha-cholestan-3-one in brassinosteroid biosynthesis. Plant Physiol. **120,** 833-840.

Ogweno, J.O., Song, X.S., Shi, K., Hu, W.H., Mao, W.H., Zhou, Y.H., Yu, J.Q., and Nogués, S. (2007). Brassinosteroids alleviate heat-induced inhibition of photosynthesis by increasing carboxylation efficiency and enhancing antioxidant systems in *Lycopersicon esculentum*. J. Plant Growth Regul.**27**, 49-57.

Ohnishi, T., Szatmari, A.M., Watanabe, B., Fujita, S., Bancos, S., Koncz, C., Lafos, M., Shibata, K., Yokota, T., Sakata, K., Szekeres, M., and Mizutani, M. (2006). C-23 hydroxylation by Arabidopsis CYP90C1 and CYP90D1 reveals a novel shortcut in brassinosteroid biosynthesis. Plant Cell **18,** 3275-3288.

Özdemir, F., Bor, M., Demiral, T., and Turkan, I. (2004). Effects of 24-epibrassinolide on seed germination, seedling growth, lipid peroxidation, proline content and antioxidative system of rice (*Oryza sativa* L.) under salinity stress. Plant Growth Regul. **42,** 203-211.

Pien, S., Wyrzykowska, J., and Fleming, A.J. (2001). Novel marker genes for early leaf development indicate spatial regulation of carbohydrate metabolism within the apical meristem. Plant J. **25,** 663-67.

Sasse, J.M., Smith, R., and Hudson, I. (1995). Effect of 24-epibrassinolide on germination of seed of *Eucalyptus camaldulensis* in saline conditions. Proc. Plant Growth Regul. Soc. Am. **22,** 136-141.

Seo, P.J., Lee, A.K., Xiang, F., and Park, C.M. (2008). Molecular and functional profiling of Arabidopsis pathogenesis-related genes: insights into their roles in salt response of seed germination. Plant Cell Physiol. **49,** 334-344.

Sharma, P., and Bhardwaj, R. (2007). Effects of 24-epibrassinolide on growth and metal uptake in brassica juncea L. under copper metal stress. Acta Physiol. Plant.. 29, 259-263.

Shimada, A., Ueguchi-Tanaka, M., Sakamoto, T., Fujioka, S., Takatsuto, S., Yoshida, S., Sazuka, T., Ashikari, M., and Matsuoka, M. (2006). The rice spindly gene functions as a negative regulator of gibberellin signaling by controlling the suppressive function of the della protein, *slr1*, and modulating brassinosteroid synthesis. Plant J. **48,** 390-402.

Shimada, Y., Fujioka, S., Miyauchi, N., Kushiro, M., Takatsuto, S., Nomura, T., Yokota, T., Kamiya, Y., Bishop, G. J., and Yoshida, S. (2001). Brassinosteroid-6-oxidases from arabidopsis and tomato catalyze multiple c-6 oxidations in brassinosteroid biosynthesis. Plant physiol. **126,** 770-779.

Shimada, Y., Goda, H., Nakamura, A., Takatsuto, S., Fujioka, S., and Yoshida, S. (2003). Organ-specific expression of brassinosteroid-biosynthetic genes and distribution of endogenous brassinosteroids in arabidopsis. Plant physiol. **131,** 287-297.

Takahashi, T., Gasch, A., Nishizawa, N., and Chua, N.H. (1995). The *DIMINUTO* gene of Arabidopsis is involved in regulating cell elongation. Genes Dev. **9,** 97-107.

Tanaka, K., Asami, T., Yoshida, S., Nakamura, Y., Matsuo, T., and Okamoto, S. (2005). Brassinosteroid homeostasis in arabidopsis is ensured by feedback expressions of multiple genes involved in its metabolism. Plant Physiol. 138, 1117-1125.

Tang, W., Deng, Z., Oses-Prieto, J., Suzuki, N., Zhu, S., Zhang, X., Burlingame, A. and Wang, Z. (2008). Proteomics studies of brassinosteroid signal transduction using prefractionation and two-dimensional DIGE. Mol. Cell Proteomics **7,** 728-738.

Upreti, K.K., and Murti, G.S.R. (2004). Effects of brassinosteroids on growth, nodulation, phytohormone content and nitrogenase activity in French bean under water stress. Biol. Plant **41**, 407–411.

Vert, G., and Chory, J. (2006). Downstream nuclear events in brassinosteroid signaling. Nature **441,** 96-100.

Vert, G., Nemhauser, J., Geldner, N., Hong, F., and Chory, J. (2005). Molecular mechanisms of steroid hormone signaling in plants. Annu. Rev. Cell Dev. Biol. 21, 177-201.

Vert, G., Walcher, C. L., Chory, J., and Nemhauser, J. L. (2008). Integration of auxin and brassinosteroid pathways by auxin response factor 2. Proc. Natl. Acad. Sci. U. S. A 105, 9829-9834.

Wang, X., and Chory, J. (2006). Brassinosteroids regulate dissociation of BKI1, a negative regulator of BRI1 signaling, from the plasma membrane. Science 313, 1118-1122.

Wang, X., Kota, U., He, K., Blackburn, K., Li, J., Goshe, M. B., Huber, S. C., and Clouse, S. D. (2008). Sequential transphosphorylation of the bri1/bak1 receptor kinase complex impacts early events in brassinosteroid signaling. Dev. Cell 15, 220-235.

Wilen, R.W., Sacco, M., Gusta, L.V., and Krishna, P. (1995). Effects of 24-epibrassinolide on freezing and thermotolerance of bromegrass (*Bromus inermis*) cell cultures. Physiol. Plant **95,** 195-202.

Yi, H.C., Joo, S., Nam, K.H., Lee, J.S., Kang, B.G., and Kim, W.T. (1999). Auxin and brassinosteroid differentially regulate the expression of three members of the 1-

aminocyclopropane-l-carboxylate synthase gene family in mung bean (*Vigna radiata* L.). Plant Mol. Biol. **41,** 443-454.

Yu, X., Li, L., Li, L., Guo, M., Chory, J., and Yin, Y. (2008). Modulation of brassinosteroid-regulated gene expression by jumonji domain-containing proteins ELF6 and REF6 in arabidopsis. Proc. Natl. Acad. Sci. U. S. A 105, 7618-7623.

Zhang, S., Cai, Z., and Wang, X. (2009). The primary signaling outputs of brassinosteroids are regulated by abscisic acid signaling. Proc. Natl. Acad. Sci. U. S. A 106, 4543-4548.

Zurek, D.M., and Clouse, S.D. (1994). Molecular cloning and characterization of a brassinosteroid-regulated gene from elongating soybean (*Glycine max* L.) epicotyls. Plant Physiol. **104,** 161-170.

CHAPTER 2

Brassinosteroid confers dehydration tolerance in *Arabidopsis thaliana*

A version of this chapter has been published as part of the following article.

Kagale, S., Divi, U.K., Krochko, J.E., Keller, W.A., and Krishna, P. (2007). Brassinosteroid confers tolerance in *Arabidopsis thaliana* and *Brassica napus* to a range of abiotic stresses. Planta **225**, 353-364.

CHAPTER 2

2.1 INTRODUCTION

Brassinosteroids (BRs) are a class of plant steroidal compounds that are essential for normal growth and development of plants. BRs regulate a wide range of biological processes, such as cell division and expansion, xylem differentiation, seed germination, vegetative growth and apical dominance (Sasse, 2003). Although the growth promoting properties of BRs were known in the early 1970s, the evidence for an essential role for BRs in plant development came through the isolation and characterization of BR-deficient and BR-insensitive mutants. BR-deficiency in biosynthetic mutants leads to phenotypic alterations such as dwarfism, small dark-green leaves, delayed flowering, senescence and reduced fertility, all of which can be rescued by exogenous treatment with BR in a dose dependent manner (Kwon and Choe, 2005). These observations indicate that BR functions as a hormone, and indeed, BR is now considered a plant hormone.

In addition to its role in plant growth and development, BR has been linked with protection of plants against a variety of environmental stresses, including high and low temperature stress, drought, salinity, herbicidal injury, and pathogen attack (Khripach et al., 2000; Krishna, 2003). However, studies confirming the ability of BR to modulate plant stress responses, as well as providing a framework under which such effects of BR can be studied in a reproducible manner are lacking. Previous studies in the lab showed that treatment of *Brassica napus* and tomato seedlings with 24-epibrassinolide (EBR), a BR, increased the basic thermotolerance of seedlings and led to higher accumulation of the major classes of heat shock proteins (hsps) as compared to untreated seedlings (Dhaubhadel et al., 1999). Further investigation into how hsps accumulate to higher levels in EBR-treated seedlings revealed that EBR modulates the translational machinery, leading to higher hsp synthesis during heat stress (HS) and more rapid resumption of cellular protein synthesis following HS (Dhaubhadel et al., 2002). Genes, other than hsps, associated with varied cellular processes were also up-regulated by EBR in *B. napus* seedlings (Dhaubhadel and Krishna, 2008).

The potential of BRs for increasing plant tolerance against drought, cold and soil salinity had been realized in preliminary studies (Krishna, 2003; Divi and Krishna, 2009). For instance, BR reduced the inhibitory effects of salt on seed germination in *Eucalyptus camaldulensis* (Sasse et al., 1995), rice (Anuradha and Rao, 2001), and *B. napus* (Kagale et al., 2007). In salt sensitive IR-28 rice, EBR reduced the extent of oxidative damage incurred by salt stress, which correlated with less lipid peroxidation, significant increase in the activity of ascorbate peroxidase (APX), higher soluble protein content and higher accumulation of the protective osmolyte proline (Ozdemir et al., 2004). Soaking the roots of *Robinia pseudoacacia* L. seedlings in brassinolide (BL), the most active BR, prior to planting increased the survival and growth of seedlings under simulated drought conditions (Li et al., 2007). These seedlings accumulated higher levels of osmolytes like proline and soluble sugars, had higher leaf water content and greater increases in the activities of antioxidant enzymes as compared to untreated seedlings. A stimulatory effect of BR on the growth of maize and cucumber seedlings was also seen under chilling stress (He et al., 1991; Katsumi, 1991). While these and other similar findings are encouraging, they do not provide the conditions in a model plant system based on which the mechanism of BR-mediated stress tolerance can be investigated in a systematic manner.

We focused on studying the effects of EBR on Arabidopsis, a genetic model system, and *B. napus*, an oil crop plant, under drought, cold and high salt conditions as a means to first confirm this ability of BR and to subsequently use the established experimental conditions to address the mechanism by which BR exerts anti-stress effects. We demonstrated that EBR treatment enhances seedling tolerance to drought and cold stresses in both Arabidopsis and *B. napus*, and helps to overcome a salt stress-induced inhibition of seed germination. The ability of EBR to confer tolerance in plants to a variety of stresses was confirmed through analysis of expression of a subset of drought and cold stress marker genes. Transcriptional changes in these genes were more apparent in EBR-treated Arabidopsis, in particular during earlier time points of stress.

The following chapter describes the standardization of experimental conditions mimicking drought stress, as well as the effects of BR on dehydration stress tolerance in Arabidopsis. EBR-treated Arabidopsis seedlings had greater survival, as compared to

untreated seedlings, under drought stress conditions, as well as higher expression of a subset of drought marker genes.

2.2 MATERIALS AND METHODS

2.2.1 Plant material and growth conditions

Arabidopsis ecotype Columbia, seeds were surface-sterilized by sequentially soaking seeds in 75% ethanol for 1 min, rinsing twice in sterile-distilled water, soaking in 1.05% sodium hypochlorite for 20 min with stirring, and rinsing 4-5 times with sterile distilled water. Surface sterilized seed were plated on 1X Murashige and Skoog medium (Sigma, St. Louis) supplemented with B5 vitamins, 1% (w/v) agar, 1% sucrose, and either 1 μM EBR or 0.01% ethanol (solvent for EBR). The plates were kept for 3 days in the dark at 4°C to encourage synchronized germination and then transferred to 22°C with a 16-h photoperiod (80 $\mu E\ m^{-2}\ s^{-1}$) and allowed to grow for 21 days.

2.2.2 Stress treatments

All experiments were repeated three times. For drought stress, 21-day-old Arabidopsis seedlings grown in the presence or absence of EBR were transplanted into pots containing coarse sand. Seedlings were allowed to re-establish growth for 5 days and then subjected to drought stress by withholding water for up to 96 h. Following drought stress, the seedlings were allowed to recover by watering them regularly for the next 2 days. Seedlings that survived and continued to grow were counted. Values in Figure 2.1B represent average percentages of data obtained in three biological replicates. Plant tissue above the sand was collected at various time points during drought stress and quick-frozen.

2.2.3 RNA isolation and northern blot analysis

Total RNA was isolated from frozen plant tissue using TRIzol reagent (Life Technologies, Burlington, ON, Canada). For northern blot analysis, 10 μg of total RNA was separated on a denaturing formaldehyde agarose gel and blotted onto a Biotrans^{+} membrane (ICN Biomedical, Aurora, OH, USA). Blots were hybridized with ^{32}P-labelled cDNA fragments under the conditions described previously (Krishna et al., 1995).

Following hybridization, the membranes were washed twice in 2 x SSC with 1% SDS at room temperature for 10 min, twice in 0.5 x SSC with 0.5% SDS at 52 ^{0}C for 15 min, and if required, twice in 0.1 x SSC with 0.1% SDS at 65 ^{0}C for 10 min, and autoradiographed. The cDNAs fragments for *RD29A* (accession no. D13044), *ERD10* (accession no. NM_180616), *RD22* (accession no. D10703), *DEHYDRIN* (accession no. NM_127721), were generated by RT-PCR using RNA isolated from drought-stressed Arabidopsis seedlings. The sequences of these cDNA fragments were verified by sequencing and were ^{32}P-labelled and used to detect the corresponding transcripts. The blots were stripped and re-hybridized with an 18S ribosomal DNA fragment to indicate RNA loading.

2.2.4 RT-PCR analysis

Total RNA (7µg) isolated from unstressed and drought-stressed Arabidopsis was reverse transcribed using the oligo $(dT)_{18}$ primer and SuperScript™ First Strand Synthesis System for RT-PCR (Invitrogen, Carlsbad, CA, USA). PCR was carried out with an initial denaturation step of 94^{0}C for 4 min followed by various cycles of denaturation (30 s at 94^{0}C), annealing (45 s at 56^{0}C), and extension (1 min at 72^{0}C). After the last cycle, a final extension was carried out for 5 min at 72^{0}C. PCR was performed for 30 cycles for *DREB2A* (accession no. NM_120623), 23 cycles for *ACTIN* (internal control). The following primers were used: *DREB2A-F* 5' TGACGGTACTACTGTGGCTGAG; *DREB2A-R* 5' GTCGCCATTTAGGTCACGTAG; *ACTIN-F* 5' TGCTCTTCCTCATGCTAT; *ACTIN-R* 5' ATCCTCCGATCCAGACACTG.

2.3 RESULTS

2.3.1 EBR increases drought tolerance in Arabidopsis seedlings

We have found EBR effects on Arabidopsis stress tolerance to be most pronounced when seedlings are grown in the presence of EBR for 21 days (Kagale et al., 2007). Since seedlings receive EBR treatment in petri dishes under sterile conditions, it was not possible to subject them to dehydration stress as such. For this reason,

Arabidopsis seedlings grown in the presence or absence of EBR for 21 days were transplanted to sand and then subjected to drought stress as described under materials and methods. The method was standardized for reproducibility and the experiment was repeated three times. Visible morphological changes in response to drought stress, such as leaf wilting, reduction in growth, and complete drying of some seedlings, were frequently observed in untreated seedlings, but were considerably reduced in EBR-treated seedlings (Figure 2.1A). In accordance with this observation, the survival rate of EBR-treated seedlings was noticeably higher than the survival rate of untreated seedlings. About 80% and 28% of EBR-treated seedlings watered at 72 and 80 h after drought stress, respectively, survived and continued to grow. In comparison, only 35% and 7% of the untreated seedlings survived (Figure 2.1B). All of the untreated seedlings were killed by 80-82 h of drought stress, whereas EBR-treated seedlings remained alive past 90 h of drought treatment. These results demonstrate that EBR treatment increases tolerance to drought stress in Arabidopsis seedlings.

2.3.2 EBR affects the expression of dehydration-responsive genes

Response to drought stress is a relatively well-characterized phenomenon in plants, which results in major reprogramming of gene expression (Ramanjulu and Bartels, 2002; Seki et al., 2002). To determine if EBR affects the expression of known dehydration-responsive genes, such as *RD29A*, *ERD10* and *RD22,* transcript levels of these genes were determined in EBR-treated and untreated seedlings under non-stress and dehydration stress conditions. Transcripts of *RD29A* and *ERD10*, encoding late embryogenesis abundant (LEA) proteins (Yamaguchi-Shinozaki and Shinozaki, 1993; Kiyosue, 1994), accumulated to higher levels (2 to 3-fold) in EBR-treated seedlings at earlier time points of stress (up to approximately 60 h of stress), but at later time points the levels were comparable between untreated and treated seedlings (Figure 2.2A). Transcript levels of *RD22*, an abscisic acid (ABA)-dependent dehydration-responsive gene (Iwasaki et al., 1995), switched from being slightly elevated in EBR-treated seedlings at earlier time points to being higher in untreated seedlings at later time point(s). The differences in the expression of these genes at 72 and 84 h, as well as of a

A

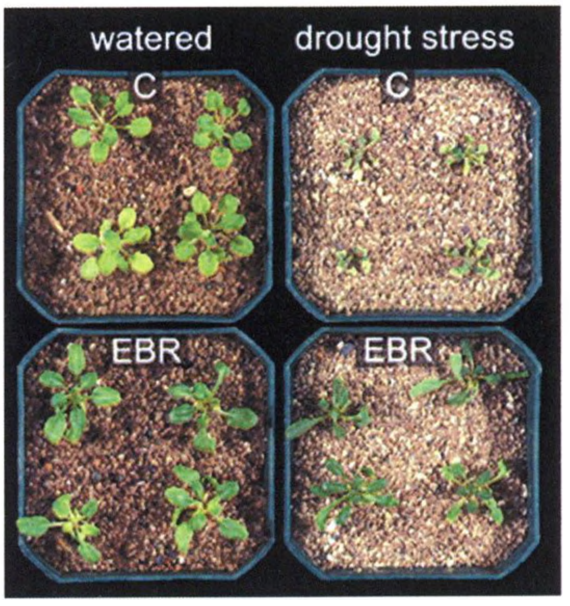
watered
drought stress
C
C
EBR
EBR

B

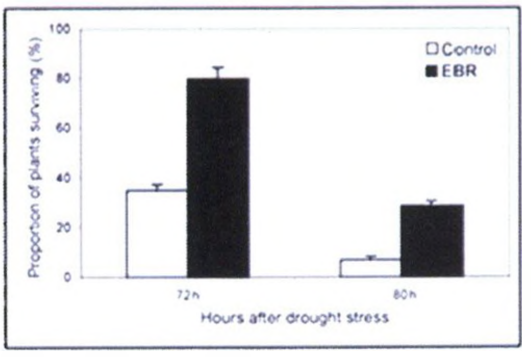
Proportion of plants surviving (%)
100
80
60
40
20
0
Control
EBR
72h
80h
Hours after drought stress

A

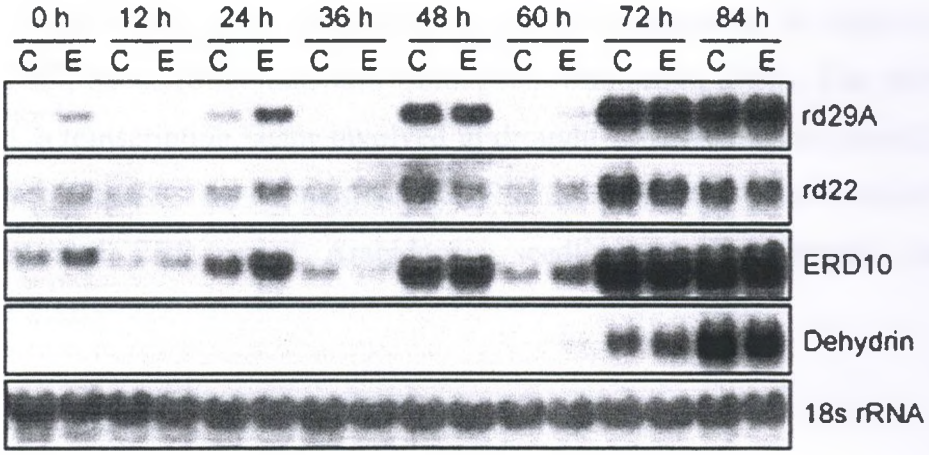
0 h
12 h
24 h
36 h
48 h
60 h
72 h
84 h
C E C E C E C E C E C E C E C E
rd29A
rd22
ERD10
Dehydrin
18s rRNA

B

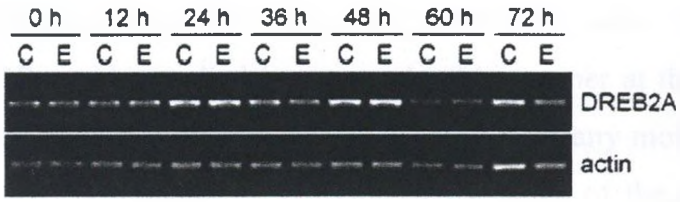
0 h
12 h
24 h
36 h
48 h
60 h
72 h
C E C E C E C E C E C E C E
DREB2A
actin

DEHYDRIN gene in the two sets of seedlings did not appear significant. Interestingly, *RD29A*, *ERD10* and *RD22* showed a circadian rhythm expression pattern at early time points of stress when transcript levels were relatively lower. This was overcome by high expression of transcripts at later time points. These experiments were repeated at least two times and the changes described were reproducible.

Transcription factors of the CBF/DREB (cold-responsive element binding factor/drought-responsive element binding factor) family in Arabidopsis bind to *cis*-acting drought-responsive elements (DRE) and regulate gene expression in response to cold, drought and salt stress (Shinozaki and Yamaguchi-Shinozaki, 2000). The mRNA levels of *DREB2A*, a transcription factor involved in drought-responsive gene expression were analyzed by RT-PCR. The expression of *DREB2A* transcripts was comparable between untreated and EBR-treated Arabidopsis seedlings during drought stress conditions (Figure 2.2B).

2.4 DISCUSSION

Though BRs have been implicated in drought, cold and salt stress responses (Divi and Krishna, 2009; Krishna, 2003), experimental conditions under which the stress alleviating effects of BR can be studied in a reproducible manner at the morphological level have not been described in literature nor have there been any molecular studies in this direction. Thus, there is a lacuna of convincing evidence of the ability of BR in modulating plant responses to a variety of environmental stresses. Our previous studies have established the role of BR in modulating plant responses to high temperature stress (Dhaubhadel et al., 1999; 2002). The present study established conditions to study the effects of BR on drought stress responses in Arabidopsis in a reproducible manner and also provides the first molecular evidence for a role of BR in drought stress tolerance.

That EBR increased drought tolerance in Arabidopsis seedlings was evident both from the reduction in visible morphological symptoms and enhanced percentage of survival (Figure 2.1A). Similar effects of EBR were seen in *B. napus* seedlings (Kagale et al., 2007). These results confirm the ability of BR to increase drought tolerance in seedlings. Further support to this end comes from the observation that EBR treatment

increased expression of marker genes with known responses to drought and cold stress, as well as of genes believed or demonstrated to enhance drought and cold tolerance of plants. However, unlike ABA, which produces dramatic increases in gene expression, we observed only 2 to 5-fold increases in the expression of some of these genes in response to EBR. This is not surprising since BR-regulated genes on average show expression changes of < 2-fold (Vert et al., 2005). Thus, although BR-induced changes in transcript levels are modest, BR-induced changes in plant phenotypes are clear, implying that either BR controls gene expression at other levels or that the changes affected by BR are together sufficient for inducing the phenotypes.

It was consistently noted that *RD29A*, *ERD10* and *RD22* mRNAs accumulated to higher levels in EBR-treated Arabidopsis seedlings at early time points of drought stress, but were either comparable in the two sets of seedlings or higher in untreated seedlings during later time points. The *RD29A* and *ERD10* genes encode a class of proteins that have molecular chaperone-like functions, preventing protein aggregation during water stress (Goyal et al., 2005). The increase in the transcript levels of these genes at earlier time points suggests that EBR-treated seedlings are likely positioned to tolerate stress better right from the beginning. Due to the positive influence of BR on gene expression at the post-transcriptional level (Dhaubhadel et al., 2002), it is possible that this effect is compounded with further increases at the protein level, at least, for some genes (this could not be tested due to unavailability of antibodies).

Similar to the effect in Arabidopsis, EBR also affected higher expression of dehydration-responsive genes *BNPIP1* and *BnD22* in *B. napus* seedlings (Kagale et al., 2007). *BnPIP1* is an aquaporin gene that is involved in water transportation during germination under stress conditions (Gao et al., 1999). The *BnD22* expression was found to be increased by progressive or rapid water stress that disappeared upon rehydration (Reviron et al., 1992). In another study, Desclos et al. (2008) showed that the water-soluble chlorophyll-binding protein (WSCP) and trypsin inhibitor (TI) activities of BnD22 lead to the protection of younger tissues from adverse conditions by maintaining protein integrity and photosynthesis. In our study, the increase in transcript accumulation of these genes correlated with increased drought tolerance of these seedlings, which, in part, may derive from the proposed functions of these genes, such as better distribution of

water, and efficient defense against the large number of proteases produced during stress conditions, respectively. A possible role for BR in controlling aquaporin activities was previously suggested in an indirect study (Morillon et al., 2001). Though further investigation is required, these results established a correlation between EBR and the expression of one aquaporin gene *BNPIP1* (Kagale et al., 2007).

The expression of structural genes in response to stress must result from a combination of factors - the degree of stress experienced by the seedling depending on its fitness, and the effectiveness by which the seedling can respond to stress. Transcript levels of transcription factors can be taken as an indirect measure of the degree by which the stress response will be launched. Transcript levels of *DREB2A*, a transcription factor that regulates drought-responsive gene expression were determined, but found to be comparable between EBR-treated and untreated Arabidopsis seedlings under no stress and drought stress conditions. This is not surprising given that DREB2 proteins require post-translational activation (Liu et al., 1998). However, in compliance with the higher stress tolerance of EBR-treated *B. napus* seedlings, transcripts of the transcription factors *BNCBF5* and *BNDREB* were present at higher levels in these seedlings, both in the absence of drought stress and under drought conditions (Kagale et al., 2007). Higher expression of transcription factors involved in activating the CBF regulon, which in turn protects plants from drought and cold stresses, supports the idea that EBR-treated seedlings are better primed than untreated seedlings to respond to stress.

In conclusion, the results of the present study along with those of the entire study as published by Kagale et al. (2007), demonstrate that EBR enhances tolerance of seedlings to a variety of abiotic stresses, and that this effect involves changes in the expression of genes encoding both structural and regulatory proteins. Analysis of global gene expression in response to EBR in the future will help in understanding how EBR improves tolerance in plants against a wide range of environmental stresses.

2.5 REFERENCES

Anuradha, S., and Rao, S.S.R. (2001). Effect of brassinosteroids on salinity stress induced inhibition of seed germination and seedling growth of rice (*Oryza sativa* L.). Plant Growth Regul. **33**, 151-153.

Desclos, M., Dubousset, L., Etienne, P., Le Caherec, F., Satoh, H., Bonnefoy, J., Ourry, A., and Avice, J.C. (2008). A proteomic profiling approach to reveal a novel role of *Brassica napus* drought 22 kd/water-soluble chlorophyll-binding protein in young leaves during nitrogen remobilization induced by stressful conditions. Plant physiol. **147**, 1830-1844.

Dhaubhadel, S., and Krishna, P. (2008). Identification of differentially expressed genes in brassinosteroid-treated *Brassica napus* seedlings. J. Plant Growth Regul. **27**, 297-308.

Dhaubhadel, S., Browning, K.S., Gallie, D.R., and Krishna, P. (2002). Brassinosteroid functions to protect the translational machinery and heat-shock protein synthesis following thermal stress. Plant J. **29**, 681-691.

Dhaubhadel, S., Chaudhary, S., Dobinson, K.F., and Krishna, P. (1999). Treatment with 24-epibrassinolide, a brassinosteroid, increases the basic thermotolerance of *Brassica napus* and tomato seedlings. Plant Mol. Biol. **40**, 333-342.

Divi, U.K., and Krishna, P. (2009). Brassinosteroids confer stress tolerance. In Plant stress biology: Genomics goes systems biology, H. Hirt, ed (Weinheim: Wiley-VCH), pp. 119-135.

Gao, Y.P., Young, L., Bonham-Smith, P., and Gusta, L.V. (1999). Characterization and expression of plasma and tonoplast membrane aquaporins in primed seed of *Brassica napus* during germination under stress conditions. Plant Mol. Biol. **40**, 635-644.

Goyal, K., Walton, L.J., and Tunnacliffe, A. (2005). LEA proteins prevent protein aggregation due to water stress. Biochem J. **388**, 151-157.

He, R.Y., Wang, G.J., and Wang, X.S. (1991). Effects of brassinolide on growth and chilling resistance of maize seedlings. In Brassinosteroids: Chemistry, Bioactivity and Applications, H.G. Cutler, T. Yokota, and G. Adam, eds (Washington: ACS Symp Ser 47, American Chemical Society), pp. 220-230.

Iwasaki, T., Yamaguchi-Shinozaki, K., and Shinozaki, K. (1995). Identification of a *cis*-regulatory region of a gene in *Arabidopsis thaliana* whose induction by dehydration is mediated by abscisic acid and requires protein synthesis. Mol. Gen. Genet. **247**, 391-398.

Kagale, S., Divi, U.K., Krochko, J.E., Keller, W.A., and Krishna, P. (2007). Brassinosteroid confers tolerance in *Arabidopsis thaliana* and *Brassica napus* to a range of abiotic stresses. Planta **225**, 353-364.

Katsumi, M. (1991). Physiological modes of brassinolide action in cucumber hypocotyl growth. In Brassinosteroids: Chemistry, Bioactivity and Applications, H.G. Cutler, T. Yokota, and G. Adam, eds (Washington: ACS Symp Ser 47, American Chemical Society), pp. 246-254.

Khripach, V., Zhabinskii, V., and de Groot, A. (2000). Twenty years of brassinosteroids: steroidal plant hormones warrant better crops for the XXI century. Ann. Bot. **86,** 441-447.

Kiyosue, T., Yamaguchi-Shinozaki, K., and Shinozaki, K. (1994). Characterization of two cDNAs (ERD10 and ERD14) corresponding to genes that respond rapidly to dehydration stress in *Arabidopsis thaliana.* Plant Cell Physiol. **35**, 225-231.

Krishna, P. (2003). Brassinosteroid-mediated stress responses. J. Plant Growth Regul. **22**, 289-297.

Krishna, P., Sacco, M., Cherutti, J.F., and Hill, S. (1995). Cold induced accumulation of hsp90 transcripts in *Brassica napus*. Plant Physiol. **107**, 915–923.

Kwon, M., and Choe, S. (2005). Brassinosteroid biosynthesis and dwarf mutants. J. Plant Biol. **48,** 1-15.

Li, K.R., Wang, H.H., Han, G., Wang, Q.J., and Fan, J. (2007) Effects of brassinolide on the survival, growth and drought resistance of *Robinia pseudoacacia* seedlings under water-stress. New Forests **35**, 255-266.

Liu, Q., Kasuga, M., Sakuma, Y., Abe, H., Miura, S., Yamaguchi-Shinozaki, K., and Shinozaki, K. (1998). Two transcription factors, DREB1 and DREB2, with an EREBP/AP2 DNA binding domain separate two cellular signal transduction pathways in drought- and low-temperature-reponsive gene expression, respectively, in Arabidopsis. Plant Cell **10**, 1391-1406.

Morillon, R., Catterou, M., Sangwan, R.S., Sangwan, B.S., and Lassalles, J-P. (2001). Brassinolide may control aquaporin activities in *Arabidopsis thaliana*. Planta **212,** 199-204.

Özdemir, F., Bor, M., Demiral, T., and Turkan, I. (2004). Effects of 24-epibrassinolide on seed germination, seedling growth, lipid peroxidation, proline content and antioxidative system of rice (*Oryza sativa* L.) under salinity stress. Plant Growth Regul. **42,** 203-211.

Ramanjulu, S., and Bartels, D. (2002). Drought- and desiccation-induced modulation of gene expression in plants. Plant Cell Environ. **25**, 141-151.

Reviron, M.P., Vartanian, N., Sallantin, M., Huet, J.C., Pernollet, J.C., and de Vienne, D. (1992). Characterization of a novel protein induced by progressive or rapid drought and salinity in *Brassica napus* leaves. Plant physiol. **100**, 1486-1493.

Sasse, J.M. (2003). Physiological actions of brassinosteroids: an update. J. Plant Growth Regul. **22**, 276-288.

Sasse, J.M., Smith, R., and Hudson, I. (1995). Effect of 24-epibrassinolide on germination of seeds of *Eucalyptus camaldulensis* in saline conditions. Proc. Plant Growth Regul. Soc. Am. **22**, 136-141.

Seki, M., Narusaka, M., Ishida, J., Nanjo, T., Fujita, M., Oono, Y., Kamiya, A., Nakajima, M., Enju, A., Sakurai, T., Satou, M., Akiyama, K., Taji, T., Yamaguchi-Shinozaki, K., Carninci, P., Kawai, J., Hayashizaki, Y., and Shinozaki, K. (2002). Monitoring the expression profiles of 7000 Arabidopsis genes under drought, cold and high-salinity stresses using a full-length cDNA microarray. Plant J. **31**, 279-292.

Shinozaki, K., and Yamaguchi-Shinozaki, K. (2000). Molecular responses to dehydration and low temperature: differences and cross-talk between two stress signaling pathways. Curr. Opin. Plant Biol. **3**, 217-23.

Vert, G., Nemhauser, J.L., Geldner, N., Hong, F., and Chory, J. (2005). Molecular mechanisms of steroid hormone signaling in plants. Annu. Rev. Cell Dev. Biol. **21**, 177-201.

Yamaguchi-Shinozaki, K., and Shinozaki, K. (1993). Characterization of the expression of a desiccation-responsive *RD29* gene of *Arabidopsis thaliana* and analysis of its promoter in transgenic plants. Mol. Gen. Genet. **236**, 331-340.

CHAPTER 3

Brassinosteroid-mediated abiotic stress tolerance in Arabidopsis involves interactions with abscisic acid, ethylene and salicylic acid pathways.

A version of this chapter has been submitted for publication

Divi, U.K., Rahman, T., and Krishna, P. (2009). Brassinosteroid-mediated abiotic stress tolerance in Arabidopsis involves interactions with abscisic acid, ethylene and salicylic acid pathways. BMC Plant Biol.

CHAPTER 3

3.1 INTRODUCTION

Brassinosteroids (BRs) are a group of plant steroidal hormones that regulate various aspects of plant growth and development, including cell elongation, photomorphogenesis, xylem differentiation, and seed germination (Sasse, 2003), as well as adaptation to abiotic and biotic environmental stresses (Khripach et al., 2000; Krishna, 2003). Molecular genetic studies of BR-deficient and BR-insensitive mutants have established an essential role for BRs in plant development and led to the identification and characterization of several BR signaling components (Clouse and Sasse, 1998; Gendron and Wang, 2007). A large number of BR-regulated genes have been identified by microarray studies; most of the known BR-regulated genes are associated with plant growth and development, such as cell wall modification, cytoskeleton formation, and hormone synthesis (Vert et al., 2005). How BR regulates gene expression is currently understood for only a small proportion of genes. In the known mechanism of BR-controlled gene expression, BR binding to BRI1 (BRASSINOSTEROID INSENSITIVE1), a plasma membrane localized leucine-rich repeat receptor-like kinase (LRR-RLK), induces association of BRI1 with its co-receptor BAK1 (BRI1-ASSOCIATED KINASE1), which enhances signaling output through reciprocal BRI1 transphosphorylation (Belkhadir et al., 2006; Gendron and Wang, 2007). BRI1 binding to BR inactivates a glycogen synthase kinase-3, BIN2 (BRASSINOSTEROID-INSENSITIVE2), and possibly activates the phosphatase BSU1 (BRI1 SUPPRESSOR1). BIN2 negatively regulates transcription factors BZR1 (BRASSINAZOLE RESISTANT1) and BES1 (BRI1 EMS SUPPRESSOR) by phosphorylating them, while BSU1 positively regulates BR signaling by dephosphorylating BZR1 and BES1. Activated BZR1 and BES1 accumulate in the nucleus and directly bind to CGTG(T/C)G motif in the promoters of BR biosysnthesis genes *CPD* and *DWF4* (He et al., 2005) and to the E boxes (CANNTG) of the *SAUR-ACI* promoter, respectively, to affect gene expression (Yin et al., 2005). The recent demonstrations that BES1 interacts with other transcription factors such as BIMs (BES1-INTERACTING MYC-LIKE) (Yin et al., 2005), MYB30 (MYB DOMAIN PROTEIN 30), which acts as a positive regulator of the hypersensitive cell-death response (Vailleau et al., 2002), and the jumonji (Jmj) domain-

containing proteins ELF6 (EARLY FLOWERING 6) and REF6 (RELATIVE OF EARLY FLOWERING 6) that are involved in regulating flowering time (Yu et al., 2008), points to recruitment of different proteins by BES1 as one of the ways by which BR affects diverse biological processes.

The role of BRs in plant stress responses has been confirmed in several studies (Dhaubhadel et al., 1999; 2002; Kagale et al., 2007; Koh et al., 2007). BR promotes tolerance in plants to a wide range of stresses, including heat, cold, drought and salinity, and this increase is generally correlated with higher expression of stress marker genes, such as *heat shock protein* (*hsp*) genes, *RESPONSIVE TO DESSICATION29A (RD29A)*, and *EARLY RESPONSIVE TO DEHYDRATION 10* (*ERD10)* (Dhaubhadel et al., 1999; Kagale et al., 2007), indicating that increased expression of stress-responsive genes is responsible, in part, for the higher stress tolerance in BR-treated plants. The mechanisms by which BR controls plant stress responses and regulates the expression of stress response genes are not known. Since different plant hormones can regulate similar physiological processes, and cross-talk between different hormones can occur at the level of hormone biosynthesis, signal transduction or gene expression (Nemhauser et al., 2006), it was proposed that BR regulates plant stress responses via cross-talk with other hormones (Krishna, 2003).

The plant growth regulators with documented roles in plant adaptation to abiotic and biotic stresses are abscisic acid (ABA), ethylene (ET), jasmonic acid (JA) and salicylic acid (SA). SA, JA and ET are important in defense against pathogen and pest attack (Bari and Jones, 2009), whereas ABA is a key molecule involved in salt and drought stress (Zhu, 2002). SA, ET, ABA and JA have also been linked to heat stress. Studies of hormone deficient and insensitive mutants have demonstrated the involvement of SA, ET and ABA in acquired thermotolerance of plants (Larkindale et al., 2005), and additionally for SA and JA, a role in basal thermotolerance of plants (Clarke et al., 2004; 2009). Although experimental evidence points to interactions of BR with auxin (Mouchel et al., 2006; Hardtke et al., 2007), gibberellic acid (GA) (Bouquin et al., 2001; Shimada et al., 2006), ABA (Steber and McCourt, 2001; Abraham et al., 2003), ET (Yi et al., 1999; Arteca and Arteca, 2001) and JA (Kitanaga et al., 2006; Müssig et al., 2006), the relationship of BR with these hormones has been documented primarily in plant growth

regulatory processes. Furthermore, with the exception of BR-auxin interaction, little is known in terms of genes how BR interacts with other hormones. Recent progress made towards understanding BR-auxin interaction can serve as a paradigm for how two hormones could interact at multi-levels. Auxin and BR share a number of target genes, many of which are involved in growth-related processes (Hardtke et al., 2007). Since promoter regions in BR-responsive genes are enriched in Auxin Response Factor (ARF)-binding sites, and binding sites of BES1 are over-represented in genes regulated by both hormones, regulatory elements in gene promoters represent a point of cross-talk between auxin and BR (Nemhauser et al., 2004). Recently, the BR-regulated BIN2 kinase was demonstrated to phosphorylate ARF2, a member of the ARF family of transcriptional regulators, leading to loss of ARF2 DNA binding and repression activities (Vert et al., 2008). Thus, in this model ARF2 links BR and auxin signaling pathways. In addition to gene coregulation, BR can also promote auxin transport (Li et al., 2005), and optimal auxin action is dependent on BR levels (Mouchel et al., 2006).

The role of BR in plant responses to abiotic stress has become well established over the last decade, but there are very few reports indicating how BR interacts with other stress-related hormones and their signaling pathways in conferring stress tolerance. While there exists evidence to indicate that BR increases ET and JA levels under normal growth conditions (Kitanaga et al., 2006; Arteca and Arteca, 2001), there appears to be only one report linking BR with increase in ABA levels in the lower plant *Chlorella vulgaris* under stress condition (Bajguz, 2009). Very recently it has been demonstrated that ABA inhibits BR signaling through phosphorylation of BES1 (Zhang et al., 2009). Currently there are no studies at the genetic level as to how BR interacts with other hormones under stress conditions. Here we asked the question whether one or more stress-related hormones, such as ABA, ET, JA or SA, have a major role in BR-mediated stress tolerance. Arabidopsis mutants with either disrupted or enhanced hormone pathways were tested for phenotypes and gene expression in response to BR under high temperature and high salt conditions. Our results indicate that in Arabidopsis the NONEXPRESSOR OF PATHOGENESIS-RELATED GENES1 (NPR1) is a critical component of BR-mediated effects on thermotolerance and salt tolerance, that BR exerts anti-stress effects both

independently as well as through interactions with other hormones, ABA inhibits BR effects during heat stress, and that BR shares transcriptional targets with other hormones.

3.2 MATERIALS AND METHODS

3.2.1 Plant material and growth conditions

The *eds5-1* (CS3735), *npr1-1* (CS3726), *cpr5-2* (CS3770), *ein2* (CS8844), *eto1-1* (CS3072), *aos* (CS6149), and *jar1-1* mutants belong to the Columbia (Col) background, while the *aba1-1* (CS21) and *abi1-1* (CS22) mutants are in the Landsberg *erecta* (L*er*) background. Accordingly, the WT Col and L*er* were used as controls in the experiments. The *aos* mutant is a T-DNA knockout line derived from Col-6, hence its parental line (CS8155) was used as control. The *jar1-1* mutant was a kind donation from Dr. Pradeep Kachroo (University of Kentucky, Lexington, KY, USA). All other mutants were obtained from the Arabidopsis Biological Resource Center (ABRC).

Seedlings were grown essentially as described by Kagale et al. (2007). Seeds were surface sterilized and plated on 1X Murashige and Skoog medium (Sigma, St. Louis) supplemented with B5 vitamins, 1% (w/v) agar, 1% sucrose, and either 1 µM EBR or 0.01% ethanol (solvent for EBR). The plates were kept for 3 days in the dark at 4^0C to encourage synchronized germination and then transferred to 22^0C with a 16/8 h photoperiod (80 µE m^{-2} s^{-1}) and allowed to grow for 21 days. For the short-term EBR treatment, 21-day-old seedlings grown in the medium without EBR were submerged for 7 h in sterile water containing 1 µM EBR or 0.01% ethanol.

3.2.2 Heat stress treatments

The thermotolerance of Arabidopsis seedlings was assayed according to Kagale et al. (2007) with minor modifications. Seedlings grown at 22^0C for 21 days were exposed to 43^0C for 4 h and scored as dead or alive after 7 days of recovery at 22^0C. Values in Figure 3.1B represent average percentages of data obtained in three biological replicates. Plant tissue was collected at different time points and quick-frozen for protein isolation and for the TBARS assay.

3.2.3. Salt stress treatments

Surface sterilized seeds were germinated on 0.5X Murashige and Skoog medium supplemented with B5 vitamins and either 1 µM EBR or 0.01% ethanol. Salt treatment was given by including 150 mM NaCl in the medium. All plates were kept for 3 days in the dark at 4^0C plates and then transferred to 22^0C. Percent germination was determined 3 days after transferring plates to 22^0C. Seeds with emerging cotyledons were scored as germinated. Percent survival was calculated by counting the number of seedlings that showed true leaves and green colour at 20 days after imbibition. Values in Figure 3.5 are average percentages of data obtained in three biological replicates.

3.2.4 Thiobarbituric Acid Reactive Substance (TBARS) assay

TBARS assay was performed according to Heath and Packer (1968). Seedlings grown at 22^0C for 21 days were subjected to 43^0C for 3 h and then allowed to recover for 2 days at 22^0C. Seedlings were quick frozen in liquid nitrogen and 0.5 g of the tissue was ground in 1 mL of solution containing buffer 1 and buffer 2 in equal proportions (buffer 1: 0.5 mL of 0.5% [w/v] thibarbituric acid in 20% [v/v] trichloroacetic acid; buffer 2: 0.5 mL 175 mM Nacl in 50 mM Tris, pH 8.0). Ground samples were heated to 94^0C for 1 h, centrifuged at 13,000 rpm for 20 min, and the absorbance of the supernatant was measured at 532 and 600 nm. The levels of TBARS were deduced from the malonaldehyde standard curve and in each case the TBARS levels in the EBR-treated samples were compared to that of untreated control. Values in Figure 3.2A were averaged from three replicates.

3.2.5 Protein extraction and western blotting

Extraction of total proteins and western blotting were carried out as described by Dhaubhadel et al. (1999). Seedlings grown at 22^0C for 21 days were either maintained at 22^0C or subjected to 43^0C for 3 and 4 h. Seedling tissue above the medium was harvested, frozen in liquid nitrogen and stored at -80^0C. Frozen tissue was ground in protein extraction buffer [25 mM Tris-HCL, 1 mM EDTA, 20 mM NaCl, 1 mM PMSF, 1 mM benzamidine, 1 µg/ml leupeptin and 2 µg/ml aprotinin] and after centrifugation at 13,000 rpm for 30 min, the supernatant was transferred to a new tube. Protein

concentration was determined by the bradford assay. Total proteins (15 µg) were separated on a 7.5% SDS-polyacrylamide gel and transferred onto nitrocellulose membrane by electroblotting using the Trans-blot Semi-Dry Electrophoretic Transfer Cell (BioRad, Hercules, CA, USA). Hsp90 was detected by sequential incubation with the polyclonal R2 antisera (Krishna et al., 1997) and the peroxidase conjugated anti-rabbit IgG, each at a dilution of 1:5,000, followed by chemiluminescent detection (ECL system, Amersham, Baie d'Urfe, QC).

3.2.6 RT-PCR analysis

RNA was extracted from 21-day-old seedlings grown at 22^0C using the SV Total RNA Isolation System (Promega, Madison, WI). Total RNA (3 µg) was reverse transcribed using the oligo $(dT)_{18}$ primer and Super Script First Strand Synthesis System for RT-PCR (Invitrogen, Carlsbad, CA). PCR was carried out with an initial denaturation step of 94^0C for 5 min followed by various cycles of denaturation (40 s at 94^0C), annealing (45 s at 53^0C), and extension (45 s at 72^0C). After the last cycle, a final extension was carried out for 5 min at 72^0C. PCR was performed for 32 cycles for *PDF1.2, HEL, WRKY70, LTP4, RD22;* 35 cycles for *LOX2, PR-1, WAK1, GST1*; and 21 cycles for *ACTIN* (control gene).

The following primers were used:

PR-1-F: 5' GATGTGCCAAAGTGAGGTG,

PR-1-R: 5' CTGATACATATACACGTCC,

WRKY70-F: 5' CGCCGCCGTTGAGGGATCTC,

WRKY70-R: 5' CGCCGCCACCTCCAAACAC,

WAK1-F: 5' GAGTTACTTTGCGACTGCCA,

WAK1-R: 5' CAGCTTCCTGGATCTCCTTC,

PDF1.2-F: 5' AATGAGCTCTCATGGCTAAGTTTGCTT,

PDF1.2-R: 5' AATCCATGGAATACACACACGATTTAGCACC,

LOX2-F: 5' CTCTTCAGAGCACGCTACG,

LOX2-R: 5' GAAGATGGAGGGAAGAGCTG,

HEL-F: 5' ACAAGGCCATCTCATTGTTG,

HEL-R: 5' GATCAATGGCCGAAACAAG,
GST1-F: 5' TTGGCTTCTGACCACTTCAC,
GST1-R: 5' ACGCTCGTCGAAGAGTTTCT,
RD22-F: 5' GCGAGCTAAAGCAGTTGCGGTATG,
RD22-R: 5' CGGCTAGTAGCTGAACCACACAAC,
LTP4-F: 5' CACCAACTGCGCCACCATCAAG,
LTP4-R: 5' GCCATCAAGACAAACAAAGAC,
DWF4-F: 5' ACGGAGCAAATTCTCGATC,
DWF4-R: 5' AGCTCTTCAACGGCTTTAG,
ACTIN-F: 5' TGCTCTTCCTCATGCTAT,
ACTIN-R: 5' ATCCTCCGATCCAGACACTG,

3.3 RESULTS

3.3.1 EBR effects on basal thermotolerance in different hormone genotypes

We have previously demonstrated that EBR enhances the basic thermotolerance of *Brassica napus*, tomato (Dhaubhadel et al., 1999; 2002) and Arabidopsis seedlings (Kagale et al., 2007). Since the effects of EBR on stress tolerance are most pronounced when seedlings are grown in the presence of EBR for 21 days (long-term treatment), we postulated the involvement of other phytohormones in this process (Krishna, 2003). Several hormone pathways, such as of ABA, ET, SA and JA, have been linked with one or more environmental stresses, including heat stress (HS). We therefore evaluated the effects of EBR on thermotolerance in a subset of Arabidopsis hormone mutants altered in either biosynthesis or signaling of these phytohormones (Table 3.1). We first studied the effects of EBR on basal thermotolerance in SA genotypes *npr1-1* (defective in SA signaling), *eds5-1* (defective in SA synthesis), and *cpr5-2* (SA-overproducer) by exposing 21 day old seedlings to 43^0C for 4 h, allowing them to recover at 22^0C for 7 days and then scoring for dead and alive seedlings. WT, *eds5-1*, *npr1-1* and *cpr5-2* seedlings grown in the absence of EBR had average survival rates of 7.5%, 4.5%, 5.5% and 13.5%, respectively, and those grown in the presence of EBR had survival rates of 69.3%, 58.3%, 13.4% and 83%, respectively (Figure 3.1A and B). From these results it is clear that the survival rates of WT and different SA genotypes were significantly

Category	Locus (AGI)	Gene	Description	Mutant allele
SA synthesis defective	At4g39030	*EDS5*	member of the MATE-transporter family; mutants do not accumulate SA after pathogen inoculation and are hypersusceptible to pathogen infection (Glazebrook et al., 1996; Rogers et al., 1997; Nawrath et al., 1999)	*eds5-1*
SA-insensitive	At1g64280	*NPR1*	similar to the transcription factor inhibitor I kappa B, and contains ankyrin repeats; key regulator of SA-mediated systemic acquiredresistance (SAR) pathway; mutants are SA-insensitive and hypersusceptible to pathogen infection (Cao et al., 1994; Delaney et al., 1995)	*npr1-1*
High SA levels	At5g64930	*CPR5*	regulator of expression of pathogenesis-related (*PR*) genes; participates in signal transduction pathways involved in plar defense; mutants exhibit increased SA levels and constitutive expression of *PR* genes (Bowling et al., 1997; Boch et al., 1998)	*cpr5-2*
ET-insensitive	At5g03280	*EIN2*	NRAMP metal transporter family; involved in ET signal transduction;mutants are ET-insensitive (Guzman and Ecker, 1990)	*ein2*
High ET levels	At3g51770	*ETO1*	encodes a negative regulator of 1-aminocyclopropane-1-carboxylic acid synthase5(ACS5), which catalyzes the rate-limiting step in ET biosynthesis; mutations elevate ET biosynthesis by affecting the posttranscriptional regulation of ACS (Guzman and Ecker, 1990)	*eto1-1*
JA-deficient	At5g42650	*AOS*	encodes a member of the cytochrome p450 CYP74 gene family that functions as an allene oxide synthase; catalyzes dehydration of the hydroperoxide to an unstable allene oxide in the JA biosynthetic pathway; mutants are JA-deficient (Park et al., 2002)	*aos*
JA-insensitive	At2g46370	*JAR1*	encodes cytoplasmic localized phytochrome A signaling component protein similar to the GH3 family of proteins; loss of function mutants are defective in a variety of responses to JA (Staswick et al., 1992)	*jar1-1*
ABA-deficient	At5g67030	*ABA1*	encodes zeaxanthin epoxidase gene that functions in first step of ABA biosynthesis; mutants are ABA-deficient (Koornneef et al., 1982)	*aba1-1*
ABA-insensitiv	At4g26080	*ABI1*	Protein phosphatase 2C; involved in ABA signal transduction; mutants are ABA-insensitive (Koornneef et al., 1984)	*abi1-1*

A

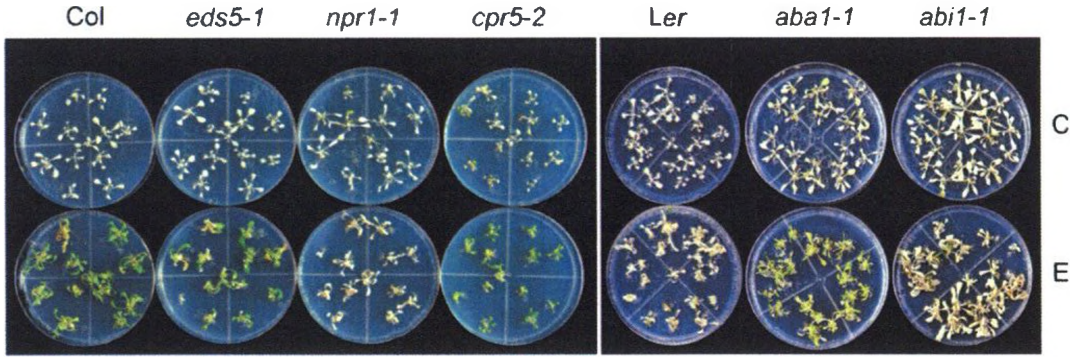
Col
eds5-1
npr1-1
cpr5-2
Ler
aba1-1
abi1-1
C
E

B

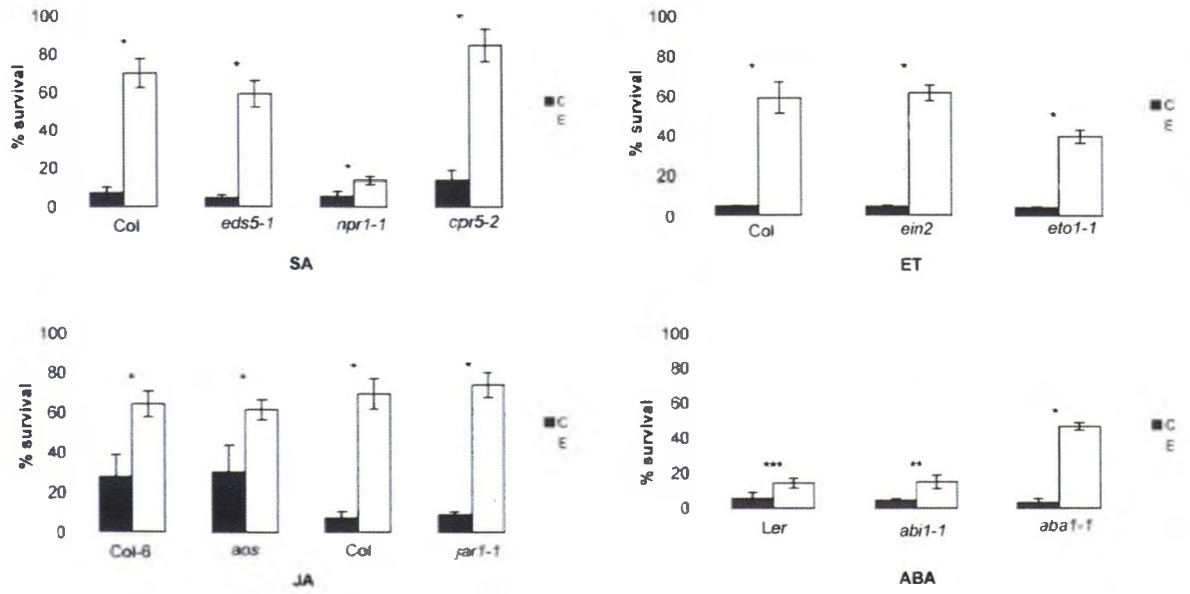
% survival
100
80
60
40
20
0
Col
eds5-1
npr1-1
cpr5-2
SA
C
E
Col
ein2
eto1-1
ET
Col-6
aos
Col
jar1-1
JA
Ler
abi1-1
aba1-1
ABA

increased by EBR treatment, but the increase was considerably less in case of *npr1-1* as compared to other genotypes within this group

For genotypes related to ethylene, EBR increased survival rates of WT, *ein2* (ET-insensitive), and *eto1-1* (ET-overproducer) seedlings to significant levels as compared to seedlings with no treatment (Figure 3.1B). The JA mutants *aos* (JA-deficient) and *jar1-1* (defective in JA response) belong to different backgrounds; *jar1-1* is in Arabidopsis ecotype Col, whereas *aos* is in Col-6 background. Under the HS conditions employed here, untreated WT Col-6 survived better than untreated WT Col. EBR effect on seedling survival was more pronounced in Col than in Col-6 background (Figure 3.1B). EBR increased survival rates of *aos* and *jar1-1* seedlings to amounts similar to corresponding WT seedlings (Figure 3.1B).

The ABA mutants *aba1-1* (ABA-deficient) and *abi1-1* (ABA-insensitive) are from the L*er* background; hence, WT L*er* was used for comparison with these mutants. Under the conditions used, EBR was less effective in WT L*er* as compared to WT Col (about 2.5-fold increase in L*er vs.* 9-fold increase in Col in survival rates in response to EBR) (Figure 1B). Since ABA has been linked with heat tolerance (Larkindale and Knight, 2002; Larkindale et al., 2005), we expected ABA mutants to be less thermotolerant than WT even in the presence of EBR. Contrary to our expectation we found that the effect of EBR was most distinct in *aba1-1* (survival rate of 43.3%) as compared to WT (14.3%) and *abi1-1* (15%) seedlings (Figure 3.1A and B). These results suggest that ABA masks BR effects on the HS response pathway of WT Arabidopsis seedlings.

From the survival data represented in Figure 3.1 it is clear that when EBR effect in any hormone genotype is viewed in reference to the effect on the corresponding WT, EBR could increase the basal thermotolerance of all hormone genotypes, but its effect was minimal in *npr1-1*. Since the SA-deficient *NahG* transgenic line (Gaffney et al., 1993) and the JA response defective *coi1* mutant (Feys et al., 1994) could not be obtained for this study, we cannot yet conclude that SA and JA are dispensable for BR-mediated increase in thermotolerance. However, from the collection of mutants used here it would appear that BR can exert anti-stress effects that are independent of ABA, ET, JA and SA, at least to some extent. The dependency of BR on NPR1 in mediating stress tolerance is a

first time observation made in this study. Whether BR modulates NPR1 activity via SA or BR pathway or both remains to be determined.

3.3.2 EBR effects on oxidative damage in hormone mutants

Heat stress produces oxidative damage, which as a result of lipid peroxidation leads to the production of thiobarbituric acid reactive substances (TBARS) (Heath and Packer, 1968; Larkindale et al., 2005). To complement the results of the HS phenotype of seedlings, oxidative damage levels were assessed in untreated and EBR-treated seedlings. Measurements of TBARS in time course experiments determined that maximum oxidative damage occurred post HS (during the recovery period). Therefore, seedlings exposed to HS and then allowed to recover for 2 days at 22^0C were used for TBARS analysis. With the exception of *npr1-1,* EBR treatment reduced the levels of oxidative damage in WT and other mutant seedlings as compared to their untreated counterparts (Figure 3.2A). WT Col and L*er* exhibited 45% and 60% reduction in TBARS production, respectively, while the mutant seedlings showed 25-50% less TBARS in response to EBR treatment. It should be noted that the data shown in Figure 3.2A do not allow a comparison of oxidative damage across genotypes, but rather a comparison of oxidative damage levels between untreated and treated seedlings of the same genotype. Consistent with its lower survival rate (Figure 3.1B), the *npr1-1* mutant showed an insignificant 4.5% reduction in TBARS production in response to EBR treatment (Figure 3.2A). However, in contrast to the relatively higher survival of *cpr5-2* seedlings, the reduction in oxidative damage in these seedlings in response to EBR measured only 25% relative to no treatment. Overall, these results demonstrated that EBR treatment can reduce oxidative damage during HS and that this effect is not critically dependent on any one hormone in question, although a functional NPR1 protein appears to be required for a complete effect of EBR on thermotolerance of seedlings.

3.3.3 EBR induces higher accumulation of hsp90 in aba1-1

We have found that EBR treatment leads to significant increases in the levels of hsps during HS in *B. napus* (Dhaubhadel et al., 1999; 2002), but the effect of EBR on hsp levels in Arabidopsis is subtle (Kagale et al., 2007). We wished to see how EBR would

A

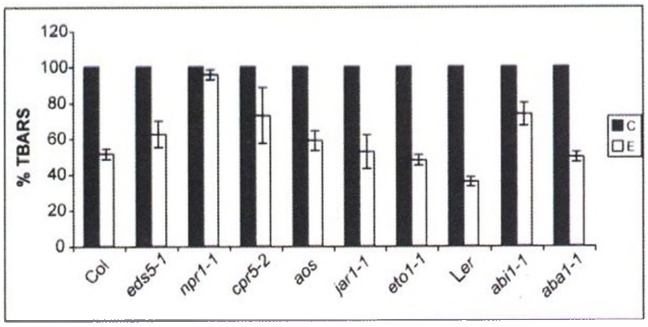
% TBARS
120
100
80
60
40
20
0
C
E
Col
eds5-1
npr1-1
cpr5-2
aos
jar1-1
eto1-1
Ler
abi1-1
aba1-1

B

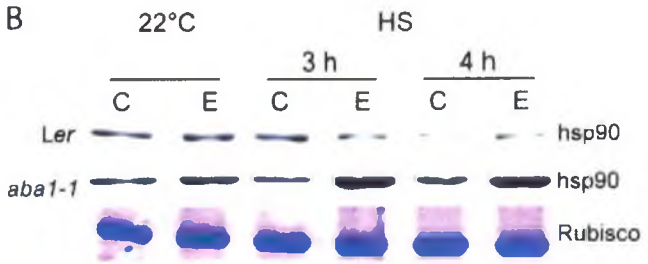
22°C
HS
3 h
4 h
C
E
C
E
C
E
Ler
hsp90
aba1-1
hsp90
Rubisco

affect the accumulation of hsp90 in various mutant seedlings in the absence of HS (22^0C) and in response to HS (3 h and 4 h exposure to 43^0C). With the exception of *aba1-1* (Figure 3.2B), no significant differences in the steady state levels of hsp90 were observed between EBR-treated and untreated mutant seedlings, including *npr1-1*. EBR-treated *aba1-1* seedlings accumulated approximately 3- and 2.5-fold higher levels of hsp90 at 3 and 4 h of HS, respectively, as compared to untreated *aba1-1* seedlings (Figure 3.2B). By contrast, EBR-treated WT seedlings showed a maximum of 1.3-fold increase in hsp90 levels at 4 h of HS as compared to untreated seedlings. The fold change values are average of three different experiments, which consistently produced the same pattern. Thus, with respect to higher survival following HS and greater accumulation of hsp90 during HS, EBR produced most distinct effects in the ABA-deficient *aba1-1* mutant. These results reinforce the idea that ABA suppresses BR effects in WT seedlings. Although convincing evidence for antagonism between BR and ABA in plant growth regulatory processes, such as germination has been provided before (Steber and McCourt, 2001; Zhang et al., 2009), the demonstration at the genetic and molecular levels of an antagonistic relationship between the two hormones in plant stress response is new.

3.3.4 EBR up-regulates the expression of SA, JA/ET and ABA response genes in both WT and corresponding mutants

Plant hormone responses in Arabidopsis have been correlated with the expression of hormone–specific marker genes. We studied the expression of few such genes that are well documented to be induced by SA, JA/ET or ABA, both before and after treatment with EBR. The *PATHOGENESIS-RELATED1* (*PR-1*), the transcription factor *WRKY70,* and the *WALL-ASSOCIATED KINASE1* (*WAK1*) genes are known to be regulated primarily by SA (Uknes et al., 1992; He et al., 1998; Li et al., 2004); *PLANT DEFENSIN1.2* (*PDF1.2*), *LIPOOXYGENASE2* (*LOX2*) and *HEAVIN-LIKE PROTEIN* (*HEL*) by JA/ET (Potter et al., 1993; Bell et al., 1995; Penninckx et al., 1996); and *RESPONSIVE TO DESSICATION22* (*RD22*) and *LIPID TRANSFER PROTEIN4* (*LTP4*) by ABA (Iwasaki et al., 1995; Arondel et al., 2000).

The steady-state levels of *PR-1*, *WRKY70* and *WAK1* transcripts were elevated by EBR in WT and SA-related genotypes, including *npr1-1*, albeit at different levels (Figure 3.3A). The *npr1-1* genotype has been noted previously to be defective in the expression of *PR* genes (Cao et al., 1994). Full-scale induction of *WRKY70* and *WAK1* by SA also requires a functional NPR1 (He et al., 1998; Li et al., 2004). Our results clearly indicate that EBR can mediate induction of *PR-1*, *WRKY70* and *WAK1* to levels seen in Figure 3.3A in an NPR1-independent manner.

EBR treatment also enhanced the expression of the JA/ET marker gene *PDF1.2* in WT, *aos*, *jar1-1* and *eto1-1* backgrounds, but not to the same extent in *ein2* (Figure 3.3A). The effect of EBR on *LOX2* expression was distinct in Col and *jar1-1* backgrounds, but not in Col-6 and *aos* backgrounds. Increase in the expression of the *HEL* gene by EBR was only slight.

The ABA-responsive *LTP4* showed dramatic induction by EBR in WT and *abi1-1* background (Figure 3.3A), but not in *aba1-1*. The transcript levels of the ABA-marker gene *RD22* were up-regulated by EBR only slightly in *aba1-1* and *abi1-1* mutant seedlings, but significantly in WT (Figure 3A), indicating interaction between ABA and BR in affecting gene expression.

To determine the interaction of EBR with SA, JA/ET and ABA in the regulation of *GST1*, a gene common to abiotic stress and defense pathways (Wagner et al., 2002), we compared its transcript levels in untreated and EBR-treated WT and mutant seedlings. EBR enhanced *GST1* transcript levels in SA (Figure 3.3B), as well as in all other hormone genotypes studied (Appendix 3.1). As would be expected, *cpr5-2* had the highest expression of *GST1* even in the absence of EBR.

Exogenous BR negatively regulates the BR biosynthetic gene *DWF4* (Tanaka et al., 2005). To ensure that transport, perception and signaling of BR is intact in *npr1-1*, which was most inert to EBR effects, *DWF4* expression was determined in WT and *npr1-1*. The fact that *DWF4* levels were reduced in EBR-treated WT and *npr1-1* seedlings as compared to untreated seedlings (Figure 3.3C) suggests that the BR pathway is intact in *npr1-1*.

Taken together, these results demonstrate that most, if not all, of the SA, JA/ET and ABA -responsive genes tested in the present study are also up-regulated by BR both

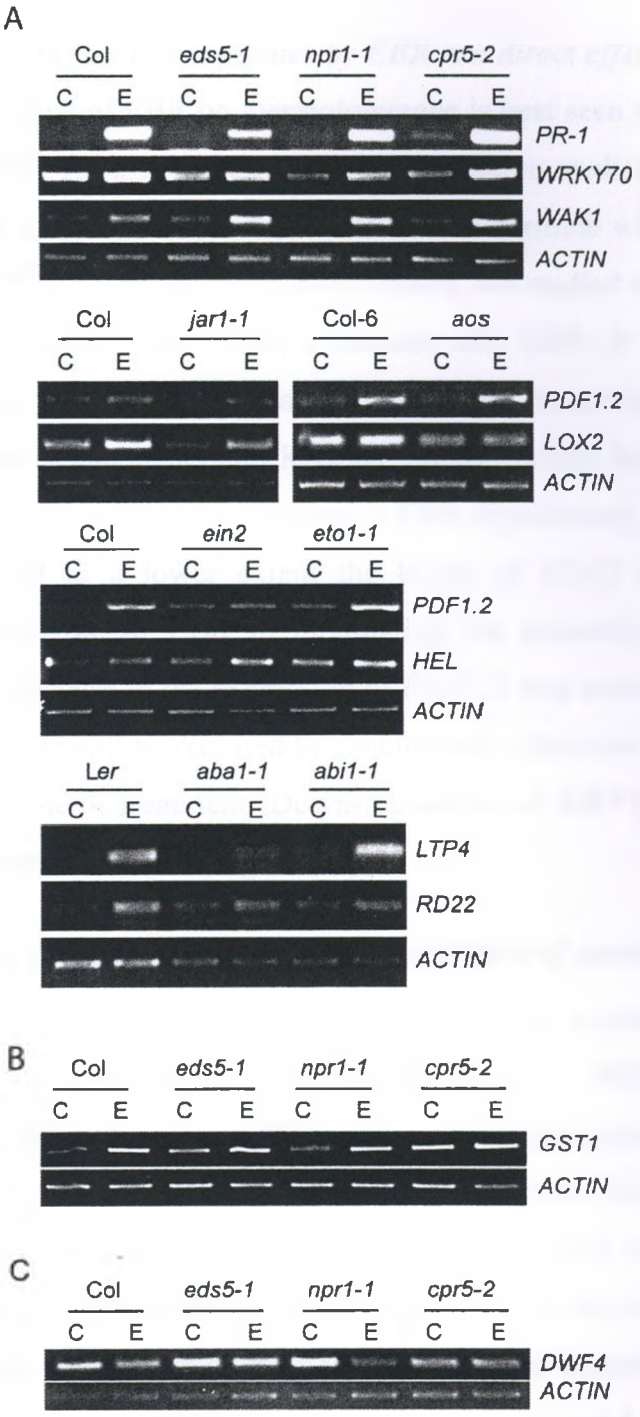
A
Col
eds5-1
npr1-1
cpr5-2
C E C E C E C E
PR-1
WRKY70
WAK1
ACTIN
Col
jar1-1
Col-6
aos
C E C E C E C E
PDF1.2
LOX2
ACTIN
Col
ein2
eto1-1
C E C E C E
PDF1.2
HEL
ACTIN
Ler
aba1-1
abi1-1
C E C E C E
LTP4
RD22
ACTIN
B
Col
eds5-1
npr1-1
cpr5-2
C E C E C E C E
GST1
ACTIN
C
Col
eds5-1
npr1-1
cpr5-2
C E C E C E C E
DWF4
ACTIN

in WT and mutant backgrounds, albeit to different levels. These results point to overlapping gene targets of ABA, JA/ET or SA and BR, as well as to hormone interactions controlling the final output.

3.3.5 Up-regulation of a subset of genes by EBR is a direct effect of EBR

Since the effect of EBR on thermotolerance is best seen when plants are grown in the presence of EBR for 2-3 weeks, our gene expression studies were also conducted in plants receiving a long-term exposure to EBR. To determine whether the effect of EBR on SA, JA/ET and ABA -responsive genes is direct, we studied the expression of a subset of genes in response to a short-term treatment with EBR. It is to be noted that up-regulation of genes by BR can take as long as 18-48 hrs even in short-term treatment (Zurek et al., 1994; Dhaubhadel and Krishna, 2008). Similar to the results of long-term treatment, the 7 h short-term treatment with EBR significantly enhanced the transcript levels of *PR-1* and to a lower extent the levels of *RD22* and *GST1* (Figure 3.4), suggesting a direct role of EBR in modulating the transcript levels of these genes. Although a small increase in the expression of *PDF1.2* was seen in replicate experiments, additional time points will be required to conclusively determine EBR effects on *PDF1.2* expression in short-term treatment. Down-regulation of *DWF4* by exogenous BR was used as an experimental control (Figure 3.4).

3.3.6 EBR rescues hypersensitivity of ein2 to inhibition of germination by salt stress

We have previously shown that EBR helps to overcome salt stress-induced inhibition of seed germination in *B. napus* (Kagale et al., 2007). More recently it was demonstrated that BR-deficient and BR signaling-defective mutants are more inhibited in germination on salt while a BRI1 overexpressing transgenic line is more resistant to salt than WT (Zhang et al., 2009). To study the effects of EBR on salt stress in hormone mutants, we selected *ein2* because of its hypersensitivity to salt stress (Wang et al., 2007), and *eto1-1* and *npr1-1* because of their relatively higher susceptibility to HS even after EBR treatment. Seeds were allowed to germinate on 150 mM NaCl in the presence or absence of EBR, and seedlings with emerged cotyledons were scored after 3 days. Inhibition of germination of *ein2* seeds by salt was significantly reduced in the presence

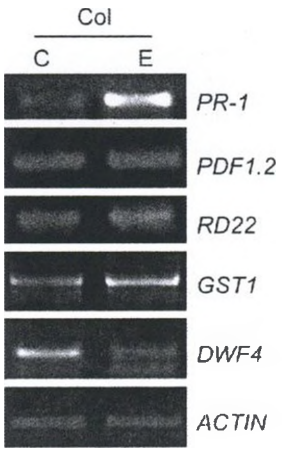
Col
C
E
PR-1
PDF1.2
RD22
GST1
DWF4
ACTIN

A

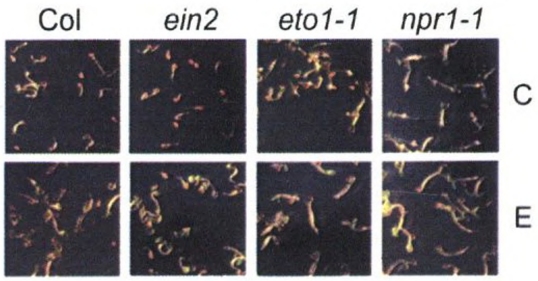
Col
ein2
eto1-1
npr1-1
C
E

B

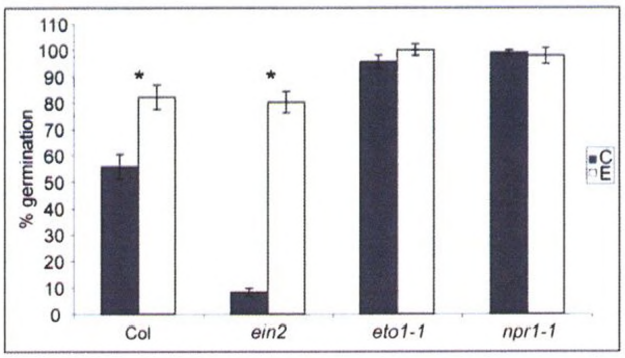
% germination
110
100
90
80
70
60
50
40
30
20
10
0
*
*
Col
ein2
eto1-1
npr1-1
C
E

C

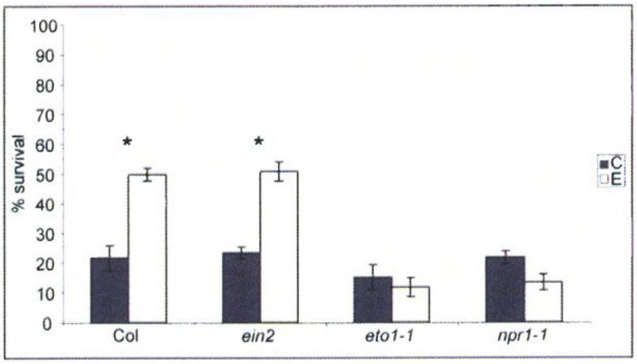
% survival
100
90
80
70
60
50
40
30
20
10
0
*
*
Col
ein2
eto1-1
npr1-1
C
E

of EBR (Figure 3.5A and B). WT seeds showed germination rates of 55% and > 80% on 150 mM NaCl in the absence and presence of EBR, respectively, while *ein2* seeds had germination rates of ~10% and 80% under the same conditions (Figure 3.5B). Seeds of *eto1-1* and *npr1-1* germinated at similar rates (> 90%) on 150 mM NaCl in the absence or presence of EBR (Figure 3.5B). However, despite the good germination efficiency on salt, the average survival rates of *eto1-1* and *npr1-1* on salt were only 15% and 22%, respectively (close to WT), but unlike WT, survival of these mutant seedlings could not be rescued by EBR treatment (Figure 3.5C). These results indicate that NPR1 has a role in salt stress and that BR effects on seedling survival under salt stress require a functional NPR1.

3.4 DISCUSSION

In the present study we focused on understanding BR interactions with other stress hormones in mediating increase in stress tolerance mainly because 1) BR is known to interact with other plant hormones in regulating plant developmental processes, and 2) multiple hormone signaling pathways play a role in acquisition of stress tolerance. We evaluated a subset of signaling, biosynthetic and constitutively active mutants of ABA, ET, JA and SA for thermo and salt tolerance in untreated and BR-treated states to assess the importance of these hormones in BR-mediated increase in stress tolerance of Arabidopsis seedlings. Here we demonstrate that NPR1, a protein well recognized for its role in SA-mediated systemic acquired resistance (SAR) and cross-talk inhibition of JA-mediated defense responses, also has a role in BR-mediated stress tolerance.

3.4.1 Thermotolerance defects of hormone mutants and BR effects

SA, and more recently JA, has been linked with thermotolerance. In case of SA genotypes, it is known that *npr1-1* is compromised in basal thermotolerance, while *cpr5-2* has greater thermotolerance than WT (Clarke et al., 2004; Larkindale et al., 2005). Recently it was demonstrated that a JAR1-dependent pathway is also required for basal thermotolerance (Clarke et al., 2009). Using a collection of genotypes with basal thermotolerance either lower or higher than WT, we found that EBR treatment could significantly increase the basic thermotolerance of these genotypes and that this increase

was comparable to the increase in WT. An exception to this result within the SA, JA and ET genotypes was *npr1-1*, indicating that a functional NPR1 is required for full manifestation of BR's effects. Although collectively our data seems to suggest that BR is not critically dependent on SA levels and JA signaling for its anti-stress effects, further confirmation is required with genotypes such as *Nahg* and *coi1* to make an unequivocal claim. Even if BR works to some extent independently of other hormones in conferring heat tolerance, the mere fact that ABA, BR, ET, JA and SA all play a role in thermotolerance of Arabidopsis plants suggests that there must be some redundant and some specific events in the mechanisms by which these hormones produce their effects. With the exception of BR where some information has been obtained (Dhaubhadel et al., 1999; 2002; Kagale et al., 2007), molecular changes mediated by ABA, ET, JA and SA that lead to thermotolerance are largely unknown. In case of ET, the Ethylene Response Factor Protein, JERF3, has been demonstrated to activate the expression of oxidative genes, resulting in decreased accumulation of ROS and, in turn, enhanced adaptation to drought, freezing, and salt in tobacco (Wu et al., 2008). A similar role for JERF3 can be envisioned in response to HS. A number of ABA-regulated genes have been implicated in drought tolerance (Zhu, 2002). Recent functional characterization of the ABA-regulated ERD10 and ERD14 indicated that these proteins could prevent the heat-induced aggregation and/or inactivation of various enzyme substrates (Kovacs et al., 2008). Thus, induction of genes functionally similar to molecular chaperones by ABA during HS may help combat the denaturing stress effects of HS.

Previous studies involving treatment with exogenous ABA (Larkindale and Knight, 2002), *aba* and *abi* mutants (Larkindale et al., 2005), and high ABA producing lines (Ristic and Cass, 1992), have demonstrated the positive effects of ABA on thermotolerance. Under our experimental conditions the differences in the survival rates of untreated WT and *aba1-1* and *abi1-1* mutant seedlings were not striking, but the most pronounced effects of EBR with respect to survival within this set of plants was seen in *aba1-1* seedlings (Figure 3.1B), indicating that endogenous ABA levels suppress BR effects. This notion is supported further by higher accumulation of hsp90, a representative of the hsp families of proteins that are known markers of thermotolerance, in *aba1-1* seedlings as compared to WT (Figure 3.2B). It should be noted that neither SA,

nor ABA or BR mutants are compromised in hsp accumulation (Larkindale et al., 2005; Kagale et al., 2007; present study). We have previously demonstrated that treatment with exogenous EBR can significantly increase hsp accumulation in *B. napus* (Dhaubhadel et al., 1999; 2002), but that this effect in Arabidopsis is subtle (Kagale et al., 2007). Thus, the clear enhancement of hsp accumulation in response to EBR during HS in *aba1-1*, but not in WT (Figure 3.2B), confirms that endogenous ABA levels suppress BR effects in WT even under stress conditions. While this work was under preparation, a study describing ABA inhibition of BR signaling was reported whereby it was shown that ABA increases the expression levels of BR biosynthesis gene *DWF4* and *CPD* to a greater extent in *aba1* than in WT, reinforcing the idea that ABA inhibits BR signaling in WT and that this inhibition is relieved in the *aba1* background (Zhang et al., 2009).

Despite an antagonistic relationship between BR and ABA, data from our microarray experiment suggest that ABA levels rise in response to HS in Arabidopsis and that this increase may be further augmented by BR treatment (Chapter 4). Indeed, ABA content has been reported to increase in pea leaves in response to HS (Liu et al., 2006) and in response to BR under HS in *C. vulgaris* (Bajguz, 2009). Based on these results it can be speculated that BR augments ABA levels and ABA-related effects during HS (Figure 3.6), but it is only when ABA levels are compromised that the BR effects of enhancing stress tolerance become apparent.

3.4.2 NPR1, stress tolerance and BR effects

Although *npr1-1* seedlings have been shown to be defective in basal thermotolerance, the heat sensitivity of this genotype is not dramatically lower than WT (Clarke et al., 2004; Larkindale et al., 2005). However, in our study the mere 2.4-fold increase in percent survival of *npr1-1* in response to EBR treatment as compared to the 9-fold increase in WT Col following HS (Figure 3.1), nearly no change in oxidative damage levels in *npr1-1* in response to EBR (Figure 3.2A), and the lack of EBR effect in increasing survival of *npr1-1* seedlings on salt (Figure 3.5B), explicitly indicates that a functional NPR1 is required for the manifestation of BR effects on seedling stress tolerance. Two questions arise from these observations; 1) what would be the function of

NPR1 during abiotic stress conditions, and 2) how could NPR1 integrate in the BR pathway?

NPR1 is a redox-controlled transcriptional cofactor, which is key to development of SAR and critical for modulating cross-talk between SA and JA signaling (Spoel et al., 2003). In the absence of stress, NPR1 is maintained in a large complex consisting of intermolecular disulfide bonded oligomers, which upon stress are reduced to an active monomeric state (Mou et al., 2003). The monomeric form interacts with TGA-bZIP transcription factors and activates defense gene expression. ROS is a common signal in plant stress responses to both abiotic and biotic stresses (Apel and Hirt, 2004; Dietz, 2008). The notion that ROS could be a signal for the HS response is derived from studies of activation of heat shock transcription factors (Hsfs). The eukaryotic Hsf1 multimerizes and binds to DNA upon either heating or oxidation with H_2O_2 (Ahn and Thiele, 2003). More direct evidence showing that endogenous ROS production is necessary for induction of the HS response comes from the observation that a dominant negative allele of Rac1, the small GTPase necessary for the activation of ROS production by membrane-bound NADPH oxidase (Abo et al., 1991), inhibits the stress-induced activation of Hsf1 (Ozaki et al., 2000). Thus, it is highly likely that ROS production during HS also activates NPR1, leading to gene expression changes critical for thermotolerance. Future studies directed at global gene expression analysis in WT and *npr1* mutant in response to HS and BR as separate and combined treatments should indicate NPR1-dependent molecular changes and help clarify the role of NPR1 in BR-mediated increase in thermotolerance.

The mechanism for how BR could function with NPR1, it is speculated that ROS-activated NPR1 monomers may bind a BR-activated regulator to affect stress-responsive gene expression critical to the survival of seedlings under stress conditions. It is unlikely that NPR1 controls BR signaling via BIN2 and BZR1 given that down-regulation of DWF4 in *npr1-1* was unaffected (Figure 3.3C).

3.4.3 Oxidative stress state in cpr5 and BR effects

The *cpr* (CONSTITUTIVE EXPRESSOR OF *PR* GENES) mutants are characterized with increased concentrations of SA, constitutive expression of the *PR*

genes, and enhanced resistance to pathogens (Bowling et al., 1994; 1997; Clarke et al., 1998). The *cpr* mutants are in a state of high-cellular oxidative stress state as compared to WT. For example, *cpr1* plants exhibited greater oxidative damage than WT under both normal growth (23^0C) and chilling (5^0C) conditions (Scott et al., 2004), and molecular changes in *cpr5* such as increased expression of several genes in the ROS gene network, including GSTs, indicate that the cellular redox balance in this mutant is de-regulated (Jing et al., 2008). We also observed higher levels of *GST1* transcript in *cpr5-2* as compared to WT (Figure 3.3B). The high-cellular oxidative stress state of the *cpr* mutants, combined with the constitutively activated SA and JA/ET-mediated pathways (Bowling et al., 1997; Clarke et al., 2000), may trigger not only defense responses against pathogens but also abiotic stress response pathways, leading to greater survival of *cpr5-2* seedlings than WT in response to HS (Figure 3.1B). EBR treatment further enhanced the survival rates of *cpr5-2* seedlings exposed to HS (Figure 3.1B), but had negligible effect on the oxidative damage levels in this mutant (Figure 3.2A), presumably due to the inherent oxidative state of the mutant.

3.4.4 BR induces expression of other hormone marker genes

Up-regulation of *PR-1* by BR in *eds5-1* and *npr1-1* backgrounds (Figure 3.3A), as well as in short-term treatment (Figure 3.4), suggests that BR directly mediates expression of this gene. Interestingly, we found *WRKY70*, a transcription factor acting downstream of NPR1 and involved in the expression of SA-induced *PR* genes (Li et al., 2004), to also be up-regulated by BR in different SA genotypes (Figure 3.3A). Thus, in addition to NPR1, *WRKY70* may be a potential point of cross-talk between SA and BR via which BR may induce a subset of SA-responsive genes. Such a scenario could explain, in part, how BR enhances plant resistance against pathogen infection (Krishna, 2003).

BR could increase the expression of *PDF1.2* in JA mutants, but not to the same extent in the ET-insensitive mutant *ein2* (Figure 3.3A). Thus, at present we favor the possibility that BR effects on *PDF1.2* expression are mediated via the ET pathway. It should be noted that *PR-1* and *PDF1.2* genes are constitutively expressed in *cpr* and *ssi1*

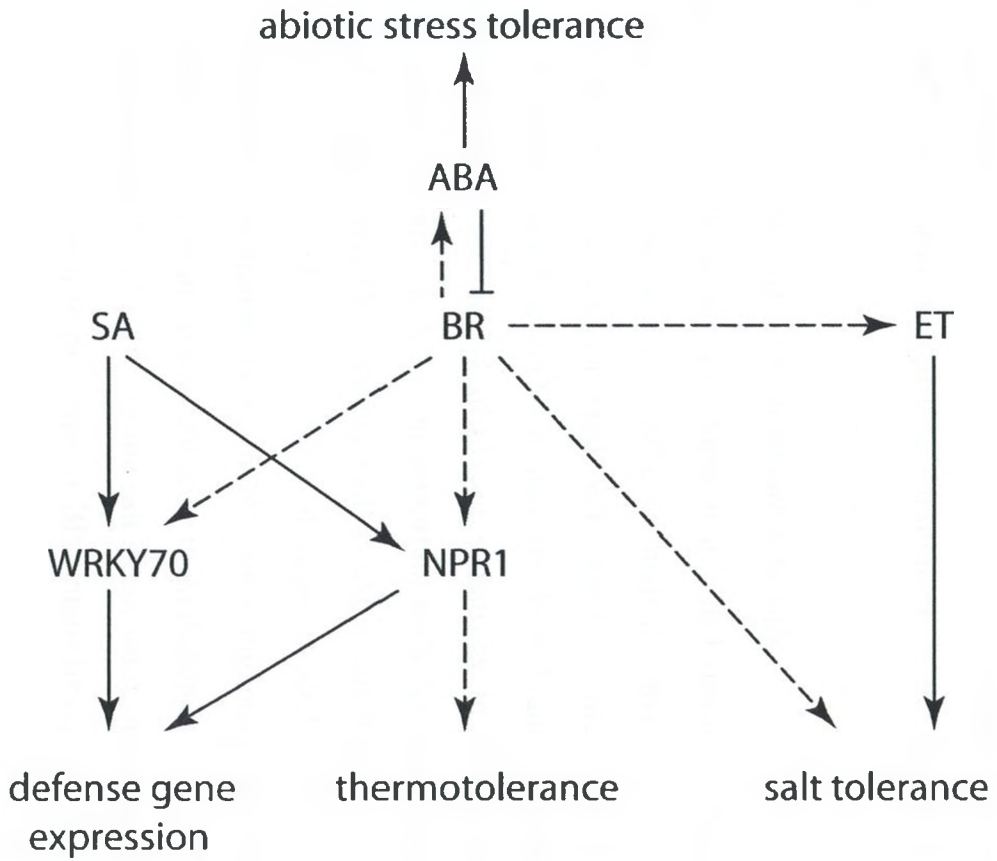
abiotic stress tolerance
ABA
SA
BR
ET
WRKY70
NPR1
defense gene expression
thermotolerance
salt tolerance

mutants of Arabidopsis in an NPR1-independent and SA, JA and ET-dependent manner (Clarke et al., 2000; Nandi et al., 2003), providing precedent for the notion that more than one pathway governs the expression of these genes. The increase in the transcript levels of the ABA-responsive *RD22* gene and the stress-induced *GST1* gene in WT and hormone mutants by EBR, including short-term treatment of WT (Figure 3.4), suggests that these genes may also be primary targets of BR. Taken together, our data indicate that BR has regulatory inputs into the expression of other hormone-responsive genes, which may result from the action of the BR pathway either on the promoters of these genes, or on the regulation of a hormone-signaling component or the biosynthesis of another hormone (Figure 3.6).

3.4.5 BR effects on inhibition of seed germination by salt

We have previously shown in *B. napus* that EBR helps to overcome inhibition of seed germination by salt (Kagale et al., 2007). To study the involvement of BR and other hormones in salt tolerance, we screened WT, *npr1-1*, *ein2* and *eto1-1* seeds for germination on 150 mM salt. The *ein2-5* mutant has been found to be hypersensitive to salt (Wang et al., 2007) and *ein2-1* displayed sensitivity to heat and osmotic stress (Suzuki et al., 2005). Clearly, EIN2 is an important node for interaction of stress and hormonal signaling pathways. The fact that EBR could rescue hypersensitivity of *ein2* to salt (Figure 3.5A and B) and increase survival rates of *ein2* seedlings following HS (Figure 3.1) with effects paralleling those in WT, unambiguously indicates that BR can bypass ET signaling in conferring stress tolerance in Arabidopsis.

We included *npr1-1* and *eto1-1* in the salt stress study due to the hypersensitivity of these genotypes to HS even in presence of BR. Interestingly, while both *npr1-1* and *eto1-1* were insensitive to salt during germination, both genotypes had survival rates comparable with those of WT and *ein2* in the absence of EBR, and notably lower survival rates than WT and *ein2* in the presence of EBR (Figure 3.5C). These results further endorse a crucial requirement of functional NPR1 in BR-mediated increase in stress tolerance and suggest further explorations of the roles of NPR1 in abiotic stress. The possibility that NPR1 mediates defense responses against abiotic stresses has been suggested in two recent reports (Quilis et al., 2008; Yasuda et al., 2008).

In summary we have demonstrated that 1) the BR-mediated increase in stress tolerance is independent, at least in part, from other hormone signals, 2) NPR1 is a critical component of BR-mediated effects on thermo and salt tolerance, 3) ABA inhibits BR effects in abiotic stress responses, and 4) several hormone-responsive genes are also BR-responsive. These findings point to possible cross-talk of BR with SA, ET and ABA signaling pathways in mediating stress responses, as depicted in Figure 3.6.

3.5 REFERENCES

Abo, A., Pick, E., Hall, A., Totty, N., Teahan, C., and Segal, A. (1991). Activation of the NADPH oxidase involves the small GTP-binding protein p21rac1. Nature **353,** 668-670.

Abrahám, E., Rigó, G., Székely, G., Nagy, R., Koncz, C., and Szabados, L. (2003). Light-dependent induction of proline biosynthesis by abscisic acid and salt stress is inhibited by brassinosteroid in Arabidopsis. Plant Mol. Biol. **51,** 363-372.

Ahn, S.G., and Thiele, D.J. (2003). Redox regulation of mammalian heat shock factor 1 is essential for Hsp gene activation and protection from stress. Genes Dev. **17,** 516-528.

Apel, K., and Hirt, H. (2004). REACTIVE OXYGEN SPECIES: Metabolism, Oxidative Stress, and Signal Transduction. Annu. Rev. Plant Biol. **55,** 373-399.

Arondel, V., Vergnolle, C., Catherine, C., and Kader, J. (2000). Lipid transfer proteins are encoded by small multigene family in Arabidopsis thaliana. Plant Sci. **157,** 1-12.

Arteca, J.M., and Arteca, R.N. (2001). Brassinosteroid-induced exaggerated growth in hydroponically grown Arabidopsis plants. Physiol. Plant **112,** 104-112.

Bajguz, A. (2009). Brassinosteroid enhanced the level of abscisic acid in *Chlorella vulgaris* subjected to short-term heat stress. J. Plant Physiol. **166,** 882-886.

Bari, R., and Jones, J.D. (2009). Role of plant hormones in plant defence responses. Plant Mol Biol.**69**, 473-488.

Belkhadir, Y., Wang, X., and Chory, J. (2006). Brassinosteroid signaling pathway. Sci. STKE. **364,** cm4.

Bell, E., Creelman, R.A., and Mullet, J.E. (1995). A chloroplast lipoxygenase is required for wound-induced jasmonic acid accumulation in Arabidopsis. Proc. Natl. Acad. Sci. USA. **92,** 8675-8679.

Boch, J., Verbsky, M.L., Robertson, T.L., Larkin, J.C., and Kunkel, B.N. (1998). Analysis of resistance gene–mediated defense response in *Arabidopsis thaliana* plants carrying a mutation in *CPR5*. Mol. Plant-Microbe Interact. **11**, 1196-1206.

Bouquin, T., Meier, C., Foster, R., Nielsen, M.E., and Mundy, J. (2001). Control of specific gene expression by gibberellin and brassinosteroid. Plant Physiol. **127,** 450-458.

Bowling, S.A., Clarke, J.D., Liu, Y., Klessig, D.F., and Dong, X. (1997). The *cpr5* mutant of Arabidopsis expresses both NPR1-dependent and NPR1-independent resistance. Plant Cell **9**, 1573-1584.

Bowling, S.A., Guo, A., Cao, H., Gordon, A.S., Klessig, D.F., and Dong, X. (1994). A mutation in Arabidopsis that leads to constitutive expression of systemic acquired resistance. Plant Cell **6,** 1845-1857.

Cao, H., Bowling, S.A., Gordon, A.S., and Dong, X. (1994). Characterization of an Arabidopsis mutant that is nonresponsive to inducers of systemic acquired resistance. Plant Cell **6,** 1583-1592.

Clarke, J.D., Liu, Y., Klessig, D.F., and Dong, X. (1998). Uncoupling PR gene expression from NPR1 and bacterial resistance: characterization of the dominant Arabidopsis *cpr6-1* mutant. Plant Cell **10,** 557-569.

Clarke, J.D., Volko, S.M., Ledford, H., Ausubel, F.M., and Dong, X. (2000). Roles of salicylic acid, jasmonic acid, and ethylene in cpr-induced resistance in arabidopsis. Plant Cell **12,** 2175-2190.

Clarke, S.M., Cristescu, S.M., Miersch, O., Harren, F.J., Wasternack, C., and Mur, L.A. (2009). Jasmonates act with salicylic acid to confer basal thermotolerance in Arabidopsis thaliana. New Phytol. **182**, 175-187.

Clarke, S.M., Mur, L.A., Wood, J.E., and Scott, I.M. (2004). Salicylic acid dependent signaling promotes basal thermotolerance but is not essential for acquired thermotolerance in *Arabidopsis thaliana*. Plant J. **38,** 432-447.

Clouse, S.D., and Sasse, J.M. (1998). Brassinosteroids: essential regulators of plant growth and development. Annu. Rev. Plant Physiol. Plant Mol. Biol. **49,** 427-451.

Delaney, T.P., Friedrich, L., and Ryals, J.A. (1995) Arabidopsis signal transduction mutant defective in chemically and biologically induced disease resistance. Proc. Natl Acad. Sci. USA **92**, 6602-6606.

Dhaubhadel, S., and Krishna, P. (2008). Identification of differentially expressed genes in brassinosteroid-treated *Brassica napus* seedlings. J. Plant Growth Regul. **27**, 297-308.

Dhaubhadel, S., Browning, K.S., Gallie, D.R., and Krishna, P. (2002). Brassinosteroid functions to protect the translational machinery and heat-shock protein synthesis following thermal stress. Plant J. **29,** 681-691.

Dhaubhadel, S., Chaudhary, S., Dobinson, K.F., and Krishna, P. (1999). Treatment with 24-epibrassinolide, a brassinosteroid, increases the basic thermotolerance of *Brassica napus* and tomato seedlings. Plant Mol. Biol. **40,** 333-342.

Dietz, K.J. (2008). Redox signal integration: from stimulus to networks and genes. Physiol. Plant **10,** 459-468.

Feys, B.J.F., Benedetti, C.E., Penfold, C.N., and Turner, J.G. (1994). Arabidopsis mutants selected for resistance to the phytotoxin coronatine are male sterile, insensitive to methyl jasmonate, and resistant to a bacterial pathogen. Plant Cell **6,** 751–759.

Gaffney, T., Friedrich, L., Vernooij, B., Negrotto, D., Nye, G., Uknes, S., Ward, E., Kessmann, H., and Ryals, J. (1993). Requirement of salicylic acid for the induction of systemic acquired resistance. Science **261,** 754–756.

Gendron, J.M., and Wang, Z.Y. (2007). Multiple mechanisms modulate Brassinosteroid signaling. Curr. Opin. Plant Biol. **10,** 436-441.

Glazebrook, J., Rogers, E.E., and Ausubel, F.M. (1996). Isolation of Arabidopsis mutants with enhanced disease susceptibility by direct screening. Genetics **143,** 973–982.

Guzman, P., and Ecker, J.R. (1990). Exploiting the triple response of Arabidopsis to identify ethylene-related mutants. Plant Cell **2,** 513–523.

Hardtke, C.S., Dorcey, E., Osmont, K.S., and Sibout, R. (2007). Phytohormone collaboration: zooming in on auxin-brassinosteroid interactions. Trends Cell Biol. **17,** 485-492.

He, J.X., Gendron, J.M., Sun, Y., Gampala, S.S., Gendron, N., Sun, C.Q., and Wang, Z.Y. (2005). BZR1 is a transcriptional repressor with dual roles in brassinosteroid homeostasis and growth responses. Science **307,** 1634-1638.

He, Z.H., He, D., and Kohorn, B.D. (1998). Requirement for the induced expression of a cell wall associated receptor kinase for survival during the pathogen response. Plant J. **14,** 55-63.

Heath, R.L., and Packer, L. (1968). Photoperoxidation in isolated chloroplasts. I. Kinetics and stoichiometry of fatty acid peroxidation. Arch. Biochem. Biophys. **125,** 189-198.

Iwasaki, T., Yamaguchi-Shinozaki, K., and Shinozaki, K. (1995). Identification of a cis-regulatory region of a gene in *Arabidopsis thaliana* whose induction by dehydration is mediated by abscisic acid and requires protein synthesis. Mol. Gen. Genet. **247,** 391-398.

Jing, H.C., Hebeler, R., Oeljeklaus, S., Sitek, B., Stühler, K., Meyer, H.E., Sturre, M.J., Hille, J., Warscheid, B., and Dijkwel, P.P. (2008). Early leaf senescence is associated with an altered cellular redox balance in Arabidopsis *cpr5/old1* mutants. Plant Biol. (Stuttg). **10,** 85-98.

Kagale, S., Divi, U.K., Krochko, J.E., Keller, W.A., and Krishna, P. (2007). Brassinosteroid confers tolerance in *Arabidopsis thaliana* and *Brassica napus* to a range of abiotic stresses. Planta **225,** 353-364.

Khripach, V., Zhabinskii, V., and de Groot, A. (2000). Twenty years of brassinosteroids: steroidal plant hormones warrant better crops for the XXI century. Ann. Bot. **86,** 441-447.

Kitanaga, Y., Jian, C., Hasegawa, M., Yazaki, J., Kishimoto, N., Kikuchi, S., Nakamura, H., Ichikawa, H., Asami, T., Yoshida, S., Yamaguchi, I., and Suzuki, Y. (2006). Sequential regulation of gibberellin, brassinosteroid, and jasmonic acid biosynthesis occurs in rice coleoptiles to control the transcript levels of anti-microbial thionin genes. Biosci. Biotechnol. Biochem. **70,** 2410-2419.

Koh, S., Lee, S.C., Kim, M.K., Koh, J.H., Lee, S., An, G., Choe, S., and Kim, S.R. (2007). T-DNA tagged knockout mutation of rice OsGSK1, an orthologue of Arabidopsis BIN2, with enhanced tolerance to various abiotic stresses. Plant Mol. Biol. **65,** 453-466.

Koornneef, M., Jorna, M.L., Brinkhorst-van der Swan, D.L.C., and Karssen, C.M. (1982). The isolation of abscisic acid (ABA) deficient mutants by selection of induced revertants in nongerminating gibberellin sensitive lines of *Arabidopsis thaliana* (L.) Heynh. Theor. Appl. Genet. **61,** 385–393.

Koornneef, M., Reuling, G., and Karssen, C.M. (1984). The isolation and characterization of abscisic acid-insensitive mutants of *Arabidopsis thaliana*. Physiol. Plant. **61,** 377–383.

Kovacs, D., Kalmar, E., Torok, Z., and Tompa, P. (2008). Chaperone activity of ERD10 and ERD14, two disordered stress-related plant proteins. Plant Physiol. **147,** 381-390.

Krishna, P. (2003). Brassinosteroid-mediated stress responses. J. Plant Growth Regul. **22,** 289-297.

Krishna, P., Reddy, R.K., Sacco, M., Frappier, J.R., and Felsheim R.F. (1997). Analysis of the native forms of the 90 kDa heat shock protein (hsp90) in plant cytosolic extracts. Plant Mol. Biol. **33,** 457-466.